Climate Signals in Coastal Deposits

Dissertation

zur Erlangung des Doktorgrades an der Fakultät für
Mathematik, Informatik und Naturwissenschaften

Fachbereich Geowissenschaften
der Universität Hamburg

vorgelegt von

Juliane Ludwig

Hamburg

2016

Tag der Disputation: 17.11.2016

Folgende Gutachter empfehlen die Annahme der Dissertation:

Prof. Dr. Christian Betzler
Dr. Sebastian Lindhorst

Hiermit erkläre ich an Eides statt, dass ich die vorliegende Dissertationsschrift selbst verfasst und keine anderen als die angegebenen Quellen und Hilfsmittel benutzt habe.

Hamburg, den 02.08.2016 Juliane Ludwig

Abstract

The purpose of this study is to reconstruct the development of Holocene coastal landscapes along the Polish Baltic Sea coast and to evaluate their potential to provide a proxy record of wind-field variations. The direct response of marine and aeolian systems to changes in the wind field makes them exceptionally valuable for serving as climate archives. A key prerequisite to access the climate record is to have a comprehensive understanding of the barrier and dune architecture and their forming processes. This study provides high-resolution stratigraphic and evolutionary models of the Wolin barrier, located in the Pomeranian Bight, and the Łeba barrier, located at the northern part of the Polish coast, and shows the potential of the transgressive dunes of Łeba to record annual wind-intensity variations. The near subsurface of barrier and dune systems were studied by an integrated approach of using ground-penetrating radar (GPR), sediment cores, and sampling trenches. GPR provides a spatial insight into barrier and dune architecture, core data gives a 1-diminensional understanding of environmental conditions. A complementing hydroacoustic data set, obtained in the Pomeranian Bight, provides an understanding of on-offshore sedimentation.

The data obtained illustrates the contemporaneous development of regressive (Wolin) and transgressive (Łeba) barrier systems along the southern Baltic Sea coast. The formation of spits and barriers is linked to a decelerating rate of sea level rise since 6500 BP and alongshore transported eroded moraine material. A complex interaction of several factors, most importantly the impact of the local sea level, the wave energy, and the sediment supply, influences the development of each barrier and evokes differences in the barrier architecture. Depending on the depositional barrier history, either foredunes or transgressive dunes cover the barrier.

The Wolin barrier is characterized by a progradational sequence comprising of an alongshore growing spit and a seaward prograding beach plain. The formation of either spits or beach plains is associated to the predominance of longshore currents or waves and depends on the progradation direction of the barrier. The alongshore-parallel spit, attached in the east to a Pleistocene headland, is the result of current-dominated sediment transport. The shift from spit to beach-plain sediments is the result of restricted accommodation space for further spit growth and is accompanied by a change towards a wave-controlled sedimentation. The seaward prograding beach succession is therefore subject to greater sediment reworking by waves, especially during storms, evident from numerous unconformities in the sedimentary record. The dominating progradational character of the barrier system is attributed to a sediment supply high enough to compensate the accommodation space, a temperate wind and wave energy, and to only small fluctuations in the local sea level. Foredunes atop the barrier, characteristic for regressive systems, indicate the direction of barrier progradation through time. Foredune development in the study

area is controlled by the beach progradation rate and the potential aeolian sediment transport rate.

The development of the landward migrating Łeba barrier is controlled by overwash and aeolian sediment influx into the adjacent lagoon. In absence of topographic barrier constraints, washover fans developed as a result of the landward sediment transfer from the coast under the influence of elevated wave and water levels during storm surges. Since barrier stabilization by vegetation and dunes prevented overwash, a significant dunal contribution guarantees an ongoing landward barrier migration. Transgressive dunes are periodically prominent on the barrier and migrated into the lagoon maintaining therefore the sediment budget of the barrier which highlights the importance of dunes for barrier development. Coastline retreat, as a result of beach erosion and subsequent sediment redistribution, is attributed to a barrier position exposed to a high wind and wave energy. Transgressive barriers are furthermore attributed to a rising sea level. However, the formation of dunes on top of the Łeba barrier since 3000 BP, as the result of barrier stabilization, is an indicator for a nearly stable sea level.

At present, the Łeba barrier is covered by a transgressive dune field, composed of eight dunes which bear a record of annual wind intensity. Integrated geophysical and sedimentological data show inter-annual changes in the sedimentary properties. Intervals dominated with quartz sands and intervals showing layers enriched in heavy minerals are imaged by GPR as alternating reflection packages of low and high amplitudes. This log of alternating reflection packages is termed a sedimentary “bar code”. The deposition of quartz-dominated intervals or layers enriched in heavy minerals is attributed to sub-yearly changes in the wind field. Hence, the annual net-sedimentation at the dune lee-side is imaged by a paired low and high amplitude package. Variations in the annual bar code thickness are directly linked to annual variations in the wind intensity. The time-based wind proxy covers the time period 1987 to 2012 and was tested and validated against a time series of instrumental weather data. Analogue to dendrochronological methods, this new approach uses sub-yearly intervals in the sedimentary record of dunes, which allows providing a proxy of annual wind-intensity variations, applicable to areas and time periods lacking of instrumental observation.

Zusammenfassung

Ziel der vorliegenden Arbeit ist es die Entwicklung holozäner Küstenlandschaften entlang der polnischen Ostseeküste unter dem Aspekt ihrer Nutzung als Windarchiv zu rekonstruieren. Marine und äolische Systeme reagieren direkt auf Änderungen des Windfeldes und werden aus diesem Grund als wertvolle Windarchive eingestuft. Eine Grundvoraussetzung, Barrieren und Dünen als Archiv für Windfeldänderungen nutzen zu können, ist ein umfangreiches Verständnis über deren Architektur und einflussnehmenden Prozesse. Prozess-basierte Modelle wurden für das Barrieresystem von Wolin, das im Süden der Pommerschen Bucht liegt, und Łeba, im Nordosten der polnischen Küste, erstellt. Die Dünen von Łeba bieten darüberhinaus ein Archiv zur Rekonstruktion jährlicher Variationen in der Windintensität.

Der nahe Untergrund von Barrieresystemen und Dünen wurde mit Hilfe des Georadars (GPR), Sedimentbohrkernen und Gräben untersucht. Das GPR erlaubt eine räumliche Erkundung der Barriere- und Dünenarchitektur; Kerndaten liefern ein 1-dimensionales Verständnis über frühere Umweltbedingungen. Hydroakustische Daten aus der Pommerschen Bucht vervollständigen den Datensatz und geben Aufschluss über on-offshore Sedimentationsprozesse.

Eine ineinandergreifende Interpretation der Daten erlaubt die Rekonstruktion der Architektur und Entwicklung beider Barrieresysteme und belegt die gleichzeitige Generierung regressiver (Wolin) und transgressive (Łeba) Barrieren entlang der polnischen Ostseeküste. Barrieren entwickelten sich im Zuge eines verlangsamten Meeresspiegelanstieges seit etwa 6500 BP unter dem Einfluss küstenparallel transportierten Moränenmaterials. Die Interaktion mehrerer Faktoren, insbesondere der Einfluss des lokalen Meeresspiegels, der Wellenenergie und der Sedimentzufuhr, beeinflussten und bestimmten marine Sedimentationsprozesse und verursachten Unterschiede in der Barrierearchitektur. Je nach Barrieresystem überlagern entweder Vordünen oder transgressive Dünen die hier untersuchten Barrieren.

Die progradierende Abfolge der Wolinbarriere besteht aus einem küstenparallel-orientiertem Spit und einer seewärtig progradierenden Strandebene. Es wird gezeigt, dass die Generierung von Spits oder Strandebenen an den dominierenden Einfluss von Küstenlängsströmungen oder Wellen geknüpft und abhängig von der Richtung des Barrierewachstums ist. Strömungsdominierter Sedimenttransport führte zur Bildung eines küstenparallelen Spits, der im Osten an die pleistozäne Landzunge anlagert ist. Der Wechsel vom Spit zur Strandebene ist das Resultat eines begrenzten Akkommodationraumes in küstenparallele Richtung und geht einher mit einem Wechsel hin zu einer wellendominierten Sedimentation. Die seewärts progradierende Strandebene unterliegt deshalb der Aufarbeitung durch Wellen, insbesondere während Stürmen, was in Form zahlreicher Erosionsdiskordanzen in der sedimentären Abfolge überliefert ist. Der progradierende Charakter der Barriere ist auf eine hohe Sedimentzufuhr, eine gemäßigte Wind- und Wellenenergie und

nur geringfügige Schwankungen im Meeresspiegel zurückzuführen. Die Barriere überlagernden Vordünen zeigen die Progradationsrichtung während des Barrierewachstums an und sind charakteristisch für regressive Systeme. Die Entwicklung der Vordünen ist durch die Rate der Strandprogradation und der potentiellen Sedimenttransportrate kontrolliert.

Die Entwicklung der landwärtig migrierenden Łeba Barriere ist von overwash und äolischem Sedimenteintrag in die Lagune dominiert. Eine flache Barriere erlaubt einen landwärts gerichteten Sedimenttransfer und die Ablagerung von washover fans im Verlauf erhöhter Wellenenergie und Wasserstände, ausgelöst durch Stürme. Eine Stabilisierung der Barriere durch Vegetation und Dünen verhindert overwash Sedimentation, jedoch wird die landwärtige Verlagerung der Barriere durch den signifikanten Beitrag von Dünen sichergestellt. Die Migration transgressiver Dünen in die Lagune erhält somit den Sedimenthaushalt der Barriere aufrecht und betont die Bedeutung äolischer Sedimentation für die Entwicklung von Barrieren. Erosion entlang der Küste führt zu deren Rückschreiten und wird auf die hohe Wind- und Wellenenergie aufgrund der exponierten Lage der Barriere zurückgeführt. Transgressive Barrieren sind darüber hinaus charakteristisch in Gebieten mit steigendem Meeresspiegel. Jedoch ist die Entwicklung von Dünen auf der Łeba Barriere seit etwa 3000 BP ein Indikator für einen nahezu gleichbleibenden und stabilen Meeresspiegel.

Heute bedeckt ein Wanderdünengürtel, bestehend aus acht Dünen, die Łeba Barriere. Die Dünen liefern ein Proxy zur Rekonstruktion jährlicher Windintensitäten, der auf saisonal variierenden sedimentären Eigenschaften basiert. Quartzsand-dominierende Intervalle und Intervalle mit Lagen angereicht mit Schwermineralen sind im GPR als alternierende Reflektionspakete mit niedrigen oder hohen Amplitude abgebildet. Dieses alternierende Muster wird sedimentärer „bar code" genannt. Quartzsand-dominierende oder Schwerminerallagen-angereicherte Intervalle entstehen aufgrund subjährlich wechselnder Windrichtungen. Die jährliche Netto-Sedimentation am Leehang der Düne spiegelt sich deshalb in einem Paar von jeweils einem Paket niedriger und hoher Amplituden wieder. Variationen der jährlichen bar code Mächtigkeit ist direkt auf Änderungen in der Windintensität zurückzuführen. Der zeit-basierte Proxy reicht 26 Jahre zurück und wurde mit meteorologischen Daten verglichen und validiert. Analog zu dendrochronologischen Methoden nutzt der vorgestellte Ansatz subjährliche Intervalle in den Sedimenteigenschaften von Dünen um anschließend ein Proxy für jährliche Änderungen in der Windintensität zu erstellen. Diese Methode zur Erstellung eines Wind-Proxys kann auf Gebiete und Zeitspannen angewendet werden, für die keine meteorologischen Daten zur Verfügung stehen.

Table of content

Chapter 1

Introduction

Barrier systems and dunes are highly dynamic coastal landforms, modified by atmospheric and hydrological factors. In wave-dominated settings, waves and longshore currents are prominent parameters affecting barrier processes and have a potential influence on regional coastal behaviour on centennial to millennial time scales (Roy et al., 1994; Goodwin et al., 2006). The geometry of barriers responds furthermore to fluctuations of various other parameters such as the relative sea level, the sediment supply, the grain size distribution, and the barrier topography. Dune processes in temperate climates are not only controlled by the immediate effect of short-term variations in the wind direction and speed, but are also influenced by vegetation and soil moisture (Pye, 1983; Tsoar and Blumberg, 2002; Hugenholtz et al., 2009). Considering the relationship between coastal landform formation and the surrounding environmental parameters, coastal deposits can be an indicator for atmospheric variations. Therefore, developing an accurate understanding of the architecture and variability of marine and aeolian landscapes is necessary to provide a reliable forecast model of barrier and dune behaviour which are important to constrain due to our anthropogenic development of coastal areas.

Holocene barrier systems account only for 15 % of the world´s coastlines, but have been studied extensively as they are most vulnerable to weather extremes and climatic changes (Davis Jr., 1994). Investigations of coastal landforms along the southern Baltic Sea were mainly performed on geomorphological and sedimentological bases (e.g. Keilhack, 1914; Borówka, 1979, 1990; Borówka et al., 2005; Borówka and Rotnicki, 1995a; Tomczak, 1995b; Osadczuk, 2002; Hoffmann et al., 2005; Rotnicki et al., 2009; Łabuz, 2013). At coasts elsewhere the application of geophysical methods, especially ground-penetrating radar (GPR), has been highlighted as an important analysis tool as it can significantly improve the ability to image barrier and dune architecture in the near subsurface (Bailey and Bristow, 2000; Neal et al., 2002; Lampe et al., 2004; Buynevich, 2006; Costas et al., 2006; Lindhorst et al., 2008, 2010; Ziekur et al., 2009; Clemmensen and Nielsen, 2010; van Dam, 2012; Lindhorst and Schutter, 2014). In addition, optical-stimulated luminescence (OSL) dating can provide a reliable chronology of barrier and dune deposits to reconstruct the coastal evolution (Bristow et al., 2005, 2010; Reimann et al., 2011; Costas et al., 2012a; Choi et al., 2014).

In non-tidal settings, as those in the Baltic Sea, climatic factors such as winds and in particular storms greatly affect marine and aeolian systems. Washover sediments of transgressive barriers are the result of significant storm events and are therefore used as a potential indicator for storm frequency and intensity (Morton et al., 2007; Wang and Horwitz, 2007; Switzer and Jones, 2008). Sedimentary gaps in the progradational succession of beach plains record intense storm activity, evident from erosional scarps and from sand layers enriched in heavy minerals (Buynevich et al., 2004; Dougherty et al., 2004; Bristow and Pucillo, 2006; Hein et al., 2013). Layers enriched in heavy minerals can furthermore indicate a record of annual beach progradation (Moore et al., 2004); however, a time-based reconstruction of atmospheric changes, such as overall shifts in the wind direction or wind intensity, from barrier successions remains yet to be addressed. Based on the close relationship between dune processes and the wind field, dunes allow for an understanding of episodic wind-strength variations on decadal to centennial time scales. This is possible due to the circumstance of enhanced dune activity during time periods with a higher frequency and intensity of storms (Forman et al., 2001; Wilson et al., 2001; Havholm et al., 2004; Aagaard et al., 2007; Clemmensen et al., 2007; Bristow et al., 2011; Costas et al., 2012a, 2013, 2016). A first successful attempt to provide a high-resolution proxy-record of wind-intensity variations is based on variations in the grain size distribution (Lindhorst and Betzler, 2016). However, the development of an annual to sub-decadal proxy-based record of wind field variations is in an early stage of scientific development and can be greatly enhanced by more studies.

1.1 Objective of the study

This study attempts to reconstruct climate variations within the last 8000 years on a yearly to centennial or millennial time scale based on sedimentary proxies. Archives to be investigated comprise of aeolian (dune) and marine (barrier) successions. A comprehensive understanding of the architecture and processes of both depositional settings is necessary in order to discern the climate record. Aeolian sediments can highlight the variability of the wind field on a high resolution while barrier deposits provide larger scale constraints to the overall wind field.

1.2 Thesis outline

The content of this thesis is presented in six chapters, with this **first chapter** being the introduction of the thesis.

The **second chapter** is a preface including the geography and geology of the research areas. The chapter opens introducing the Holocene evolution of the Baltic Sea, its oceanography, and its climate. Subsequently, the location and general background of each investigated barrier (Wolin and Łeba) are introduced. The chapter concludes with a description of the barrier associated coastal dune types.

The stratigraphy and evolution of the regressive Wolin barrier system is presented in the **third chapter** and is based on an integrated approach by combining off- and onshore obtained data sets. The barrier system is comprised of alongshore prograding spit deposits, which subsequently change into a beach plain with seaward dipping foresets. The change in the progradation direction is associated with a change in the predominance of either longshore currents or waves. Foredunes on top of the barriers indicate the shift from alongshore barrier progradation to the seaward beach progradation.

In **chapter four**, geophysical and core data reveal the internal architecture of the transgressive Łeba barrier. The overall landward barrier migration is the result of marine overwash and aeolian processes. The chapter highlights the importance of aeolian sediment accumulation into a lagoon by transgressive dunes that significantly contribute to the landward barrier migration and maintain the sediment budget of the barrier.

Chapter five introduces a new method to access annual wind-field variations provided by the sedimentary record of dunes. The development of a sedimentary log, termed “bar code”, which reflects seasonally changes in the sedimentary properties allows for the reconstruction of annual variations in the wind intensity. Six bar codes extracted from dunes of the transgressive dune field in Łeba were combined into one composite bar code, which was subsequently tested and validated by meteorological data.

The concluding **chapter six** summarizes results of the preceding three chapters (3 to 5) and addresses the effect of interacting controlling factors have on the development of either transgressive or regressive barriers.

Chapter 2

Research area

This study has been conducted along the Polish Baltic Sea coast. The coast of the southern Baltic Sea is characterized by spits and barriers attached to moraine cliffs (Rotnicki and Rotnicka, 2010). Coastal landforms to be investigated comprise the barrier complex of the Wolin Island (Fig. 2.1: A), and the barrier system located west of the village Łeba and its active dune field atop (Fig. 2.1: B). The Wolin barrier is part of the Woliński National Park and the barrier and dunes of Łeba belong to the Słowiński National Park.

2.1 Baltic Sea : oceanography and climate

The Baltic Sea is an intra-continental and tideless sea of the Atlantic Ocean connected to the North Sea by the Danish straits, specifically the Great Belt, Little Belt, and Øresund. The salinity decreases from 25 ‰ in the Danish Straits to between 3.5 ‰ to 7 ‰ in the north and east of the basin (Bothnian Sea and Bay; Gulf of Finland) as a result of increased freshwater input by river discharge (Leppäranta and Myrberg, 2009). The resulting density differences between freshwater- and saltwater-dominated water masses and the wind are the main drivers of the hydrodynamic surface circulation (Fig. 2.1). The small size of the sea causes friction by the bottom and shores which dampen the current velocity, being low with an average speed of 5 cm s^{-1}. The Baltic Sea is characterized by a halocline, separating low-salinity-surface waters of seasonally changing temperatures from high salinity and stable temperate deep waters (Emeis et al., 2003; Uścinowicz, 2014).

The long-term sea level trend of the semi-enclosed Baltic Sea is linked to the global sea level and isostatic land movement, whereas oscillations in wind conditions stress the importance of meteorological factors to control short-term sea level changes (Uścinowicz, 2006; Łabuz, 2013; Deng et al., 2014; Hünicke et al., 2015). Depending on the wind direction, intensity, and continuity, winds raise or lower the water level of the Baltic Sea in various areas of the basin. Winds can raise the water level in the order 1.5 m, reaching up to 2.80 m in the southwestern part of the basin, as a result of storm surges and also affect processes along the coast, such as seabed erosion and transport of sediment (Uścinowicz, 2006, 2014; Zhang et al., 2013). Winds from the southwest and west dominate throughout the year. The average yearly wind speed ranges between 6 m s^{-1} and 8 m s^{-1}, showing top speeds during the autumn and winter months (Uścinowicz, 2014; Hünicke et al., 2015). Westerly winds are closely related to the North Atlantic Oscillation (NOA), where a positive

NAO is associated with warm and humid winters and strong westerly winds and a negative NAO relates to cold and dry winters (Hünicke et al., 2015).

2.2 Holocene history of the southern Baltic Sea coast

The southern part of the present Baltic Sea was ice free since 15.5 ka – 14.5 ka BP (Uścinowicz, 2014). The ice-sheet retreat is associated with isostatic uplift of the earth's crust. Glacio-isostatic rebound along the southern coast started 17 ka BP and reached a total uplift rate of 100 m to 150 m along the present southern Baltic coast (Uścinowicz, 2014). The evolution of the Baltic Sea

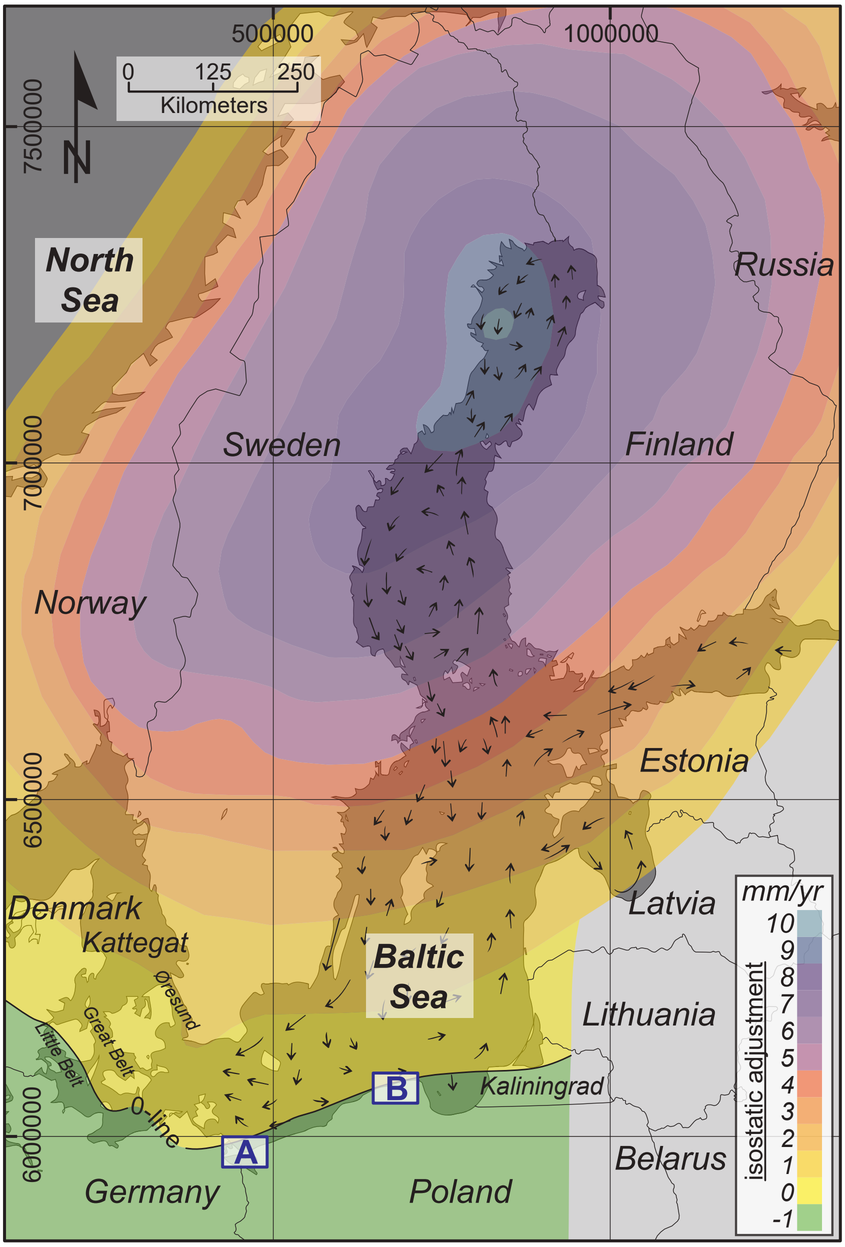

Fig. 2.1: Location of research areas in north Poland facing the Baltic Sea. A: Wolin barrier; B: Łeba barrier and dune field. The surface current direction is based on Leppäranta and Myrberg (2009); the present vertical crustal displacement is adopted from Harff and Meyer (2011).

during the Holocene is characterized by three transgressive stages – the Yoldia Sea, the Ancylus Lake, and the Littorina Sea – each reported by different faunal occurrences (Björck, 1995). The first stage, the Yoldia Sea, is accompanied with a rapid warming. This time period is named after the marine bivalve *Portlandia* (old: *Yoldia*) *arctica* that migrated into the Baltic area through the narrow straits of the southcentral Swedish lowland indicating a connection to the open ocean at this time (11.7 ka – 10.7 ka BP) (Andrén et al., 2011). High uplift rates of Scandinavia blocked further water exchange through the straits and the freshwater-dominated Ancylus Lake, named after the snail *Ancylus fluviatilis*, which developed by a large input of meltwater (10.7 ka – 9.8 ka BP). The re-connection of the Baltic basin to the Atlantic is indicated by the presence of marine deposits, first in the western and southern parts of the Baltic basin (Uścinowicz, 2014). The shift from freshwater to marine conditions around 8.5 ka BP was accompanied with the initiation of the Littorina Sea, named after the marine slug *Littorina littorea*. The rapid sea-level rise of 1.5 cm a^{-1} at the beginning of the Littorina transgression caused inundation of the paraglacial landscapes and promoted the erosion of the Pleistocene headlands (Tomczak, 1995a; Hoffmann et al., 2005; Hoffmann and Lampe, 2007). Eroded moraine material, transported alongshore by currents, accumulated in the form of spits and barriers, characterized by a straightening of the coastline. A decelerated sea-level rise since 7 ka BP allowed for compensation of the new provided accommodation space (Hoffmann et al., 2005). Since the early Atlantic the effect of glacio-isostatic movements diminished in the southern Baltic Sea and uplift rates ceased at around 3 ka BP (Lampe, 2005; Uścinowicz, 2014). The small sea-level rise along the southern Baltic coast since this time increased the influence of meteorological fluctuations (Uścinowicz, 2006). In late Atlantic (5.8 ka BP) the Littorina sea level reached its highstand at 1.5 m to 2 m below the present sea level in the southwest of the Baltic Sea (Lampe, 2005). The last pronounced sea-level fluctuation with a sea-level rise of 0.18 m is associated with the Little Ice Age between 0.45 ka and 0.15 kaBP (Lampe, 2005). At present, the polish Baltic Sea coast is seen to be attributed to minor subsidence as a result of the northward shifting of the transition zone (0-line) separating subsidence in the south from uplift in the north (Fig. 2.1) (Hansen et al., 2012; Uścinowicz, 2014).

2.3 Geographic-geological setting of studied barriers

2.3.1 Wolin barrier

The Wolin (Wollin in German) barrier is located at the border of Poland and Germany (Fig. 2.1: A) and separated from the Uznam (Usedom in German) spit by the Świna Channel that is part of the Oder river mouth area. Both barriers combined belong to the Świna Gate barrier system, which separates the freshwater-dominated Szczecin Lagoon from the Pomeranian Bight in the north. Each barrier is connected to a Pleistocene headland and consists of a continuous series of established and stabilized foredune ridges. In the past, the investigation of the barrier system and the Szczecin Lagoon comprised geomorphological, pedological, and sedimentological studies (e.g. Keilhack, 1914; Osadczuk, 2002; Witkowski et al., 2004; Borówka et al., 2005; Łabuz, 2005). A four-step evolution of the prograding barrier system was provided based on the orientation of the foredune crests (Osadczuk, 2002). Reimann et al. (2011) established a comprehensive chronology of the foredune ridge plain by using optical-stimulated luminescence (OSL).

Foredune ridge plains or a series of beach ridges atop marine deposits are characteristic features of progradational barrier systems. The development of prograding (regressive) barriers is linked to either stable or falling sea levels and characterized by a seaward directed displacement of the shore (Roy et al., 1994; Davis Jr. and FitzGerald, 2004; Clemmensen and Nielsen, 2010; Hein et al., 2013). Under the circumstances of the global sea-level rise during the Holocene, stable or falling sea-levels are the result of an isostatic rebound, which is common at paraglacial coasts (Forbes et al., 1995; Short, 1999). Seaward prograding beaches or alongshore growing spits develop when the rate of sediment supply exceeds the rate of creation of accommodation space (Reading and Collins, 2007; Nielsen and Johannessen, 2009). Regressive barriers are not influenced by overwash and the well preserved sedimentological record of progradational successions are most suitable to serve as recorders for palaeo-environmental changes.

2.3.2 Łeba barrier

The Łeba barrier is located in the northeast of Poland around 150 km northwest of Gdansk and encloses the Lake Łebsko (Fig. 2.1: B). The barrier belongs to the Gardno-Łeba coastal plain and is up to 1.6 km wide. Foredunes, 4 m - 15 m high, occur along the WSW-ENE striking coast of the Łeba barrier (Rotnicka, 2011). To the west, the Łeba barrier is connected to a late Pleistocene moraine (13.5 ka BP) (Rotnicki, 1995). In depths between 10 m to 12 m below the present sea-level Pleistocene glacio-fluvial sediments are covered by Holocene sands of the Łeba barrier (Rotnicki and Rotnicka, 2010; Rotnicki et al., 2009). Sedimentological and palaeontological studies of the barrier indicate the deposition of marine and freshwater sands (Rotnicki et al., 2009). The barrier shifted to its present position 4.5 ka to 3 ka BP and dunes appeared around 3 ka BP on top of the barrier. At present, plaeosols and tree stumps crop out at the coast (Borówka and Rotnicki, 1995b) representing remnants of a vegetated backbarrier environment that was shifted to the coast by coastal retreat. This is a distinct indicator for transgressive barriers, also observed elsewhere (e.g. Maio et al., 2014). The beach and shoreline eroded sediment is either transported landward by overwash or redistributed along the coast depending on the barrier topography, the vegetation density, the sediment availability, and the frequency and intensity of storms (Kahn and Roberts, 1982; Morton and Sallenger, 2003; Timmons et al., 2010; Lima et al., 2013; Maio et al., 2014). Overwash contributes to an overall landward migration of the barrier maintaining its sediment budget. The shape of transgressive barriers is long, narrow, with only few inlets along wave-dominated coasts and they are generally related to rising sea levels (Davis Jr., 1994; Short, 1999). At a late stage, transgressive barriers are often associated with an aeolian dune field atop the barrier.

2.4 Barrier associated coastal dune forms

2.4.1 Foredunes of the Wolin barrier

A complex foredune ridge plain covers the marine succession of the prograding Wolin barrier system. Foredunes were subdivided into three groups depending on foredune height and crest orientation as well as the degree of podsolization (Keilhack, 1914). Oldest dunes strike in S-N direction and have a well-developed illuvial horizon whereas youngest dunes are W-E aligned and lack an illuvial horizon. The mobilization of a transgressive dune that migrated landward is attributed to the Little Ice Age (LIA) as the result of increased winds (Reimann et al., 2011). The west-east striking coastline of the Wolin Island is dominated by a wind direction parallel to the beach. Such coast-parallel and –oblique winds are responsible for the major aeolian sediment transport rate along the lower to the middle part of the beach (Arens, 1996b; Hesp, 2002; Rotnicka, 2011; Łabuz, 2013). Alongshore transported sand is trapped by vegetation in the backshore area of a prograding beach succession leading to foredune development.

Foredunes are relict, semi-parallel, multiple ridges of wind origin. Their beach parallel alignment is understood to result from the seaward extent of vegetative growth controlled by the storm wave inundation (Davis Jr. and FitzHerald, 2004; Hesp et al., 2005). Wrack lines, berms or erosional scarps along the beach are furthermore regarded to trap sediment by vegetation allowing foredune initiation (Davis Jr. and FritzGerald, 2004; Lindhorst et al., 2010). Along the southern Baltic Sea coast halophytes occur where shells, algae, and wood fragments accumulate (Łabuz, 2013). However, first sand binding vegetation (e.g. the sea sandwort *Honckenya peploides* and *Ammophelia arenaria*) is present in the backshore area that is only affected by intense storm waves during the winter (Łabuz, 2013). As a result, incipient dunes develop in form of several discrete mounds parallel to the coastline in the upper part of the beach and generate under continuous sand supply a new foredune ridge which is associated with a change in the vegetation community being dominated by e.g. *Ammophila arenaria* or *Calammophila baltica* (Hesp, 2002; Łabuz, 2005). Stabilized foredunes of the Wolin barrier are covered by pine trees and willow shrub. The evolution and stability of foredunes is linked to a number of factors, like a seasonal variation of sediment supply, the degree and type of vegetation cover, the rate of aeolian sand accretion and erosion, the wave and wind regime, and a potential human impact (Hesp, 2002).

2.4.2 Transgressive dunes of Łeba

A dune field, comprising eight dunes, migrates on top of the Łeba barrier towards the east due to the prevalence of westerly winds. Dunes, up to 27 m high, cover an area of 2.2 km^2 and were studied in the past by using sedimentological methods (Borówka, 1980, 1990). On top of primary dunes mesobarchans vary seasonally in size and volume depending on variations in the wind velocity and precipitation rate. Łeba dunes are composed of 99.5 % quartz sands and less than 1 % heavy minerals (amphiboles, garnets, and small amounts of zircon, ilmenite and others) that are enriched in 1-2 mm thick layers (Borówka, 1979). Such layers enriched in heavy minerals are known from dunes elsewhere and expected to develop under the influence of winnowing (Hamilton and Collins, 1998; Buynevich et al., 2007a; Devi et al., 2013).

Transgressive dunes are mobile, partially, or fully vegetated aeolian sediment complexes that migrate, when active, transversely, oblique, or alongshore to the coast depending on the predominating wind field (Hunter et al., 1983; Hesp, 2013). Wind is typically not a limiting factor in the formation of coastal dunes, but sediment supply may be and vegetation is an important control on sediment availability (e.g. Havholm et al., 2004; Hugenholtz et al., 2008). According to Hesp (2013) the evolution of transgressive dune fields is attributed to three conceptual models. This includes the development of dunes directly from the backshore, by foredune destruction, and by the merging of parabolic dunes. Internally, dunes are characterized by foresets, cross stratification, bounding surfaces, and post-sedimentary deformation surfaces, each indicating phases of either dune accretion or erosion (McKee, 1966; McKee and Bigarella et al., 1972; Hunter, 1977; Bailey and Bristow, 2000; Oliveira Jr. et al., 2008). By dating the sediment or by using aerial images, transgressive dunes can be used to reconstruct phases of aeolian activity, associated to time periods of enhanced storm activity, and to determine phases of dune stabilization, indicated by the formation of soils and attributed to wetter conditions (Orford et al., 2000; Havholm et al., 2004; Clemmensen et al., 2007; Forman et al., 2008; Girardi and Davis, 2010; Buynevich et al., 2011; Reimann et al., 2011; Costas et al., 2012a; Dobrotin et al., 2013).

Chapter 3

Sedimentary architecture and development of a non-tidal prograding barrier system (Baltic Sea, Poland)

Abstract

The internal architecture of the regressive Wolin barrier (Pomeranian Bight, Baltic Sea) is revealed by an integrated approach comprising ground-penetrating radar (GPR), hydroacoustic and sedimentological data. The Wolin barrier comprises of two genetic units. First, the coast-parallel Wolin spit which grew under the control of longshore currents and second, a beach plain, that grew in shore-normal direction. The Wolin spit consists of spit platform deposits characterized by sigmoidal foresets; whereas the beach plain shows seaward-inclined internal beds attributed to a foreshore-shoreface succession. The composite architecture of the Wolin barrier is the result of a turnover from longshore-current dominated to wave-controlled sedimentation, which took place at about 1.66 ka BP, as the result of restricted accommodation space. The internal architecture of the shore-normal prograding beach plain is characterized by numerous erosional unconformities that are the result of wave-erosion triggered by strong onshore winds, especially during the winter months. This substantial erosional impact contrasts with the preceding continuity of the shore-parallel spit growth. The enhanced erosion that affected the beach plain results in a progradation rate of the Wolin spit being twice as high as the growth rate of the foreshore-shoreface succession that forms the beach plain. Differences in progradation direction are also documented by different crest orientations of the foredunes on the Wolin spit and the attached beach plain. Dune ridges on the spit are coast-normal oriented, whereas the foredunes covering the beach plain strike parallel to the present day coastline. Foredunes are nourished with sediment from the beach by coast-oblique winds. Sediment accretion patterns in the dunes change from aggrading to prograding, depending on foredune height. Development and shape of foredunes strongly depend on barrier progradation rate and beach width.

3.1 Introduction

During the Holocene, barriers and barrier-related landforms developed worldwide along coastlines attached to the mainland or off the coast. The classification of these barriers is controversially discussed (Otvos, 2012). In general, a coastal barrier is characterized by shore-parallel sand and gravel-built islands and spits that separate open marine from paralic inshore environments (Hesp and Short, 1999; Otvos, 2012). Spits represent shore-elongated sedimentary bodies that transform into bay- or lagoon-enclosing barriers when separating a water body from the open sea. By ground-penetrating radar (GPR) such spits internally show steep inclined, mostly parallel and sigmoidal foresets that are interpreted as formed by along-coast sediment transport (e.g. Nielsen et al., 1988; Shaw and Forbes, 1992; Daly et al., 2002; Smith et al., 2003; Nielsen and Johannessen, 2009; Ziekur et al., 2009; Hein et al., 2012; Lindhorst et al., 2013). The downdrift progradation of these systems contrasted with the seaward progradation of mainland strandplains (Otvos, 2012), which are composed of foreshore-shoreface sediments reflecting shore-normal sediment accumulation. Sediments of the foreshore and shoreface are imaged by GPR as seaward inclined beach foresets and are often associated with multiple erosional unconformities interpreted to result from individual storm (e.g. van Heteren et al., 1998; Neal et al., 2002; Moore et al., 2004; Engels and Roberts, 2005; Bristow and Pucillo, 2006; Lindhorst et al., 2008, 2010; Tamura et al., 2008; Dickson et al., 2009; Nielsen and Clemmensen, 2009; Clemmensen and Nielsen, 2010; Garrisson et al., 2010; Costas et al., 2013; Lindhorst and Schutter, 2014). Characteristic architectural elements of regressive barrier systems are spits as well as foreshore-shoreface deposits (e.g. Mäkinen and Räsänen, 2003; Lindhorst et al., 2010).

Prograding barrier systems are often associated with a series of beach ridges or foredunes (Roy et al., 1994). The definition of berms, beach ridges and foredunes varies between different authors and the terms are often used for deposits generated under different sedimentary regimes (Otvos, 2000; Hesp et al., 2005; Tamura, 2012). In contrast to wave-built beach ridges, foredunes are relict, semi-parallel, multiple ridges formed by trapping of wind-blown sediment by pioneer vegetation (Otvos, 2000; Hesp, 2002; Łabuz, 2005, 2013). Davis Jr. and FitzGerald (2004) and Hesp et al. (2005) argued that the regular, parallel nature of foredunes is not necessarily governed by the shore-parallel orientation of berms or beach ridges. They also attributed the initiation of foredune ridges to wrack or swash lines on the backshore or to any obstacle where wind transported sand accumulates. In temperate climates, vegetation is the most effective anchor for wind-blown sand, with the seaward extension of beach vegetation being controlled by storm wave inundation. Numerous (semi-) parallel foredunes that are oriented parallel to the shoreline are termed foredune-ridge plain (Hesp, 2002; Hesp et al., 2005; Barboza et al., 2009) to punctuate the presence of aeolian generated foredunes in the study area.

This study aims to decipher the internal architecture of the Wolin barrier system based on an amphibian approach combining onshore sedimentological- and ground-penetrating radar data with an offshore hydroacoustics survey. The genesis of the Wolin barrier is characterized by a profound change from alongshore current-dominated spit growth to wave-dominated beach-plain progradation. This shift is interpreted to result from a restricted accommodation space under

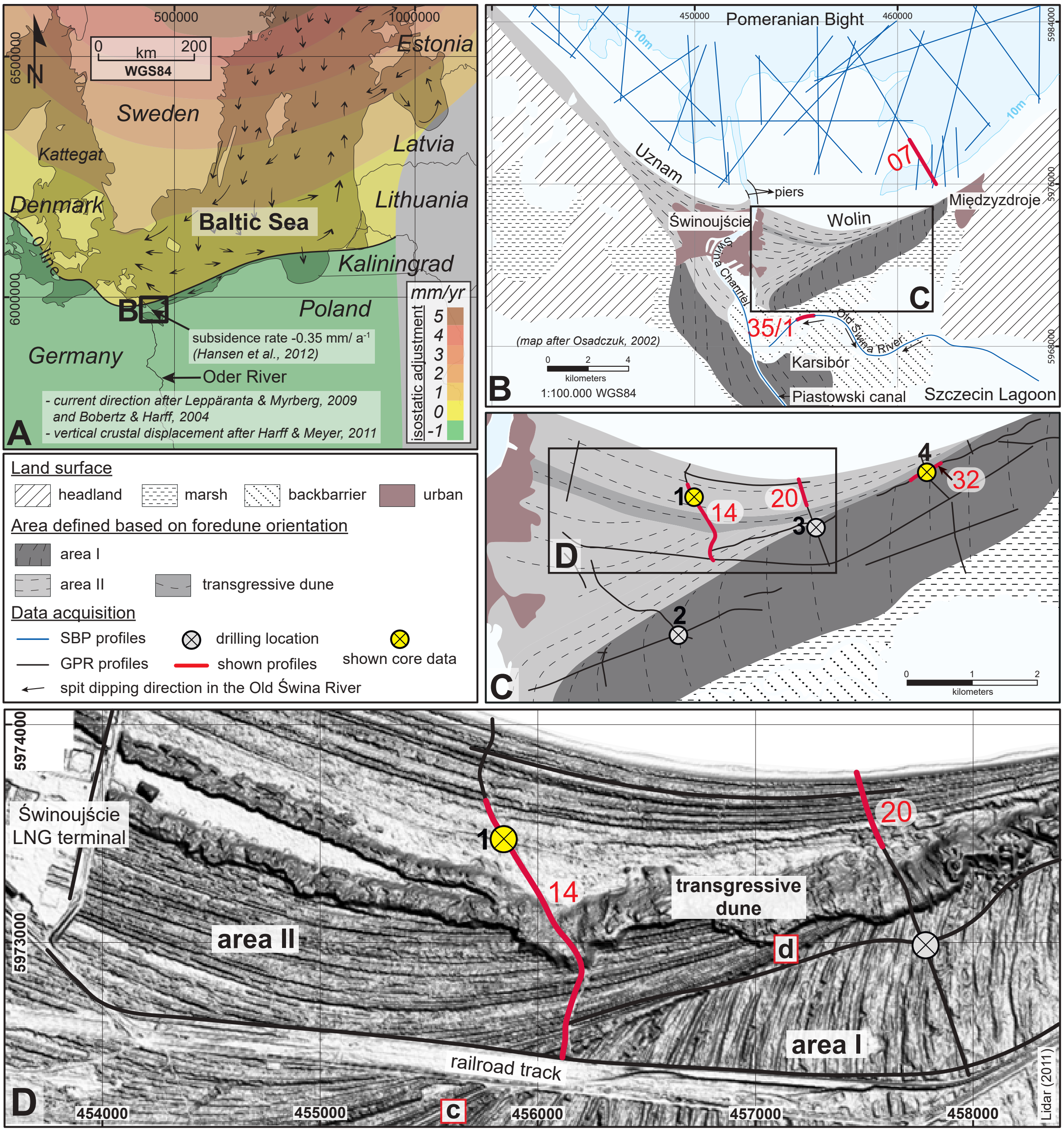

Fig. 3.1: A) Isostatic adjustment of the Baltic Sea area with subsidence south and uplift north of the 0-line. The surface circulation of the Baltic Sea is indicated by black arrows; **B)** Barrier systems of Uznam and Wolin are connected to headlands. The 10 m isobath line bases on the chart of the Bundesamt für Seeschifffahrt und Hydrographie, Hamburg (2011). Blue lines indicate the SBP survey in the Pomeranian Bight and Old Świna River; **C)** Area I is differentiated from area II based on foredune crest orientation. GPR survey is indicated by black lines. Red lines represent SBP and GPR profiles shown in this study. Four sediment cores were obtained; presented core information is indicated in yellow; **D)** DTM based on Lidar data (data provided by ProGea Consulting, Kraków, Poland). Artificial constructions (eg. the liquefied natural gas (LNG) import terminal or the railroad track) interrupt the foredune ridge trend. The contact between foredunes of area I and area II is concordant in the western part of the barrier (c) and discordant in the east (d). The stabilized transgressive dune covers foredunes of area II and partly of area I.

constant sediment supply. An evolutionary model for the barrier system is presented, illustrating current- and wave-dominated stages of barrier development.

3.2 Study area

3.2.1 Geographical setting and Geomorphology

The southern Baltic Sea coast is characterized by spit and barrier systems attached to moraine cliffs. The Świna Gate barrier system is located in the Pomeranian Bight and comprises the barriers of Uznam and Wolin (Musielak and Osadczuk, 1995; Osadczuk, 2002; Łabuz, 2005; Reimann et al., 2011) (Fig. 3.1 A, B). Both barriers are separated by the Świna Channel, which is a part of the Oder river mouth area. The Świna Channel connects the freshwater dominated Szczecin Lagoon in the south with the Pomeranian Bight in the north. The Uznam barrier is attached to a 60 m high cliff in the west that retreats with a rate of 0.4 m a^{-1} (Schwarzer et al., 2003). The up to 115 m high Wolin cliff, east of the barrier, retreats with rates between 0.1 m a^{-1} to 0.9 m a^{-1} (Cieślak, 1995; Rotnicki and Rotinicka, 2010).

The study area comprises the barrier system of Wolin and extends from the city Międzyzdroje in the east towards the Świna Channel in the west (Fig. 3.1 B, C). Foredunes on the Wolin barrier were grouped into three dune generations depending on dune height, dune crest orientation and degree of podsolization (Keilhack, 1914). The oldest foredunes strike north-south and are 2 m high and characterized by a well-developed illuvial horizon (Musielak and Osadczuk, 1995; Reimann et al., 2011). The second generation of foredunes comprises west-east oriented ridges, 3 m to 10 m high. These foredunes show weak podsoil development and a yellow illuvial horizon. The youngest, up to 5 m to 10 m high, west-east stretching foredunes lack an illuvial horizon. In addition, there is an up to 24 m high transgressive dune, which differs in height, shape and genesis from the foredunes (Osadczuk, 2002). This transgressive dune is genetically decoupled from the foredunes and buried older foredune ridges. In general, the orientation of foredune crests is parallel to the former coastline and as so indicates the progradation direction of the barrier system (Osadczuk, 2002). The Wolin barrier system is subdivided based on the orientation of the foredunes (Fig. 3.1 B, C). Area I comprise north-south oriented foredunes, whereas area II is characterized by east-west oriented foredunes.

3.2.2 Holocene sea-level history of the southern Baltic and development of the Wolin barrier

The relative sea level of the Baltic Sea is not only controlled by the post-glacial sea-level rise during the Holocene but also by vertical crustal displacement that strongly varies from the north to the south of the Baltic Sea (Fig. 3.1 A) (Lampe et al., 2010; Harff and Meyer, 2011; Hansen et al., 2012). The last Scandinavian glacial ice sheet vanished from the southern Baltic coast around 14 ka BP and as a result of post-glacial rebound the Scandinavian crust still experiences uplift, whereas the southern Baltic Sea coast, including the study area, subsides (Lampe et al., 2010; Andrén et al., 2011; Harff and Meyer, 2011).

The sea-level rise during the Littorina transgression since 8 ka BP is accompanied with enhanced erosion of Pleistocene headlands that provides the material to build up coastal barriers (e.g. Nielsen et al., 1988; Forbes et al., 1995; Dillenburg et al., 2000; Mäkinen and Räsänen, 2003; Hoffmann et al., 2005; Doughty et al., 2006; Lima et al., 2013). Along the Polish coast longshore currents transport the eroded sediment within the nearshore zone towards the east, except for the coast of the Wolin Island where sand transport towards the west is governed by local coastline configuration (Leppäranta and Myrberg, 2009; Rotnicki and Rotnicka, 2010; Deng et al., 2014). Sediment in suspension bypasses the nearshore zone and settles in deeper basins of the Pomeranian Bight (Arkona basin and Tromper Wiek) (Musielak and Osadczuk, 1995; Emeis et al., 2002). Fluvial sediment input acts as a potential secondary source of sediment; however, the fine sediment load from the river Oder is trapped in the Szczecin Lagoon or deposited in depressions of the Tromper Wiek and the Arkona Basin (Emeis et al., 2002; Borówka et al., 2005).

During the initial sea-level rise between 8 ka to 7 ka BP the sediment supply was insufficient to compensate the increase in accommodation space resulting in a drowning of the landscape (Kliewe and Janke, 1982; Hoffmann and Barnasch, 2005; Hoffmann and Lampe, 2007). Around 6 ka BP the rate of sea-level rise decelerated to 1 mm a^{-1} and the sea level reached 2 m below the present sea level (Hoffmann et al., 2005). Under a constant sediment supply the Wolin and Uznam spit started to develop in along-coast extension of the morainic plateaus. South-north striking foredunes of the westward prograding Wolin barrier formed since 5.33 ± 0.37 ka BP (Osadczuk, 2002; Reimann et al., 2011; age conversion to BP). The formation of the youngest foredunes of the Wolin spit, 2.39 ± 0.15 ka BP, was accompanied by a change in the diatom- and malacofauna in the Szczecin Lagoon to freshwater taxa which indicates the separation of the Szczecin Lagoon from the Pomeranian Bight (Witkowski et al., 2004; Borówka et al., 2005). Seaward progradation of the Wolin barrier system started around 1.66 ± 0.12 ka BP (Reimann et al., 2011). Increased summer storminess during the Little Ice Age remobilized foredunes and initiated the landward migration of a transgressive dune (Reimann et al., 2011).

3.2.3 Wave and wind climate

The Baltic Sea is a semi-enclosed tideless epicontinental shelf sea that is connected with the North Sea by the Danish Straits in the west. The surface salinity decreases towards the east and reaches a value of around 7 ‰ in the Pomeranian Bight (Osadczuk et al., 2007; Leppäranta and Myrberg, 2009). The Pomeranian Bight is located in the southern-most part of the Baltic Sea and has mean depth of 13 m (Lass et al., 2001). Where the tide-range is negligible, meteorological effects become important to influence the local sea level (Hünicke et al., 2015). Hence, meso- to large-scale wind-driven littoral drifts and local wind-induced waves dominate in the Baltic Sea and control the local sea level (Deng et al., 2014). Westerly winds account for 65% of the total wind-direction spectrum (Łabuz, 2005; Deng et al., 2014). The sheltered position of the Pomeranian Bight prevents wave heights even during westerly storms. Storm surges that develop under strong winds blowing from the north and east increase the water level in the Pomeranian Bight (Łabuz, 2005; Deng et al., 2014). Such strong but infrequent wind conditions predominantly occur in the meteorologically more variable winter months and generate water levels up to 2 m above average level (Łabuz, 2005; Sztobryn et al., 2005; Hünicke et al., 2015). Heaviest storms correlate with north-east winds and occur with an annual probability of 1% (Łabuz, 2013), resulting waves have the potential to erode beaches and foredunes (Schwarzer et al., 2003; Łabuz, 2005).

3.3 Methods

3.3.1 Ground-penetrating radar (GPR)

GPR data was acquired on the Wolin barrier system in the years 2013 and 2014 by means of a Geophysical Survey Systems Inc. (GSSI) SIR-3000 GPR system equipped with a 200 MHz antenna. GPR is a non-invasive method, based on the emission of short electromagnetic pulses into the subsurface and the partly reflection of energy at electromagnetic discontinuities (Neal, 2004). Each reflection is recorded as a function of two-way-travel time (TWT). Based on the shape of diffraction hyperbolas the subsurface radar-wave velocity in the studied sediments was determined to 0.06 m ns^{-1} for saturated and 0.12 m ns^{-1} for unsaturated sands. The topography along the survey lines was measured either manually with a theodolite or extracted from a LIDAR-based digital terrain model (DTM) obtained in 2011. Topographic heights were extracted from the DTM using the software package Surfer 10 and a grid cell size of 1 m. Processing of raw GPR data was carried out by means of Reflex-Win v. 7.1.6 (Sandmeier, 2013). Post-processing steps include static correction, subtract-mean (dewow), 1D-filter (time-independent), background removal, migration, and gain correction. In some profiles the GPR signal was attenuated by a high content of organic matter (e.g. on the Karsibór Island) or by concrete and gravel pathways (e.g. on the Uznam Island). Dense shrub vegetation limited GPR measurements off pathways.

3.3.2 Parametric sediment echosounder (SBP)

Hydroacoustic data was obtained in the Pomeranian Bight and Szczecin Lagoon in October 2013 using the hull mounted sub-bottom profiler (SBP) SES-2000 Compact of the research vessel FS Ludwig Prandtl. The presence of numerous fishing nets restricted data acquisition especially close to the coast. Probably as the result of the partially coarse grained seafloor (Schwarzer et al., 2003), the penetration depth in the study area was restricted to 15 m (progradation velocity 1600 m s^{-1}). The SBP makes use of the parametric effect, the interference of two signals with different frequencies, resulting in a lower frequency parametric signal which penetrates the subsurface (Westervelt, 1963; Lurton, 2010). SBP data were not real-time corrected for pitch, roll and heave and are therefore afflicted with a swell induced displacement of the seafloor. Data was recorded in time-domain and post-processed by the Innomar Software ISE v. 2.9.2.

The interpretation of SBP and GPR data followed the concepts for seismic interpretation after Mitchum Jr. et al. (1977). Reflection patterns of similar geometry and character were classified as certain seismic and radar facies (Baker, 1991; Bristow, 1995) (Fig. 3.2) with seismic/radar surfaces separating different facies (Baker, 1991). In this study vertical positions are given in meter (m) above or below the present sea level (asl/bsl), because the sea level determines the groundwater level as the result of hydrodynamic coupling between both systems.

3.3.3 Sediment cores and ^{14}C-dating

Sedimentological analysis of the near subsurface is based on four vibrocores along the GPR profiles. Core material was obtained by 1 and 2 m long sampling tubes of 36 mm and 50 mm in diameter. Core information is incomplete as a result of sediment compression or sediment wash-out when retrieving the gouge due to high pore-water contents. After a visual description of the core the sediment was sampled in 5 cm intervals for laboratory analysis. To measure the spectrum of the grain-size distribution with a Sympatec Helos KF Magic laser diffractometer the sediment was prepared with H_2O_2 and 30 % acetic acid in order remove organic and calcite components. The calculation of grain size statistics was done using the program Gradistat (Blott and Pye, 2001) and mean grain size, sorting, and skewness values were plotted using the logarithmic phi scale after Folk and Ward (1957).

Radiocarbon dating was performed by Beta Analytic Miami Inc. (USA) using AMS ^{14}C. Calibration was done using the program Calib 7.0.4 (Stuiver and Reimer, 1993) and the Marine13 calibration curve (Reimer et al., 2013). The local reservoir is 200 years (Lougheed et al., 2013).

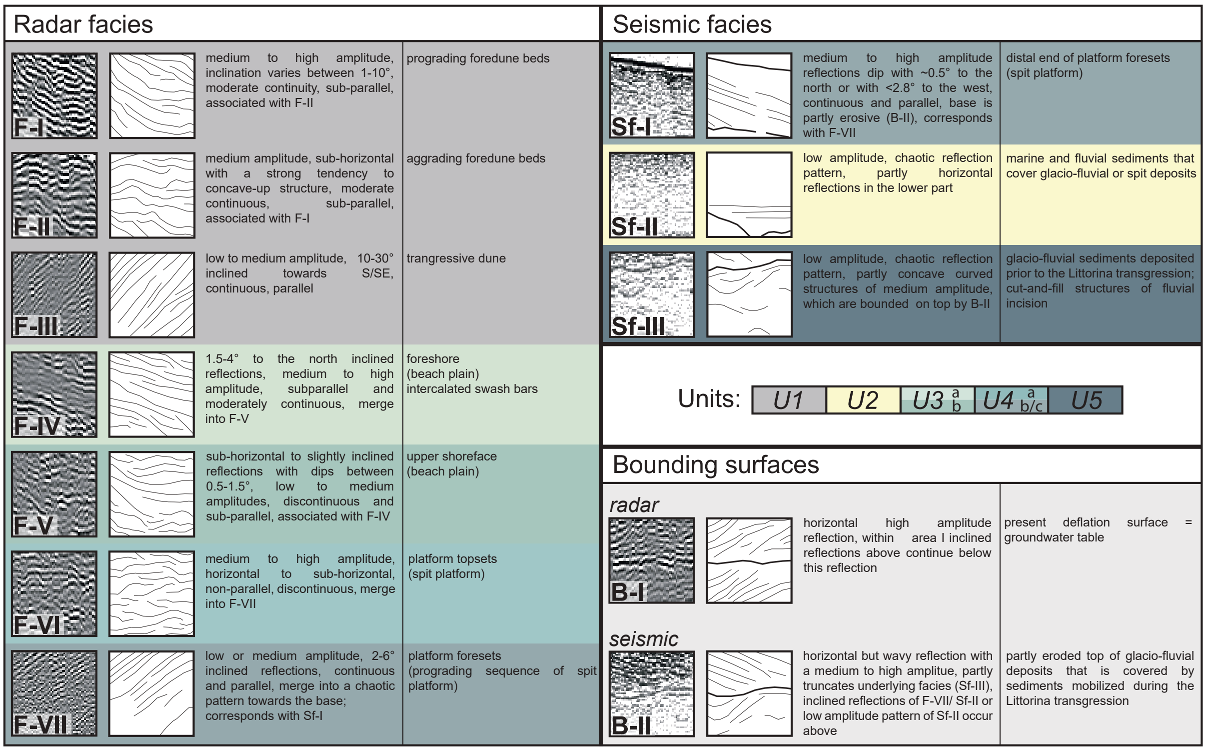

Fig. 3.2: Radar facies (F), seismic facies (Sf) and bounding surfaces (B) defined for classification of the GPR and SBP profiles. Colour code defines different units (U1 – U5).

3.4 Results

The internal architecture of the Wolin barrier system and the subseafloor of the Pomeranian Bight is documented by a total of 45 km GPR data, 260 km SBP data and 4 vibrocores (Fig. 3.1 C, D). The integration of GPR, SBP and sedimentological data allows to differentiate five genetic units (U1-U5), composed of seven radar facies (Fs-I to -VII), three seismic facies (Sf-I to -III) and two bounding surfaces (Bs-I to Bs-II) (Fig. 3.2).

The orientation of the foredune ridges of the Wolin barrier system allows to differentiate two geomorphological areas: north-south striking foredunes of area I contrast with east-west oriented foredune ridges which belong to area II (Fig. 3.1 D).

3.4.1 Pomeranian Bight

The near subseafloor of the Pomeranian Bight is exemplarily shown by the SBP profile 7 (Fig. 3.3). This line is located close to the Wolin barrier and allows for a jump correlation with the onshore GPR data.

The profile 7 images three units (U2, U4b-c, U5). Sediment penetration is down to a depth of 6 ms TWT which corresponds to 5 m. Chaotic reflections with intercalated discontinuous horizontal reflections characterizes the up to 1.5 m thick U2 (Sf-II). 0.5° north-dipping reflections (Sf-I) dominate U4b, which occurs only in the most southern part of the SBP survey. A chaotic reflection pattern characterizes U4c, which occurs in depressions. The bounding surface B-II truncates U5 at depths between 10 m and 12.5 m bsl. Concave curved reflections, which reach down to 4 m below the sea floor, are embedded into the chaotic reflection pattern of U5. Concave curved reflections occur in almost all profiles, but there is no linkage between adjacent profiles.

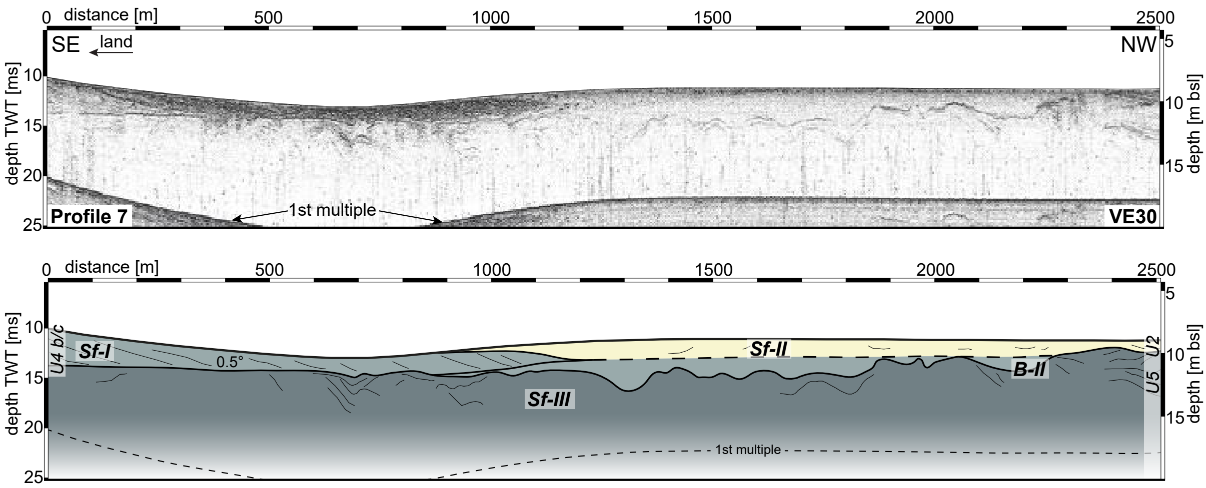

Fig. 3.3: SBP data obtained in the Pomeranian Bight. Processed data (above) and interpretation (below). The distal part of platform foresets (U4b) merges into marine sediments (U2) towards the sea. Cut-and-fill structures indicate fluvial incision into glacial sediments prior to the Littorina transgression (U5). Infilling of incised river channels during the sea-level rise (U4c).

3.4.2 Wolin barrier, area I

The internal architecture of area I is exemplary shown by the GPR profile 32 (Fig. 3.4) and by the SBP profile 35/1 (Fig. 3.5). Profile 32 images the units U1 and U4a to U4b. Signal penetration is restricted to a depth of 350 ns TWT, corresponding to 9 m. SBP data obtained in the Old Świna River (Fig. 3.5) show a sediment penetration of up to 5 m and images U2 and U4. Sediment characteristics and grain-size distribution of area I are exemplarily shown by core 4 (Figs. 3.6 A). The 16 m long core 4 reaches down to 14.5 m below present sea level (bsl) and covers three units (U1; U4a-c; U5) (Fig. 3.6 A).

Unit 1 is characterized by westward inclined and sub-horizontal reflections of medium to high amplitude (F-I; F-II). The unit reaches up to 5 m asl and down to 1.5 m bsl. At mean sea level a horizontal high amplitude reflection (B-I) intercepts reflections of F-I and F-II (Fig. 3.4). Unit 1 is characterized by medium grained sands (Fig. 3.6 A).

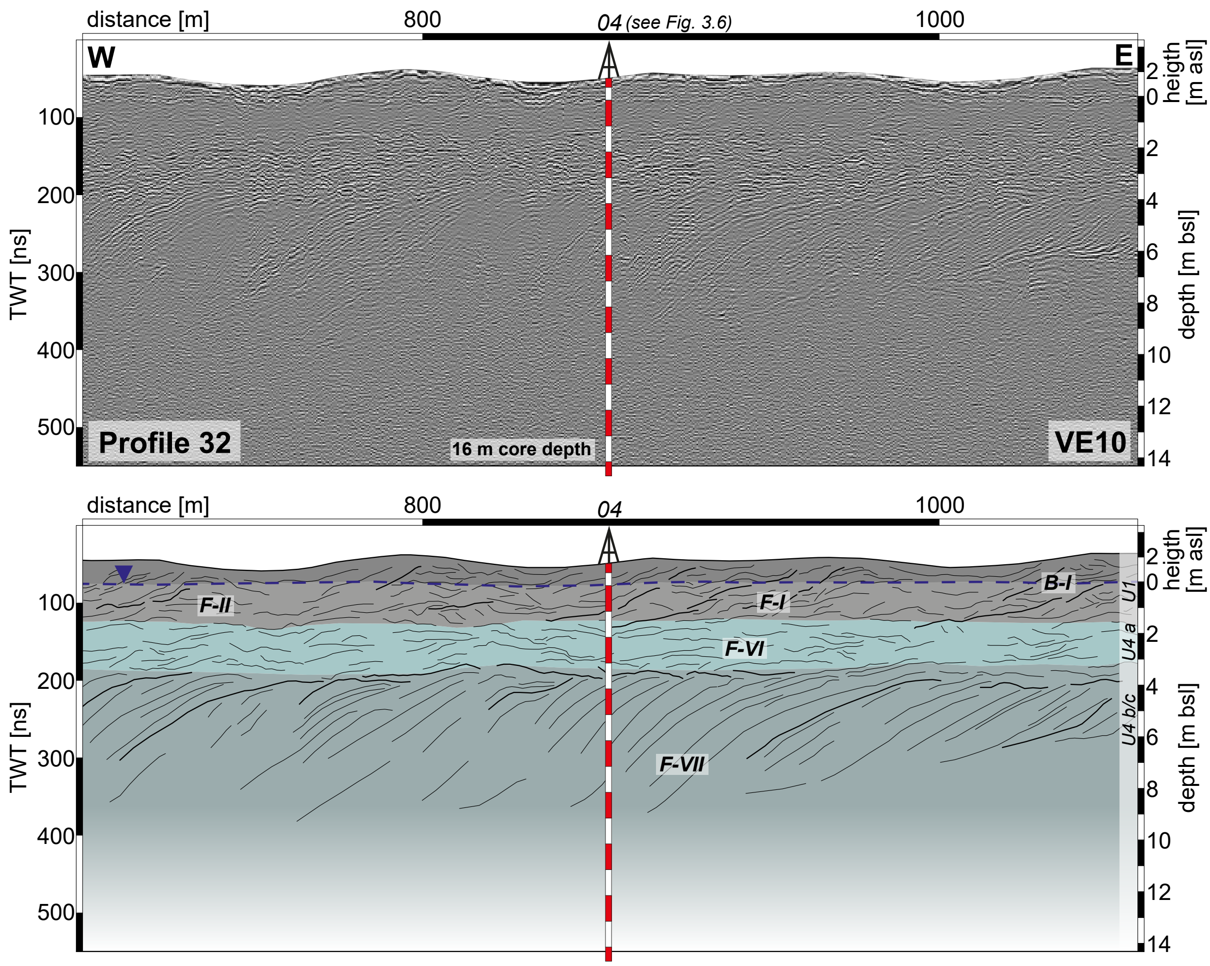

Fig. 3.4: GPR data obtained in area I. Note different migration velocities for dry (0.12 m ns^{-1}) and water saturated (0.06 m ns^{-1}) sediments and hence a different thickness-arrangement for dry and wet deposits (apply to all profiles). The 16 m long core 4 reaches down to 14.5 m bsl and includes foredune and spit platform sediments. The groundwater table intercepts foredune deposits.

Unit 4 comprises the sub-units U4a to U4c. The up to 2 m thick U4a is characterized by sub-horizontal discontinuous reflections (F-VI). At a depth of 3.5 m bsl the strata of U4c passes into 2° to 6° westward inclined parallel reflections of U4b (F-VII). Towards the base, inclined reflections fade out into a chaotic reflection pattern due to a reduced signal-to-noise ratio of GPR data. The radar facies F-VII (U4b) coincides in SBP data with 0.8° to 3.5° to the west and south inclined reflections of the seismic facies Sf-I (Fig. 3.5). The structure-less up to 2 m thick U2 covers U4b. Towards the north and south the top of U4 deepens down to 7 m bsl (Figs. 3.3, 3.5, 3.7, 3.8).

The medium grained sediments of U4a and U4b are moderately well sorted and symmetrical skewed (Fig. 3.6). At a depth of 9.50 m bsl the grain-size spectrum changes to poorly sorted and positively skewed fine sands (U4c). At 12.50 m bsl medium-coarse grained, moderately sorted and symmetrical skewed sands characterize U5. Wood and organic remains are scattered over the entire core length, whereas shells are only present between 2 m and 12 m bsl. Most shells and shell fragments belong to the mollusk species *Cerastoderma glaucum* and only few are identified as *Astarte sulcata* and *Bythinia* sp. (after Ziegelmeier, 1966) or can not be classified due to poor preservation. A shell of *Cerastoderma glaucum* sampled at 8 m bsl (U3) was dated using AMS ^{14}C revealing an age of 4.8 ± 0.09 ka cal BP.

3.4.3 Wolin barrier, area II

The architecture of area II is exemplary shown by the GPR profiles 14 and 20 (Figs. 3.7, 3.8). Both profiles image three units (U1, U3, U4). Data quality is good down to a depth of 250 ns TWT, corresponding to 7 m. The GPR signal is attenuated towards the coast due to brackish groundwater (Fig. 3.8). The 10 m long core 1 reaches down to 9.50 m bsl and allows for a description of the sedimentary characteristics of U3 (a, b) and U4 (b, c) (Fig. 3.6 B).

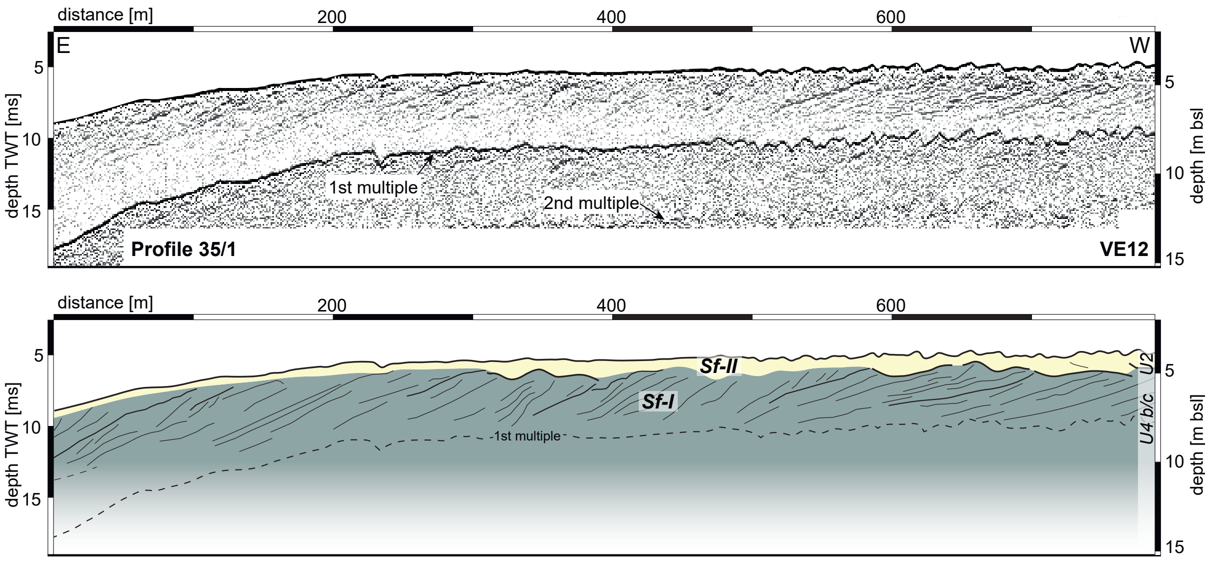

Fig. 3.5: SBP data obtained in the Old Świna River. The first and second multiple of the seafloor partly mask primary structures. Foresets of the here shown distal platform are lower inclined than in the central part of the spit. Truncation of foresets due to fluvial reworking.

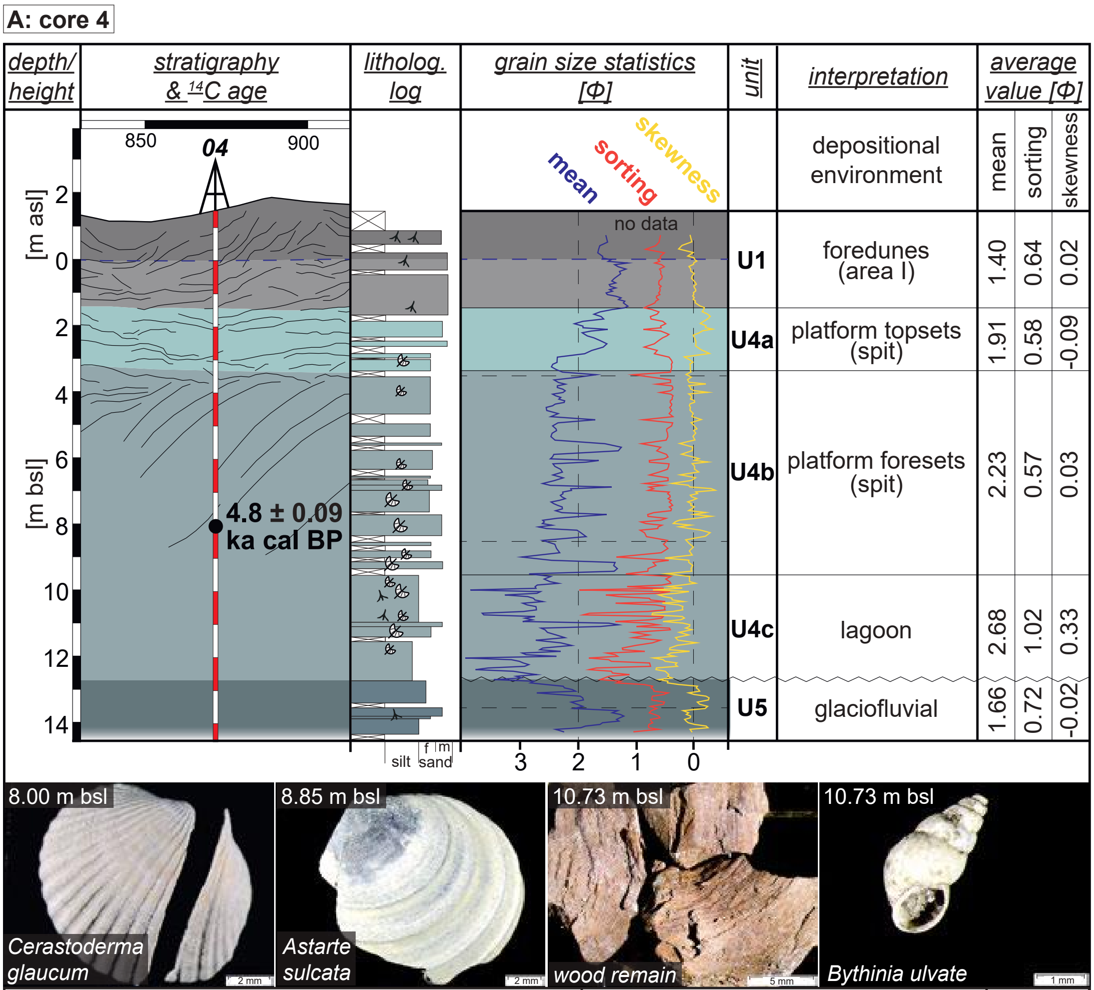

Radiocarbon dating						calibrated age [2-sigma range]			reservoir
Sample ID	Material	core depth [m]	depth bsl [m]	^{14}C age [ka BP]	^{12}C/^{13}C [o/oo]	calib curve (Reimer, P.J. et al, 2013)	range [ka cal BP]	median probability [ka cal BP]	ΔR [years]
SWINA-04_950	shell	9.5	8	4.37 ± 0.03	0.5	Marine13	4.68 - 4.86	**4.8 ± 0.09**	-200

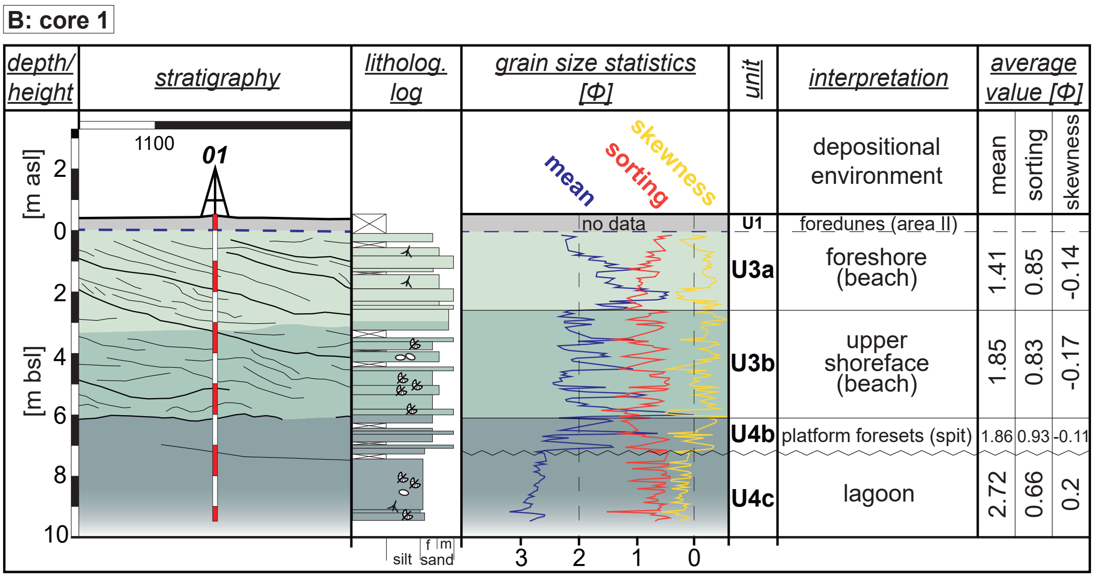

shells and shell fragments of mainly Cerastoderma glaucum ○ gravel
roots/ organic matter (wood/ reed) ● ^{14}C dating position

Unit 1 comprises two facies: up to 10° northward dipping reflections (F-I) which alternate with sub-horizontal to concave-up reflections (F-II). Both facies are partly separated from each other by bounding surfaces. Highest elevations (24 m asl) in the study area internally associate with steep (up to 30°) south-inclined reflections (F-III) (Fig. 3.7).

The top of U3 is linked to the groundwater table. The bottom of this unit descends towards the east from 4 m to 6 m bsl. U3 is characterized by high to medium amplitude GPR reflections, and is separated into the two sub-units U3a and U3b (Figs. 3.6 B, 3.7, 3.8). Unit 3a comprises up to 4° to the north inclined reflections (F-IV). At a depth of 2 m bsl in the eastern part and 3 m bsl in the western part of the barrier U3b is characterized by up 1.5° northward dipping reflections (F-V). The dipping angle of north-inclined reflections of U4b decreases from east to west from 1.5° to 2° in profile 20 to 0.5° in profile 14. The unit is characterized by a low signal-to-noise ratio in the GPR data.

Sediments of the units U3a and U3b are medium grained, with U3a being characterized by a general fining upward trend (Fig. 3.6 B). Sediments of both units are moderately sorted and negatively skewed. Shells occur from U3b to U4c and wood remains are scattered over the entire core length. Up to 3 mm large pebbles are common in the U3 and U4. Sediments of U4b are medium grained and moderately sorted. At a depth of around 7.5 m bsl the U4c grain size decreases and sediments are moderately well sorted and positively skewed.

3.5 Discussion

3.5.1 Sedimentary architecture of the Wolin barrier

A sedimentary model for the genesis of the Wolin foredunes is presented in figure 3.9. Figure 3.10 provides a coast-normal oriented cross section (A), a model of the sedimentary architecture (B) and a close-up of each building block (C) of the Wolin barrier system.

3.5.1.1 Nearshore zone

Three sedimentary units are distinguished in the nearshore area north of the Wolin barrier system (Figs. 3.3, 3.10). Up to 4 m deep cut-and-fill structures of the lower most U5 incise into irregular reflections, probably glacial tills. Prior to the Littorina transgression the south and west of the Pomeranian Bight and the Szczecin Lagoon belonged to the early post-glacial Oder river valley (Borówka et al., 2005). Cut-and-fill structures are therefore interpreted to reflect fluvial incision

Fig. 3.6: ←
Sedimentological analysis of core 4 (**A**) and 1 (**B**). Core 4 is located in area I and covers spit platform deposits. Core 1 is located in area II and comprises sediments of the beach plain. The interpreted GPR section with the core position and the lithological log are shown on the left side. Depths and heights are given in m asl and m bsl. Grain-size statistics and the depositional environment of each unit are given on the right side. Note that averaged values of each unit represent strongly varying single values; **A)** Examples of the fossil record and information to the radiocarbon dated shell found in 8 m bsl.

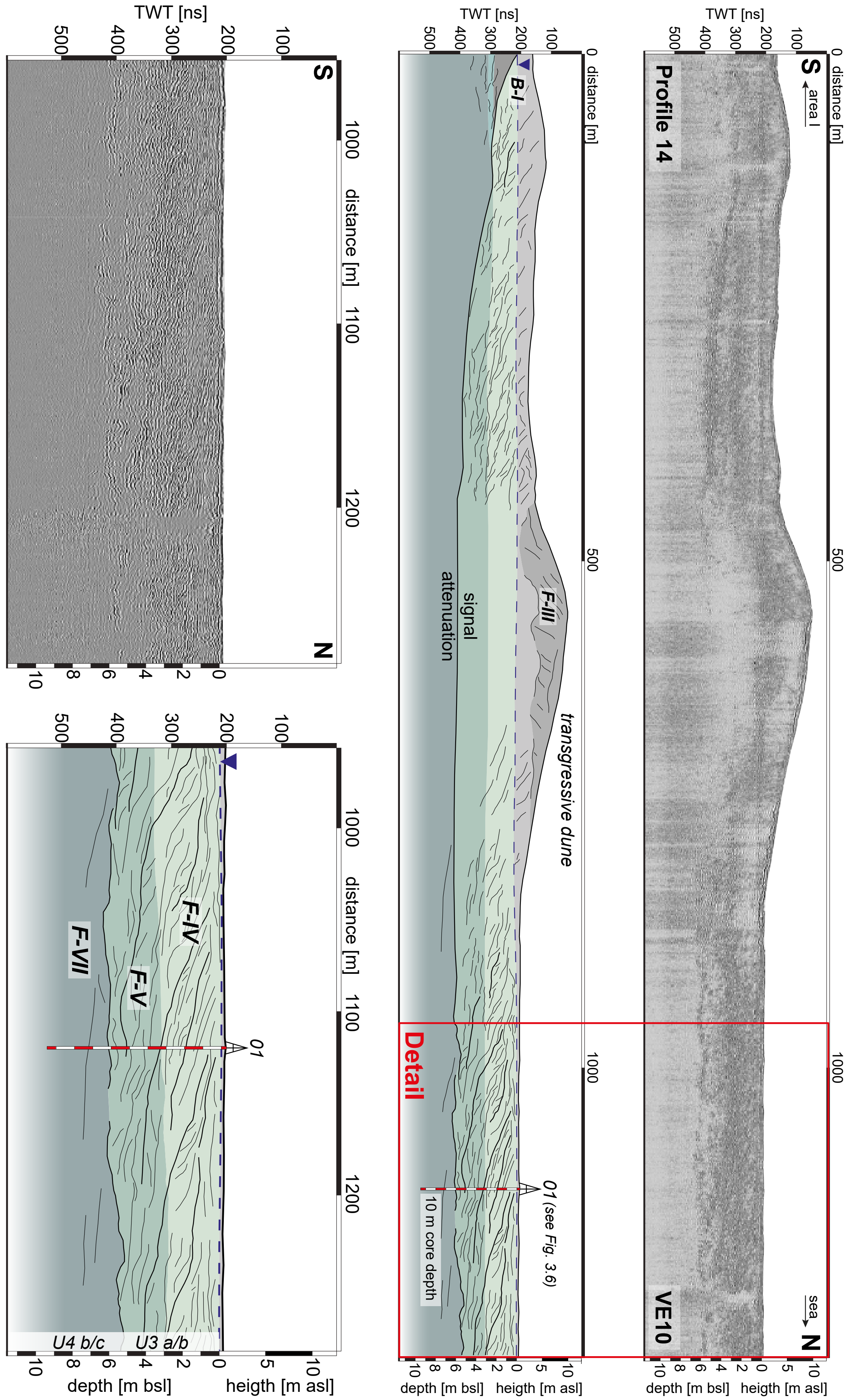

Fig. 3.7: GPR data from area II. Half way, signal attenuation in the barrier sediments is attributed to the presence of the transgressive dune above. A close up of the seaward part of the profile is shown below. The 10 m long core 1 includes sediments of the foreshore-shoreface and the distal spit platform.

into the late-glacial land surface. Cut-and-fill structures can not be correlated between the different profiles. This indicates a complex architecture of the river system, with several individual river channels. This interpretation is in accordance with studies by Borówka et al., (2005), who described the glacial and post-glacial development of the Szczecin Lagoon.

In the Pommeranian Bight, coarse grained glacio-fluvial sediments (U5) are unconformably overlain by up to 2 m thick fine-grained marine sands (U2), which often occur in patches (Schwarzer et al., 2003; Bobertz and Harff, 2004; Ostrowski and Purszak, 2011). Seaward inclined foresets (U4b) that occur in the southern part of the Pomeranian Bight are linked to the Wolin barrier and are interpreted to represent distal parts of their foreshore-shoreface sediments (Figs. 3.3, 3.10).

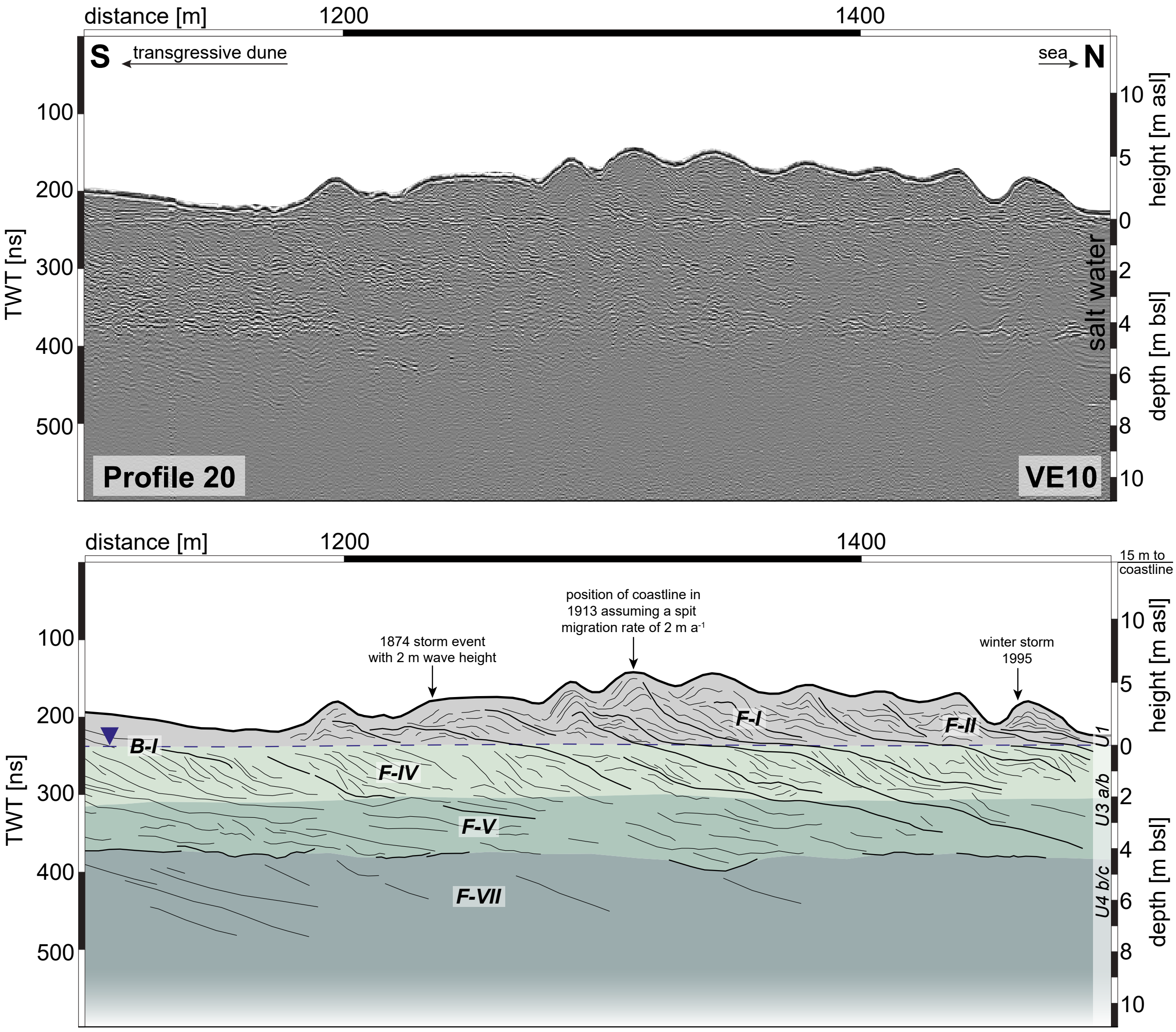

Fig. 3.8: GPR data obtained in area II. The internal architecture of foredunes is characterized by an aggrading to prograding pattern that is partly separated by erosional unconformities. Some of these unconformities reach down to the foreshore-shoreface succession and relate to observed storm events. The position of the coastline in 1913 is based on a migration rate of 2 m a^{-1} (Reimann et al., 2011).

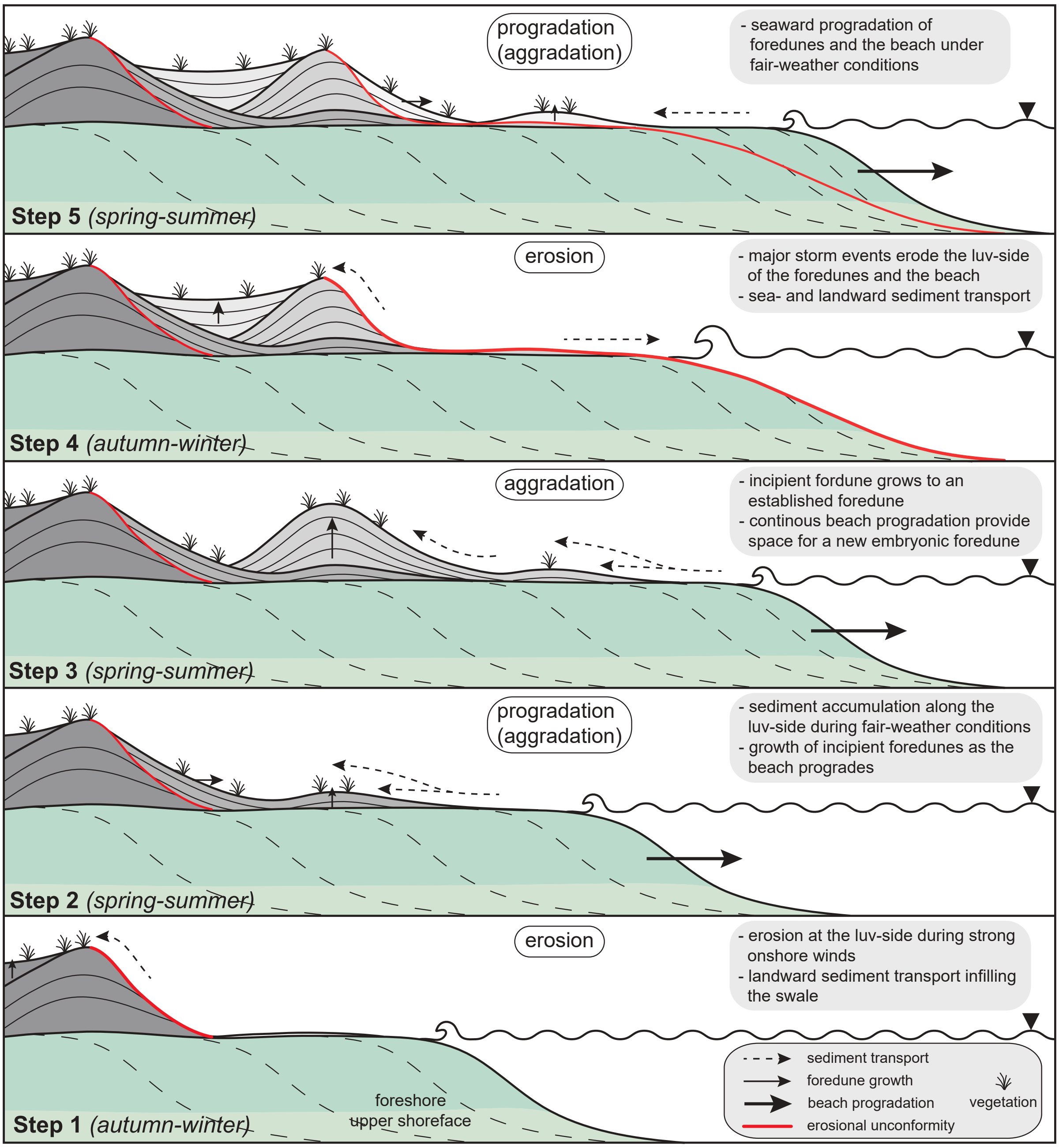

Fig. 3.9: Schematic model of foredune development. Accretion or erosion along foredunes is controlled by seasonal changing wind conditions. During spring strong winds oblique to the coastline transport sediment to foredunes trapped by vegetation (foredune growth) (steps 2, 3, 5). During autumn and winter strong winds coming from the north occur and erode the luv-side of the foredunes. Sediment is transported landward, accumulating in swales behind the foredune (step 1). Major storm events reach down and affect beach-plain deposits (step 4).

3.5.1.2 Foredunes

The internal architecture of the foredunes is shown in profile 20 which covers west-east striking dunes of area II (Fig. 3.8). The terminology used in this study for the description of foredune internal architecture follows Bristow et al. (2000), Bristow and Pucillo (2006), Hesp (2013) and Choi et al. (2014). Foredunes are internally characterized by seaward dipping (prograding) and sub-horizontal (aggrading) sedimentary beds (Fig. 3.9). Aggrading beds are partly separated from the prograding succession by a seaward-dipping unconformity. Some of these unconformities pass into bounding surfaces of the foreshore and upper shoreface (Figs. 3.7, 3.8). This internal architecture is consistent throughout the Wolin foredune ridge plain. Foredune development is closely linked to the progradation of the barrier as indicated by age dates (Fig. 3.6). Spit platform deposits of area I revealed an age of 4.8 ± 0.09 ka cal BP (this study); overlaying foredunes were dated to 4.68 ± 0.25 to 4.22 ± 0.30 ka BP (Reimann et al., 2011).

Łabuz (2013) found that growth of foredunes predominantly takes place in the spring and summer months during prevailing west winds that blow oblique to the coast and have the highest potential for aeolian sediment transport along the lower and middle part of the beach (Fig. 3.9 steps 2, 3, 5) (Arens, 1996b; Hesp, 2002; Rotnicka, 2011), whereas erosional processes prevail during autumn and winter due to strong onshore winds from the north (Fig. 3.9 steps 1, 4). These processes are described in the following.

Foredunes grow either under aggrading or prograding processes. Aggradation occurs when sand is trapped by vegetation at incipient foredunes (Fig. 3.9 steps 2, 3, 5). Progradation of foredune sedimentary beds occur when the dunes reach a certain height and sand predominantly accumulates in the lower part of the seaward foredune slope (Fig. 3.9 step 5). Arens (1996a) stated that at a certain foredune height wind deflection prevents further sediment transport to the crest, especially if the slope is vegetated. This limits the maximum height of foredunes and explains why a critical foredune height leads to sediment accumulation along the luv-side of the foredune resulting in seaward dipping sedimentary beds and a decrease of the effective slope angle. Foredune height in the study area is furthermore controlled by a combination of beach progradation rate and the potential aeolian sediment transport rate. As the result of a higher sediment transport rate along wide (dissipative) beaches, large foredunes are expected in the western part of the Wolin barrier where the beach width exceeds 100 m and during the summer months when beaches are wider (Davidson-Arnott and Law, 1996; Hesp, 2002; Schwarzer et al., 2003). However, the rapid prograding coast of the barrier (2 m a^{-1} after Reimann et al., 2011), which would result in the formation of low foredunes (Bristow and Pucillo, 2006), balances the effect of high sediment supply rate and results in foredunes up to 7 m high.

During the autumn-winter season erosional processes occur along the foredunes (Łabuz, 2013). Sediment removal is documented by erosional unconformities, accompanied with a steepening of the foredune luv-slope (Fig. 3.9 steps 1, 4). Erosion and slope steepening are attributed to strong onshore winds. The eroded sediment is transported to the dune crest and the lee-side of the foredune infilling the swale (Fig. 3.9 step 1) (Arens, 1996a; Łabuz, 2005a; Hesp, 2013). The degree of inter-seasonal morphological changes along the coast depends amongst others on the storm intensity (Ollerhead et al., 2013). Persistent or several closely spaced storm events affect also the foreshore and partly the upper shoreface (Figs. 3.8, 3.9 step 4). Wind conditions that generate water levels of 1 m asl cause major erosion along the beach and at foredunes up to 3.5 m asl and modify the coastline relief by a lowering of the beach profile (Schwarzer et al., 2003; Łabuz, 2013). In 1995 a storm resulted in a significant lowering of the backshore and beach relief (Łabuz, 2005; Furmańczyk, 2012). This event is interpreted to be imaged as a sub-horizontal reflection in the GPR data (Fig. 3.8). The highest water level so far, 2 m asl, was observed 1874 in Świnoujście. The coastal erosion attributed to this event is interpreted to be imaged in the GPR data as an erosional truncation (Fig. 3.8).

Following Łabuz (2013), after a 1 to 2 year period of incipient growth, new foredunes stabilize within 5 to 8 years. However, a higher storm frequency or intensified storm-wave activity may enlarge the time period of active foredune development. The effect of storms on foredunes also depends on the beach width (Ollerhead et al., 2013). This is visible in the eastern part of the Wolin barrier near the city of Międzyzdroje, where a small beach results in a higher storm impact on the foredunes. As a result, stabilized foredunes are absent and only incipient foredunes are present, which are frequently eroded (Fig. 3.1 B). By contrast, in the central part of the Wolin barrier the beach is wide and progrades with 2 m a^{-1} (Reimann et al., 2011). Linearly interpolated back in time, six foredune ridges developed within the last 100 years (Fig. 3.8). Consequently, the formation of one dune required 16 years in average in this area.

3.5.1.3 Spit (building block I)

Foredunes in area I unconformably overlay spit platform deposits that form the building block of the west-east extending Wolin spit. Sub-horizontal beds (unit U4a) interpreted as platform topsets merge at a depth of 3.5 m bsl into 7 m thick 2° to 6° westward inclined platform foresets (unit U4b) (Figs. 3.4, 3.10 B, C). The alongshore-parallel progradation of the spit is the result of sediment transport along the coast and sediment accumulation at the spit front where wave energy decreases (Davis Jr. and FitzGerald, 2004). Post-sedimentary reworking of spit-platform foresets is a dominant process in spit systems elsewhere and results from destabilization of the slope (slumping) or storm-wave impact (Nielsen et al., 1988; Mäkinen and Räsänen, 2003; Bristow & Pucillo, 2006). By contrast, there are only few erosional unconformities in the sediments of the Wolin spit (Figs. 3.4, 3.5, 3.10). The lack of strong erosion is attributed to the sheltered position of the Wolin spit and the small fetch of westerly winds, which both protected the active spit front from erosion. Atop platform foresets, platform topset develop under the influence of waves (Nielsen et al., 1988), and therefore lack a clear internal sedimentary bedding pattern. The mean wave base in the Pomeranian Bight is less than 2 m (Zhang et al., 2013). This depth correlates with the thickness of the Wolin spit topsets (2 m). Sediments of the platform topsets are negatively skewed (Fig. 3.6 A), a further indicator of high energetic conditions, which cause winnowing (Friedman, 1961; Chappell, 1967). There are no topset beds in the southern part of the spit. Here, platform foresets are covered by up to 1 m thick sediments of U2 that is interpreted as fluvial sediments of the Old Świna River. A reworking of former platform topsets in this part of the spit is therefore most likely (Fig. 3.5). The deepening of the top of U4 and the decrease in foreset dipping angle towards the

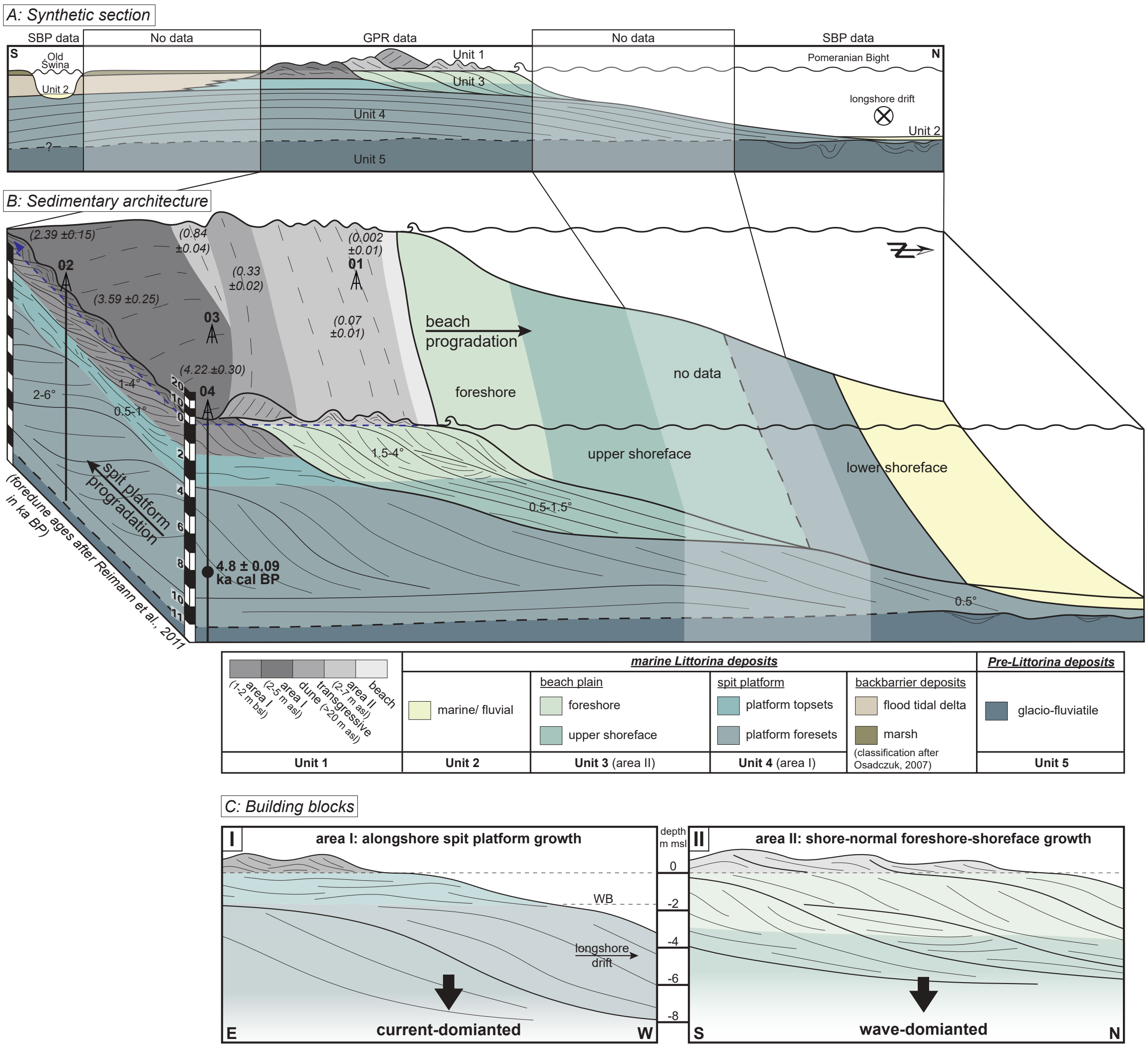

Fig. 3.10: Depositional model of the Wolin barrier system; **A)** The synthetic coast-normal oriented cross section of the barrier illustrates the position of the GPR and SBP obtained data; **B)** Block model of the sedimentary architecture: Foredunes of area I overlie spit platform sediments, prograding parallel to longshore currents towards the west. Note that the base of foredunes reach down to 1.5 m bsl. Foredunes of area II cover seaward – shore-normal – prograding beach-plain deposits. The transgressive dune covers foredunes of area I and II. Core positions and selected OSL ages (transferred into BP from Reimann et al., 2011) are shown. For areas where no data is available, different interpretation approaches are possible; **C)** The barrier system consists of two main architectural elements, named building blocks. The development of each block is either dominated by longshore currents or waves. Depths in m msl (mean sea level) refer to depths during deposition. The wave base (WB) in a depth of 2 m of the spit separates topsets from foresets.

north and south (Figs. 3.3, 3.5, 3.7, 3.8) is attributed to a focussing of sediment accumulation at the spit front and less sediment supply to the side of the spit.

Growth of the Wolin spit was towards the west, i.e. parallel to the mainland coast. Longshore currents are therefore seen as driver of spit progradation (Fig. 3.10 B, C). The impact of waves seem to be negligible as the wave base only reaches down to the base of topset beds and profound erosion of the spit platform front by storms was prohibit by its sheltered position (Nielsen et al., 1988; Mäkinen and Räsänen, 2003).

At a depth of 9.50 m bsl sediment changes to very fine grained, poorly sorted and positively skewed sands (U4c; Fig. 3.6 A). Unit 4c is not imaged in the GPR data due to signal attenuation; however their grain-size characteristics are distinctive for lagoonal deposits and indicate that the sediments were not transported for a considerable time or distance (Avramidis et al., 2008; Lima et al., 2013). The positive skewness is an indicator for the lack of winnowing (Friedman, 1961). Interbedded coarse-grained sand sheets are interpreted as storm layers caused by mobilization of larger grains under high energy conditions, probably as overwash sediments, comparable to lagoonal systems described from elsewhere (Sedgwick and Davis Jr., 2003; Donnelly et al., 2004; Buynevich and Donnelly, 2006; Switzer et al., 2006; Switzer and Jones, 2008). Below 12.50 m bsl medium to coarse grained sands are associated with an absence of marine shells (U5). This depth correlates well with cut-and-fill structures imaged in the SBP data (Fig. 3.3). Both, textural and architectural characteristics of U5 indicate a high energetic and non-marine environment, probably a fluvial system. There is a coarsening trend from unit U4c upwards to U1. Such a coarsening upward trend is characteristic for prograding non- and micro- tidal coasts (Ollerhead and Davidson-Arnott, 1995; Hoffmann et al., 2005; Garrison et al., 2010; Lindhorst et al., 2010). The mean grain size of the foredune sediments towards coarser grains compared to the spit (Fig. 3.6 A) is probably the result of aeolian winnowing under strong winds where small grains are transported further inland (Arens et al., 2002).

3.5.1.4 Beach plain (building block II)

In area II, the foredunes unconformably overlie sediments of a prograding beach plain. Beach-plain internal architecture is characterized by foreshore-shoreface clinoforms with up to 4° seaward-inclined foreshore beds (U3a) in the upper part down to 2-3 m bsl and less inclined (>1.5°) and less continuous beds of the upper shoreface (U3b) in greater depths (Figs. 3.7, 3.8, 3.10 B, C). At a depth of 5 m to 6 m bsl sediments of the prograding beach plain cover the distal foresets of the spit-platform sediments of the building block I (U4b) (Figs. 3.7, 3.8, 3.10 B). Medium to coarse and only moderately sorted sands of the distal spit platform change at a depth of 7.50 m bsl into fine grained and positively skewed sands, which reflect the low energy depositional environment of a lagoon (U4c). Swash bars are occasionally intercalated in the foreshore-shoreface clinoforms and indicate a landward migration of distinct sand bodies. The described geometry represents a typical foreshore-upper shoreface succession (Goy et al., 2003; Tamura et al., 2008; Barboza et al., 2013; Hein et al., 2013; Moulton et al., 2013). In the study area, sands of the foreshore and upper shoreface are moderately sorted and negatively skewed (Fig. 3.6 B), indicating a high energetic environment characterized by winnowing (Martins, 2003). Consequently, sediments of the foreshore and upper shoreface are regarded as being significantly reworked by wave energy (McCubbin, 1982). The observed fining upward within the foreshore is associated with a trend towards better sorting. Coarser grained sands accumulate in the lower part of the clinoforms where the slope inclination decreases; better-sorted sands are associated with steeper gradients in the upper part of the foreshore (McLean and Kirk, 1969).

The depositional environment of the foreshore-shoreface clinoforms that build up the beach plain of area II is dominated by waves and contrasts with the deposits of the spit platform, which deposited under the predominance of longshore currents and show only minor reworking (Fig. 3.10).

The seaward-directed progradation of a foreshore-shoreface succession in marco- to microtidal environments is attributed to fair-weather winds and abundant sediment supply (e.g. Jol et al., 2002; Goy et al., 2003; Dougherty et al., 2004; de Oliveira Caldas et al., 2006; Lindhorst et al., 2008; Clemmensen and Nielsen, 2010; Garrison et al., 2010; Hein et al., 2013). Landward inclined swash bars at the transition from the foreshore to the shoreface also develop during fair-weather conditions, but contribute only minor to the overall beach progradation. This contrasted with spit systems in the North Sea where swash bars are a major contributor to barrier progradation (Lindhorst et al., 2008, 2013) and probably reflects the lower wave energy in the Baltic Sea. However, the continuous progradation of the foreshore-shoreface clinoforms is interrupted by numerous unconformities that either truncate underlying beds or are characterized by downlap termination above (Figs. 3.7, 3.8). Unconformities are characterized by a lower inclination than foreshore-shoreface clinoforms and are interpreted to develop during periods of high wave energy, i.e. strong storms which predominantly occur during the autumn and winter months (Łabuz, 2005). This further underlines the strong wave impact onto the beach plain. The beach recovers after storms as it receives sand transported back onshore under fair-weather conditions predominating during the summer months (McCubbin, 1982; Łabuz, 2005; Tamura et al., 2012). Consequently, the shore-normal growth of the beach plain is characterized by an alternation of deposition and erosion showing a steep beach front during the summer months and a gentle beach slope during the winter according to Schwarzer et al. (2003). Only severe storms significantly affect and erode the shoreface-foreshore and thus it is hypothesized that not every storm is memorized in the sedimentary record. There is indistinct evidence that such high erosional events become more frequent in the younger part of the foreshore-shoreface succession (Figs. 3.7, 3.8). However, the available data set is partially incomplete due to signal attenuation in the subsurface and allows only for speculating a changed wind field towards more frequent or stronger winds during the last hundreds of years. Hünicke et al. (2015) found evidence for increased intensification of storm surges in some parts of the Baltic Sea within the last decades.

3.5.2 Holocene evolution of the Wolin barrier

3.5.2.1 Stage 1 (>6.5 ka BP)

The low base level prior to the Littorina transgression caused lowstand incision by the Oder river into the post-glacial subsurface (Fig. 3.11 stage 1). At a sea level position 10 m below the present level, during the Younger Dryas, the Oder river delta was located further north close to the Rügen Island (Lampe, 2005; Osdczuk, 2007). Up to 2 m deep depressions, developed from river incision, were filled accompanied with the onset of the Littorina transgression and the resulting flooding of the Pomeranian Bight (Fig. 3.3). The absence of basal peats within the study area is attributed to an early drowning of the Pomeranian Bight and erosion due to a rapid sea-level rise at the beginning of the Littorina transgression (Figs. 3.6, 3.11). This interpretation is corroborated by results of Lampe (2005) and Choi et al. (2014), who studied the partial erosion of glacial deposits and peatlands during a rapid marine transgression.

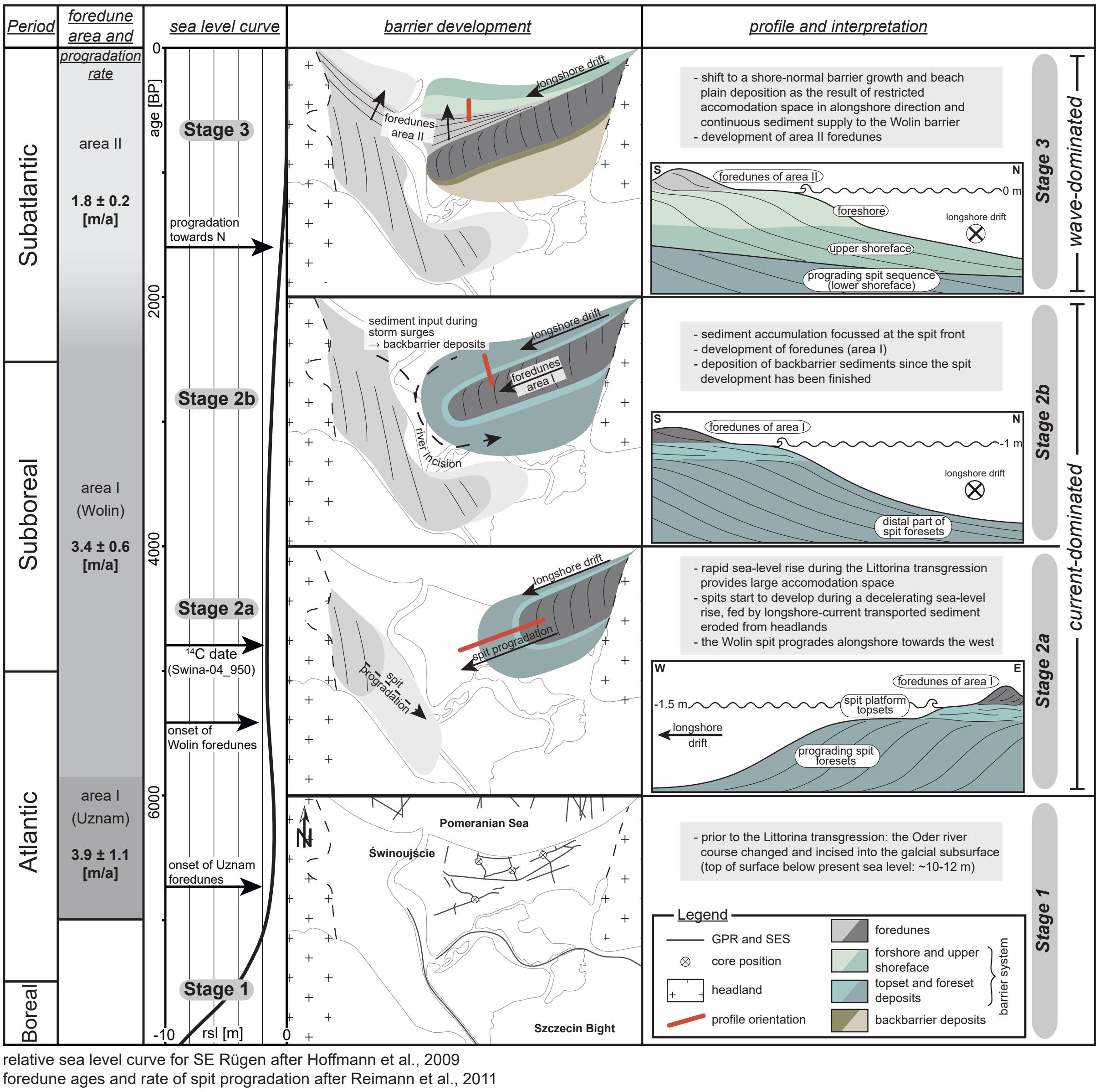

Fig. 3.11: Evolutionary model of the Wolin barrier in three steps. Prior to the Littorina transgression the Oder river incised into glacial deposits (**stage 1**). After the sea-level rise decelerated, spits developed under the predominance of longshore currents and were covered by N-S striking dunes (**stage 2a /b**). Backbarrier deposits accumulate on top of the distal spit platform in the south. A limited accommodation space and continuous sediment supply forced the barrier to prograde seaward, resulting in the deposition of wave-controlled beach-plain sediments (**stage 3**). The relative sea level curve used for this study was provided for Rügen (Hoffmann et al., 2009).

3.5.2.2 Stage 2a and 2b (6.5 – 2.5 ka BP)

The late Pleistocene to Holocene glacio-fluvial land surface is overlain by lagoonal fine sands accumulated behind a proto-barrier which preceded the present Wolin spit. This is comparable to systems described from the Canadian and Korean coast (Ollerhead and Davidson-Arnott, 1995; Choi et al., 2014). The presence of marine shells indicates a constant water exchange between the lagoon and the Baltic Sea.

Around 6.5 ka BP, the sea level reached a position 1 m to 2 m below the present level and the rate of sea-level rise decreased, giving space for the formation of barriers and spits along the southern Baltic Sea coast (Osadczuk, 2002; Hoffmann et al., 2005) (Fig. 3.11 stage 2a). The Uznam spit started to grow 6.56 ± 0.42 ka BP towards the east; growth of the westward-prograding Wolin spit began 5.33 ± 0.37 ka BP (Reimann et al., 2011; Zhang et al., 2013; Deng et al., 2014). Both spits are kept separated by the Świna Channel (the Oder river), which connects the Szczecin Lagoon with the Pomeranian Bight (Fig. 3.1). The Wolin spit continued its westward progradation until 2.39 ± 0.15 ka BP (Reimann et al., 2011).

Spit platform deposits are associated with north-south striking foredunes (area I) (Figs. 3.4, 3.10). The base of the foredunes represents the position of the sea level at the time of dune formation and therefore allows reconstructing past sea-level positions (van Heteren and van de Plassche, 1997; van Heteren et al., 2000; Goy et al., 2003; Bristow and Pucillo, 2006; Rodriguez and Meyer, 2006). The spit – foredune contact (marine – aeolian) in the GPR data indicates a sea level located 1.5 m below the present level between 5.33 ± 0.37 and 2.39 ± 0.15 ka BP (Figs. 3.4, 3.10 B). This is in accordance with published sea-level curves for the southern Baltic (e.g. Hoffmann et al., 2009) (Fig. 3.11 stage 2a-b). The spit – foredune contact elevates by around 0.80 m towards the western end of the spit platform. This is attributed to an incipient sea-level rise around 2.5 ka BP. The contact between foredunes of area I to area II is either concordant in the western part of the Wolin barrier or discordant in the eastern part (Fig. 3.1 D: c, d). This discordant contact is interpreted to result from a further northward extension of area I foredunes, which overlie the spit, subsequently eroded by longshore currents before deposition of beach plain deposits and area II foredunes. A phase of non-deposition or erosion is also indicated in OSL ages, which show a hiatus of around 400 years between the termination of spit progradation and the onset of beach-plain progradation (Reimann et al., 2011).

Backbarrier deposits accumulated south of the spit as a result of storm surges that raised the water level in the southern Pomeranian Bight and caused barrier overwash or upstream sediment transport in the Old Świna River (Musielak and Osadczuk, 1995; Osadczuk, 2002). The sediment was deposited in a low energy environment alongside the Old Świna River course and overlies the southern part of the spit platform (Figs. 3.1, 3.10, 3.11 stage 3). Backbarrier sedimentation in the area around the Old Świna River stopped since the construction of the artificial Piastowski canal in the late 19th century (Fig. 3.1 B) (Musielak and Osadczuk, 1995).

3.5.2.3 Stage 3 (< 2.5 ka BP)

Onset of foredune development on top of the beach plain (area II) is at about 1.66 ± 0.12 ka BP (Reimann et al., 2011). The shift in progradation direction from alongshore to shore-normal sediment accretion is attributed to the presence of the Uznam spit and the Świna Channel (river Oder) in the west, which restricted further westward-directed spit growth. As a consequence of continuous sediment supply, sand started to accumulate along the seaward flank of the existing spit (Fig. 3.11 stage 3) resulting in a change from current-dominated spit progradation towards a wave-controlled and seaward directed barrier growth. The change in the progradation direction also accompanies with a change in the progradation rate (Reimann et al., 2011). The Wolin spit prograded towards the west with a mean rate of 3.4 m a^{-1}, whereas the northward-directed progradation of the beach plain averages to 1.8 m a^{-1} (Fig. 3.11). The lower progradation rate of the beach plain is attributed to a greater reworking of sediments, especially during storms, shown by numerous unconformities in the sedimentary record. By contrast, only the seaward flank of the spit suffered erosion during strong onshore winds. The eroded sediment was transported by longshore currents towards the spit front resulting in an additional sediment supply for the continuous spit progradation.

An up to 24 m high transgressive dune covers foredunes of area I and area II (Fig. 3.1 C, D). 10° to 30° south-inclined foresets indicate a landward dune migration (Fig. 3.7). (Re-)activation of such landward migrating dunes is attributed to higher wind speeds during the Little Ice Age (LIA) (Aagaard et al., 2007; Buynevich et al., 2011). The transgressive dune formed between 0.39 ± 0.02 and 0.32 ± 0.03 ka BP as the result of increased (summer) storminess during the LIA.

3.6 Conclusion

Based on an amphibian data set comprising geophysical on- and offshore-data as well as sediment cores, a stratigraphic and evolutionary model of the Wolin barrier system has been presented. The Wolin barrier system is nourished with sediment from adjacent headlands by shore-parallel longshore currents. The system consists of two genetic units: a coastparallel prograding spit composed of spit platform deposits and seaward-prograding foreshore-shoreface foresets of a beach plain. Formation of the spit is seen as the result of alongshore sediment transport, whereas the beach plain shows a dominance of wave-related deposition. Reorganization of the barrier system and subsequent start of beach-plain progradation occurred between 2.39 and 1.66 ka BP, as the result of limited accommodation space towards the west that hindered further spit growth. Only severe storm events erode sediments along the foreshore and shoreface and are preserved in the sedimentary succession as unconformities. Increased erosion of beach-plain deposits in perpendicular progradation direction results, compared to the spit sediments, in a progradation rate of the beach plain being only half the rate of spit-growth.

Beach sediments of the barrier are unconformably overlain by aeolian foredunes which show a N-S strike on the Wolin spit and E-W striking crests on the beach plain. The internal architecture of the foredunes is characterized by aggrading and prograding beds, partly truncated by erosional unconformities. Foredune growth is seen as the result of sediment trapping by vegetation. Sediment aggrades at incipient foredunes that grow in height. Subsequent seaward foredune progradation relates to a certain foredune height which is controlled by the beach progradation rate and the potential aeolian sediment transport rate. During the winter months strong onshore winds erode the foredunes. Factors that control dune erosion are vegetation coverage, wind velocity and direction, and beach width.

The presented data show that the predominance of either longshore currents or waves during barrier formation correlates with the development of distinct sedimentary geometries. Spits form parallel to the coastline under the influence of longshore currents; whereas beach plains prograde perpendicular to the present coastline in seaward direction, reworked by waves. Here, the re-organization of the coastal sedimentary system is attributed to limitations in accommodation space.

Chapter 4

Architecture and development of a transgressive barrier system – the role of aeolian sedimentation in barrier development (Łeba, Poland)

Abstract

The stratigraphic architecture and evolutionary history of the transgressive barrier system of Łeba, located off the polish Baltic Sea coast, is presented. Ground-penetrating radar (GPR) data and sediment cores show that landward barrier migration is dominated by overwash processes and by the infill of subaerial and subaquatic accommodation space by aeolian sediments.

Barriers along the southern Baltic Sea formed on top of glacio-fluvial sediments contemporaneous with the deceleration of sea-level rise since the younger Atlantic, around 6 ka BP. In the study area, Holocene sediments comprise marine lagoonal sands, washover, and dune deposits. Fine-grained lagoonal sands deposited in an environment protected by a barrier located further seaward. Washover deposits overlie the lagoonal sands and consist of proximal sub-parallel beds that pass into distal landward dipping foresets. Washover foresets developed when coast-eroded sediment entered a standing water body. They are associated with mound-shaped beds that represent the central part of washover fan deposits. The sediment was transported landward and into the lagoon through overwash throats, morphological depressions within the barrier. Different washover generations that are separated from each other by an unconformity are attributed to a change in the overwash-throat position. Shells of freshwater molluscs indicate barrier stabilization since the early Subboreal, between 5 and 4 ka BP. Barrier stabilization was accompanied with an increase in barrier height by dunes and limiting overwash processes into the lagoon.

First transgressive dunes appear around 3.3 ka BP. The upper most sedimentary unit of the barrier comprises steep landward inclined foresets bounded by sub-horizontal beds. Foresets represent preserved bottom-sets of dunes that migrated into the lagoon. Sub-horizontal beds developed when active dunes are separated from the lagoon and when sand was blown into the lagoon during strong onshore winds. During periods of absent aeolian activity the lake shoreline was stabilized by vegetation. Today, dunes migrate on top of the barrier and partially into the lagoon. This shows the direct coupling between aeolian activity and landward barrier progradation.

4.1 Introduction

Holocene barriers developed worldwide where coasts were inundated due to the global sea-level rise and sediment was available to be transported alongshore. The occurrence of barrier systems is accompanied with a straightening of the coastline (Davis Jr. and FitzGerald, 2004; Falqués, 2006; Hein et al., 2013) which can also be observed along the southern Baltic Sea coast. Sea-decoupled lagoons develop when barriers are attached to the mainland at both sides (Otvos, 2012). Waves and tides play a predominant role during the formation of barrier systems. Wave-dominated barriers are long and narrow with only few inlets, which tend to be unstable in size and location; washover fans are a building block of these systems (Davis Jr., 1994). Barriers are classified into progradational, aggradational or transgressive barriers according to the preserved facies associations (Reading and Collinson, 2007). The stratigraphy and evolution of transgressive Holocene barrier systems was intensively investigated based on sediment cores (Dillenburg et al., 2004; Hoffmann et al., 2005) combined with ground-penetrating radar (e.g. Buynevich and FitzGerald, 2003; Møller and Anthony, 2003; Costas et al., 2006; de Oliveira Caldas et al., 2006; Lima et al., 2013) and by aerial images and historic charts (Buynevich and Donnelly, 2006; Donnelly et al., 2004; Forbes et al., 2004). Roy et al. (1994) stated that transgressive barriers are linked to coasts with a low topographic gradient and represent sediment bodies that are in equilibrium with the rising sea level due to the permanent landward transfer of sand eroded from the shoreface. Overwash sedimentation is the main process that maintains the landward movement of the coastline. This cannibalistic process conserves the coastal eroded sediment volume which results in a retrogradational stacking pattern of the sedimentary units (Cattaneo & Steel, 2003). Overwash events are associated with storms, but are considered at the same time as a quasi-continuous process in shaping barriers (Davis Jr., 1994; Sedgwick and Davis Jr., 2003; Donnelly et al., 2004; Forbes et al., 2004; Switzer et al., 2006; Wang and Horwitz, 2007). Washover deposits were studied to investigate the sedimentary architecture (Schwartz, 1982; Horwitz and Wang, 2005) and to extract information about the frequency or intensity of storms and tsunamis (Switzer et al., 2006; Switzer and Jones, 2008). The impact of storms and the redistribution of sediment from offshore erosion to overwash deposits strongly depend on the barrier morphology (Morton and Sallenger, 2003; Houser et al., 2008). Well-developed and closely-spaced foredunes or backbarrier dunes reduce overwash into the lagoon. However, the intensity and duration of storm surges relative to the barrier elevation and the vegetation cover are, besides others, controlling factors affecting the grade of morphological barrier destruction and washover penetration (Morton, 2002; Morton and Sallenger, 2003).

Transgressive barriers are often associated with an aeolian dune field on top of the barrier, which represents a late stage of barrier formation (Bailey and Bristow, 2004; de Oliveira Caldas et al., 2006; Buynevich et al., 2007b; Dillenburg et al., 2013). Coastal dune fields evolve either directly from the backshore or develop due to foredune destruction (Hesp, 2013). The application of radiocarbon dating and optical-stimulated luminescence dating allows to determine time periods of dune movement, often associated with a change in wind conditions towards more stormy conditions (Clemmensen et al., 2001a; Wilson et al., 2001; Clemmensen and Murray, 2006; Reimann et al., 2011; Costas et al., 2012).

This study aims to unravel the architecture and genesis of a transgressive barrier system by means of ground-penetrating radar (GPR) and sedimentological data.

4.2 Study site

The study area is located at the polish Baltic Sea coast, west of the village Łeba. The Baltic Sea is a semi-enclosed intracontinental sea that is affected by glacio-isostatic rebound since the last deglaciation (Fig. 4.1 A). Vertical crustal displacement along the southern coastline started 17 ka ago; today, a subsidence of up to 1 mm a^{-1} is recorded for the area around Łeba (Kowalczyk, 2006;

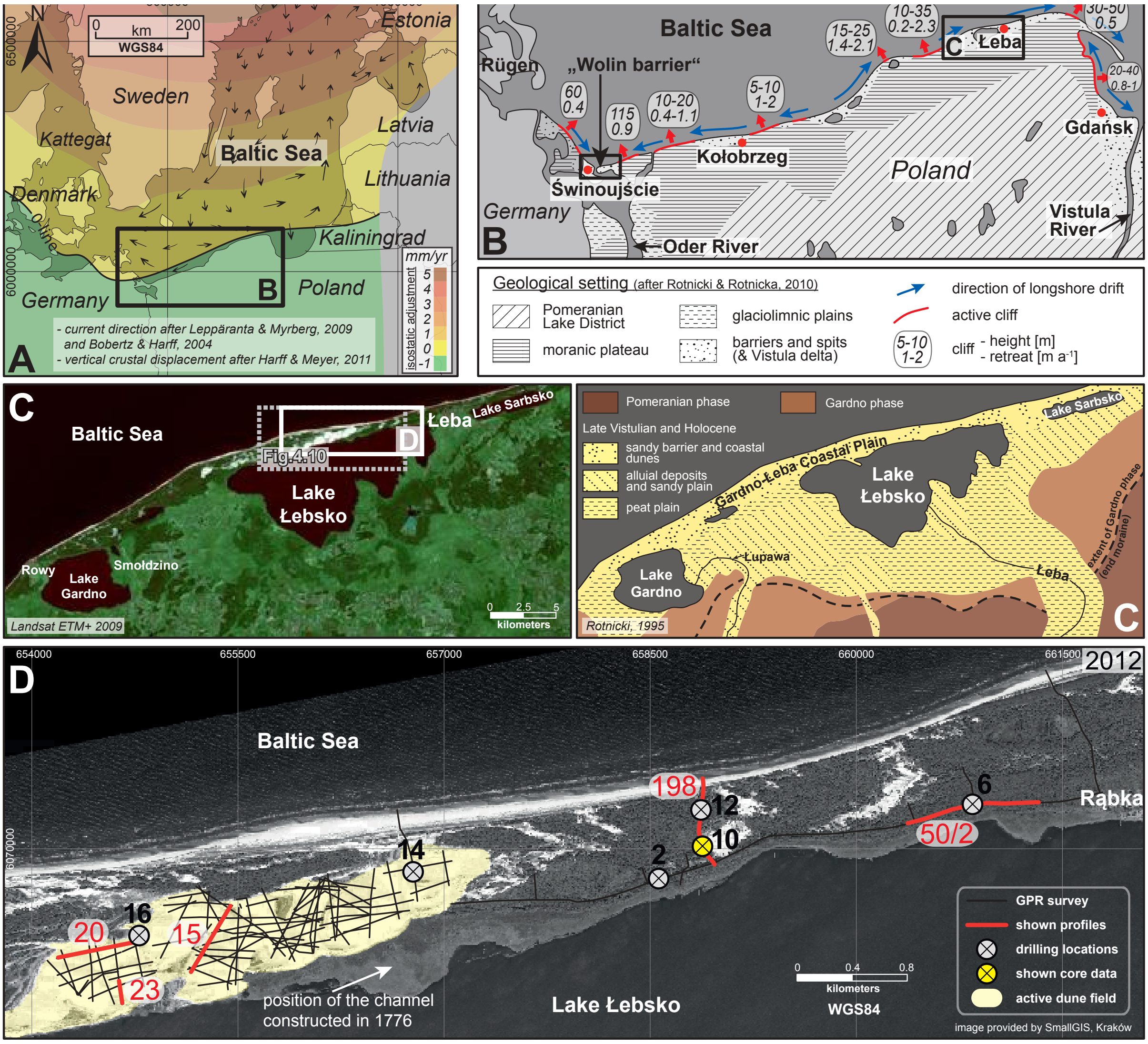

Fig. 4.1: A) Southern Baltic Sea with the surface current direction. At present, the Polish Baltic Sea coast is attributed to subsidence. Increase of uplift rates towards the north of the Baltic Sea; **B)** Geological setting of north Poland with given cliff heights at the coast and rate of retreat. Longshore currents distribute eroded moraine material east- and westward direction; **C)** Location of the studied barrier enclosing the Lake Łebsko. The geological map shows the maximum ice sheet advance in the area during the Gardno phase and sandy Holocene deposits; **D)** GPR survey and core position. Red lines indicate profiles shown in this study; Out of six cores the presented core data is indicated by yellow.

Harff and Meyer, 2011; Uścinowicz, 20014). Hydrodynamics of the tide-less Baltic Sea is dominated by complicated meso-to-large scale wind-driven currents and local wind-induced waves (Zhang et al., 2013). Alongshore currents transport eroded Pleistocene moraine material along the coast, which accumulates to barriers and spits, often enclosing former embayments (Rotnicki and Rotnicka, 2010). The largest polish lake along the Baltic Sea coast is the Lake Łebsko; with an average depth of 2.3 m (max. 6.3 m) (Wojciechowski, 1995) (Fig. 4.1 C). The lake is separated from the sea by the WSW-ENE oriented 17 km long and 0.5 to 1.6 km wide Łeba barrier which belongs to the Gardno-Łeba coastal plain. The present beach has a low gradient and is locally up to 150 m wide, seasonally alternating between dissipative and reflective (Rotnicka, 2011). Foredunes, 4 m to 15 m high, occur only along the coastline, whereas the backbeach area is covered with active migrating dunes up to 27 m high that migrate towards the east and partially into the lagoon of Lake Łebsko (Fig. 4.1 D). Psammophytes and pine trees, the dominating vegetation, restrict sand export from the beach to the dunes (Borówka and Rotnicki, 1995a).

The development of the study area before the Littorina transgression reached the area is characterized by the deposition of fluvial sands that are partly overlain by a thin early Holocene peat layer (Rotnicki et al., 2009). Glacio-fluvial sediments deposited during the last cold period, the Gardno phase, when the sea level was 60 m lower (Rotnicki and Borówka, 1995; Tomczak, 1995a). The late glacial sands and peats represent the basement of the sandy Łeba barrier at 10-12 m depth (Borówka, 1990), and were inundated at the beginning of the Littorina transgression (8 – 6.5 ka BP) during a period of rapid sea-level rise with a rate of up to 1.5 cm a^{-1} (Tomczak, 1995a; Hoffmann and Lampe, 2007). Barrier sediments started to accumulate during the Atlantic period (after 6.5 ka BP), under the circumstances of a decelerating sea-level rise (Uścinowicz, 2006; Rotnicki et al., 2009; Rotnicki & Rotnicka, 2010). The Łeba barrier comprises Holocene marine sediments and sands deposited in a freshwater lagoon (Rotnicki et al., 2009; Wojciechowski, 2011). At the onset of barrier development a high molluscan-species diversity coincides with highest salinity values (12-15 ‰) (Wojciechowski, 2011). *Cerastoderma glaucum* is the prominent species during the Littorina stage (7.5 ka to 4 ka BP). During the early Subboreal species composition changed towards freshwater-dominated taxa. Since 4 ka BP *Theodoxus fluviatilis* is most common during the lower Lymnea stage and *Valvata piscinalis*, *Bithynia tentaculata* and *Lymnea peregra* dominate the upper Lymnea stage (Wojciechowski, 2011). The sea level at the beginning of the Subboreal was 2.5 m lower than at present and under a declined rate of sea-level rise to less than 0.5 mm a^{-1} a marsh plain developed (Uścinowicz, 2006; Rotnicki et a., 2009). Between 4.5 ka and 3 ka BP the barrier reached its present position and first dunes appeared (Borówka, 1990; Rotnicki et al., 2009). During the past 3000 years the sea level rose with a mean rate of 0.3 mm a^{-1} to 0.25 mm a^{-1} and approached the present state 200-100 years ago (Uścinowicz, 2006).

Today, the Łeba barrier is covered by an extensive active dune field that migrates parallel to the coastline (Fig. 4.1 D). As documented by palaeosols, phases of dune activity and stabilization were reconstructed (Borówka, 1975, 1990, 1995). Dune migration occurred during the younger Holocene during the time periods 4 ka to 3.5 ka BP, 3.3 ka to 2.5 ka BP, 1.5 ka BP and since the 15th century. The initiation of the latest stage of dune mobilization was probably triggered by human activity around the Łeba town and harbour (Borówka, 1990 and 1995). The eastward migration of the dunes is attributed to predominating westerly to south-westerly winds (Rotnicka, 2011; see chapter 5). Strong onshore winds from north and northeast occur during the winter months and cause erosion not only at cliffs, but also along sandy barriers (Borówka and Rotnicki, 1995a; Schwarzer et al., 2003). A strong storm surge destroyed the village Łeba in 1570. Today, fossil trees and paleaosols crop out along the Łeba beach and indicate continued coastal retreat (Borówka and Rotnicki, 1995b). In the year 1776 a channel between the Lake Łebsko and the sea was built for the purpose of land improvement (melioration), but abandoned some years later after a severe storm surge (Fig. 4.1 D).

4.3 Methods

4.3.1 Ground-penetrating radar (GPR)

The internal architecture of the Łeba barrier was imaged in the years 2012 and 2013 by means of a Geophysical Survey Systems Inc. (GSSI) SIR-3000 ground-penetrating radar (GPR) equipped with a 200 MHz antenna. The radar-wave velocity was estimated based on the shape of diffraction hyperbolas to 0.065 m ns^{-1} for the water-saturated barrier sediments and to 0.13 m ns^{-1} for the overlying dry sands. Vertical time-inverted depths are given in meter (m) below the present sea level (bsl). Topography along GPR lines was obtained by either a Leica GS09 differential GPS or a theodolite when the GPS-signal coverage was insufficient.

GPR raw data was processed using the software Reflex-Win (v7.1.6, Sandmeier, 2013). Post-processing include static correction, subtract-mean (dewow), 1D-filter (time-independent), background removal, migration, and gain correction. Seismic interpretation concepts after Mitchum Jr. et. al (1977) were adopted for the interpretation. Radar facies are bound by radar surfaces and represents distinctive reflection patterns, differing in reflection shape, inclination, continuity, and amplitude (Gawthorpe et al., 1993; Neal, 2004).

4.3.2 Sediment cores and ^{14}C-dating

Sediment cores were obtained in the year 2014 along the GPR profiles using 1 and 2 m long sampling tubes of 36 mm and 50 mm in diameter. Incomplete core information is the result of sediment compaction or wash-out during coring. A visual core description and sediment sampling in a 5 cm interval was performed in the field. In the lab, the sediment was prepared with H_2O_2 and acid in order to remove organic and calcitic components. The spectrum of the grain-size distribution was determined with a Sympatec Helos KF Magic laser particle-size analyzer. Gradistat (Blott and Pye, 2001) was used to calculate the grain-size statistics, which is based on the graphical method (Folk and Ward, 1957) and provided in logarithmic phi values.

The age model for the Łeba barrier is based on dating of shells and paleaosols using radiocarbon. Radiocarbon dating was performed by Beta Analytic Miami Inc. (USA). Conventional ^{14}C-ages were calibrated using Calib 7.0.4 (Stuiver and Reimer, 1993) and the Marine13 calibration curve (Reimer et al., 2013). A ΔR of -200 years was applied following the recommendations of Lougheed et al. (2013).

4.4 Results

4.4.1 Architecture

The sedimentary architecture of the Łeba barrier was studied based on 52 km of GPR data. Five genetic units (U0 to U4) encompass eight radar facies (F-0 to F-VII) (Fig. 4.2). Three major bounding surfaces were distinguished based on different radar facies above and below (B-I to B-III). Sedimentary architectural elements of each unit are presented in figure 4.3.

The GPR profiles 20, 15, 50/2, 198 and 23 were chosen to document the internal architecture of the barrier (Figs. 4.4, 4.5, 4.6, 4.7, 4.8). Grain-size statistics and organic components were provided from sediments of the 11 m long core 10 (Fig. 4.9), which reaches down to 10 m bsl and covers all five genetic units.

The lowermost U4 is characterized by low inclined and low amplitude reflections, embedded in a reflection free or chaotic reflection pattern (F-VII) (Figs. 4.4, 4.5). The sand-size sediment is coarse-grained and moderately sorted. Unit 4 is partly truncated by a high amplitude and horizontal to wavy reflection (B-III) at a depth of 8 to 10 m bsl. At a depth of around 9.50 m bsl there is a 10 cm thick horizon of sand enriched with decayed plant remains.

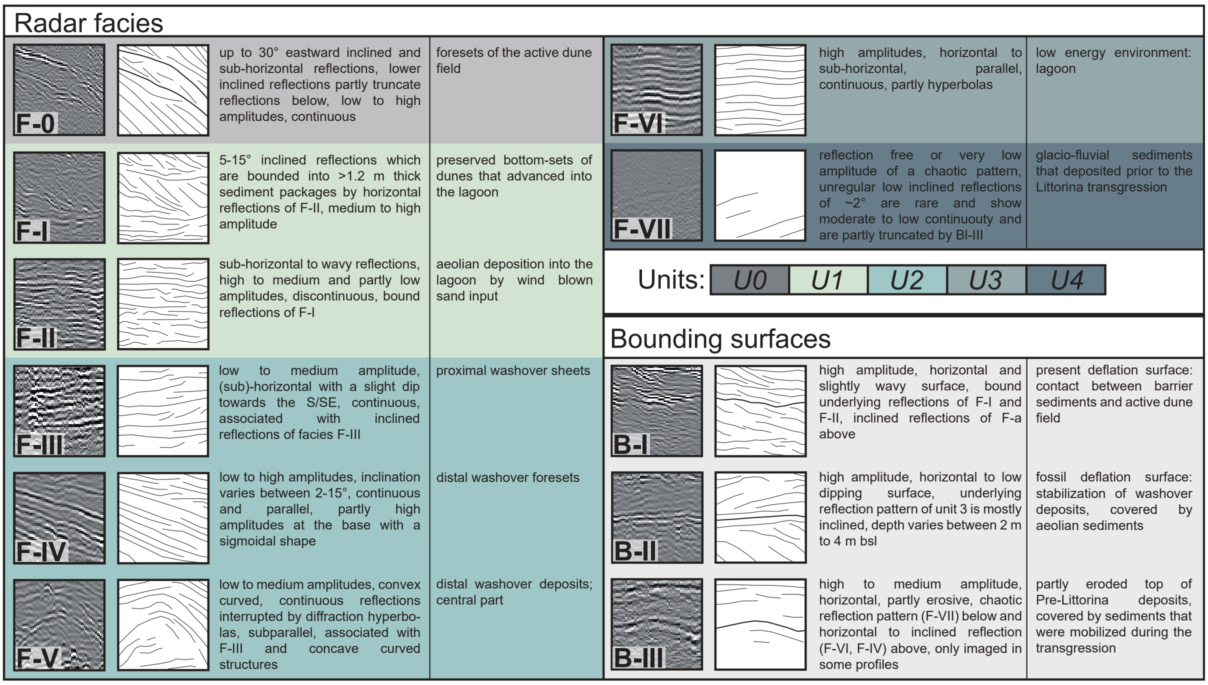

Fig. 4.2: Radar facies (F) and bounding surfaces (B) identified in the GPR profiles. Note a vertical exaggeration of 5 for 10 or all shown profiles. Given dipping angles are corrected.

Unit 4 is overlain by U3, characterized by high amplitude, horizontal, and continuous GPR reflections (F-VI) (Figs. 4.4, 4.7). The thickness of U3 ranges from a few centimeters to 4 m and thins towards the south. Unit 3 extends from 7.40 m to 9.90 m bsl and is composed of coarse silts, which are very poorly sorted, and positively skewed (Fig. 4.9). Beds of coarser grained sands are intercalated in the fine grained sediments of U3. Macrofossils are shells and shell fragments of *Cerastoderma glaucum* and others (after Ziegelmeier, 1966).

Unit 3 is conformably overlain by U2 that comprises three different radar facies, each present either in the northern or southern part of the barrier. The northern part of the barrier is characterized by sub-horizontal reflections which slightly dip to the south/southeast (F-III) (Figs. 4.5, 4.7). In the southern part, shore-normal oriented profiles image reflections dipping 15° to the south (Figs.

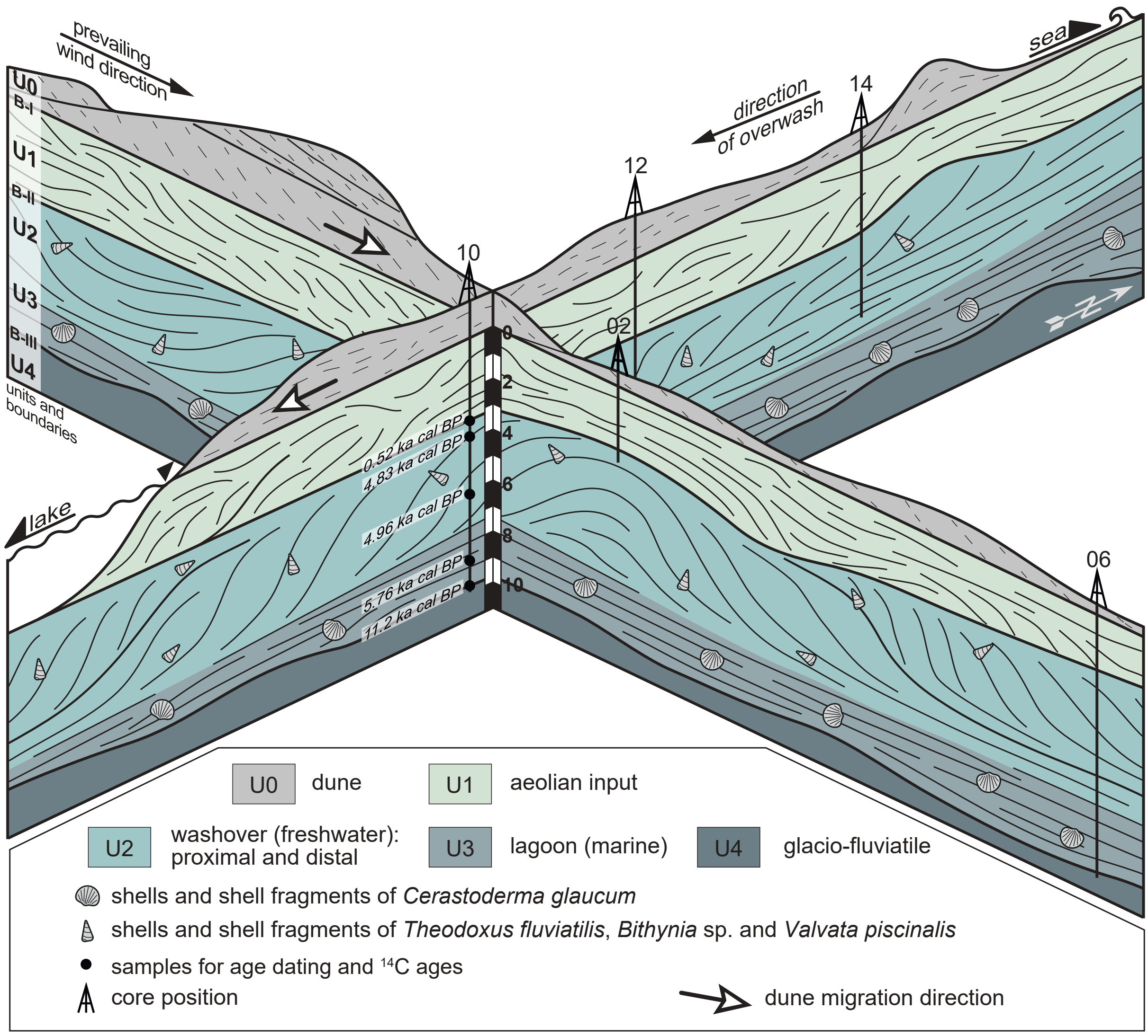

Fig. 4.3: Architectural elements of the Łeba barrier integrated in a sedimentary model. The barrier comprises four units (U1-U4). Marine and freshwater shells indicate environmental conditions at a certain time of barrier development. Age assessment of the barrier succession is based on radiocarbon dated shells and soils sampled from core 10. Dune (U0) movement on top of the barrier is controlled by the prevailing wind direction. The deflation surface is determined by the ground-water table that resembles the sea level.

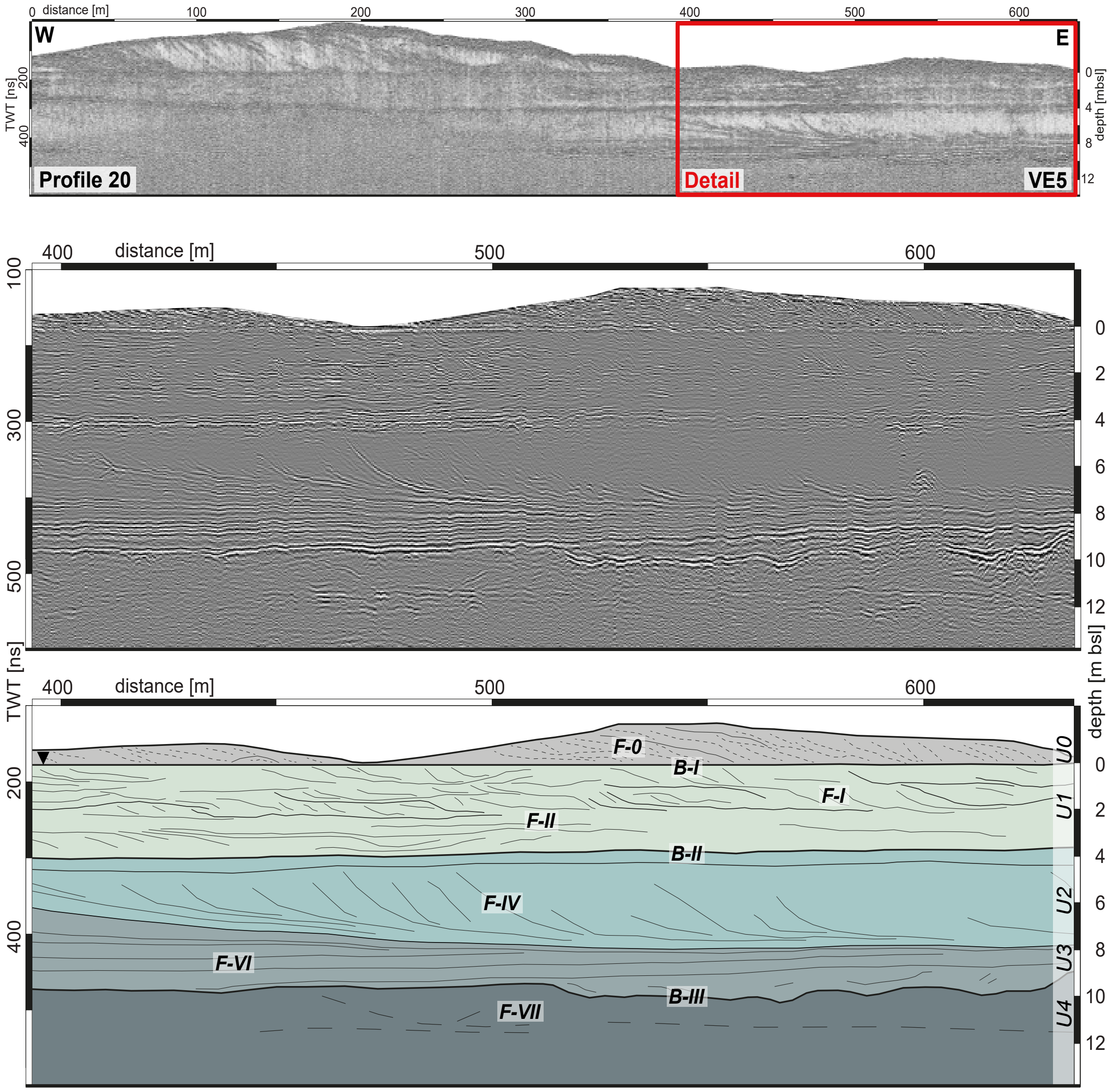

Fig. 4.4: Coast-parallel aligned GPR profile 20 comprises of U0 – U4. Overall eastward dipping beds indicate a predominant migration of the barrier towards the east. Foreset packages of U1 represent preserved bottom sets of dunes that migrated into the lagoon.

4.5, 4.7, 4.8). Reflections in shore-parallel aligned profiles dip with an angle of up to 15° either towards the west or to the east (F-IV), with the eastward-dip being most prominent. East- and westward inclined reflections are associated with up to 80 m wide convex-curved reflections (F-V) (Fig. 4.6). In the southern part of the barrier, the lower part of U2 is characterized by (very) fine-grained, poorly sorted and positively skewed sands (Fig. 4.9). The sediment texture changes in the upper part to fine- to medium-grained sands which are well sorted and slightly negatively skewed. Shells and shell debris of *Valvata piscinalis* and *Theodoxus fluviatilis* are the dominant macrofossils of U2. *Bithynia* sp. is less common (after Ziegelmeier, 1966). The radar surface B-II terminates U2 towards the overlaying sediments at depths between 2 m and 4 m bsl. This surface is associated with a 10 cm thick horizon of sand enriched with decayed plant remains, which is only missing in the cores 2 and 12.

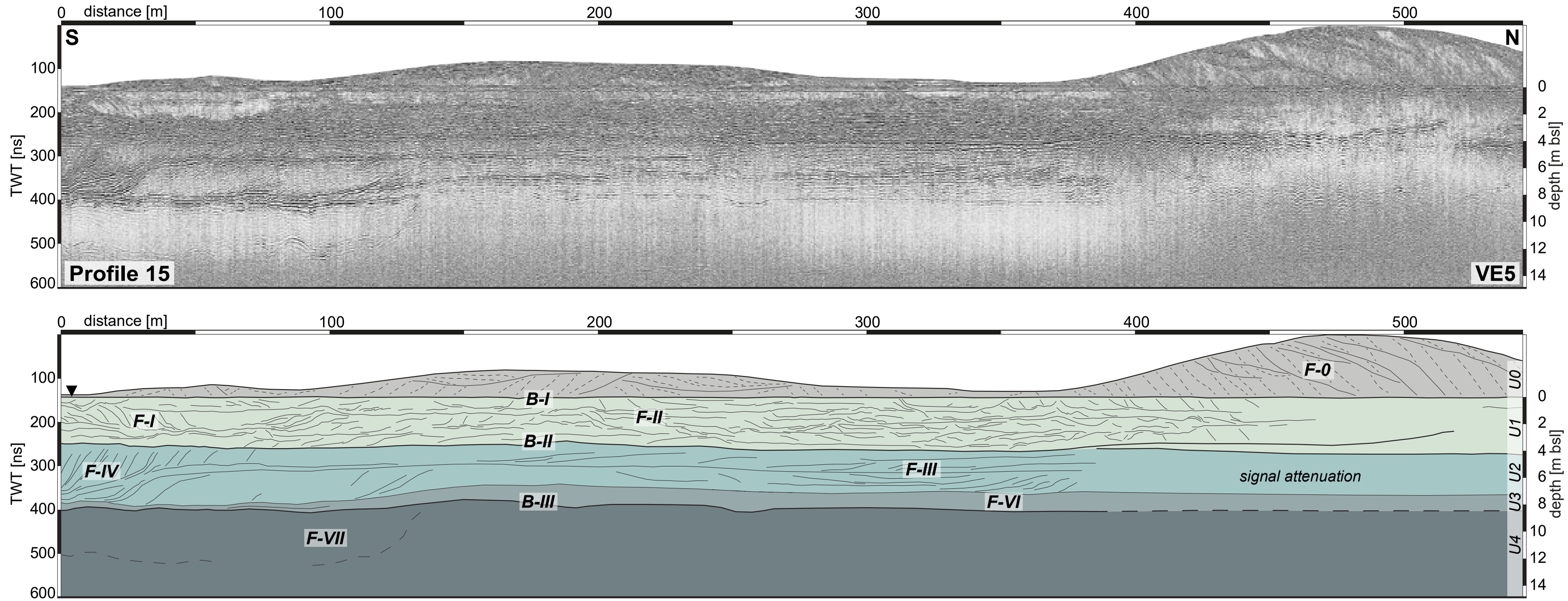

Fig. 4.5:
GPR profile 15 oriented perpendicular to the present coastline. Sub-parallel beds of proximal washover in the northern part of U2 are associated with southward inclined foresets of distal washover in the south.

Fig. 4.6:
GPR profile 50/2 oriented parallel to the coast. Foresets (F-IV) of U2 dipping to the east and west are associated with convex shaped beds (F-V) of the central washover fan. Sediments of core 6 comprises the units U1 to U4.

Fig. 4.7:
Coast-perpendicular aligned profile 198. Unit 4 is not resolved in the data due to decreasing signal-to-noise ratio with increasing depths. The contact U3 - U4 was determined based on core data. The 11 m long core 10 reaches down to 10 m bsl and covers all units (U0-U4). Results of the sedimentological analysis are presented in figure 4.9.

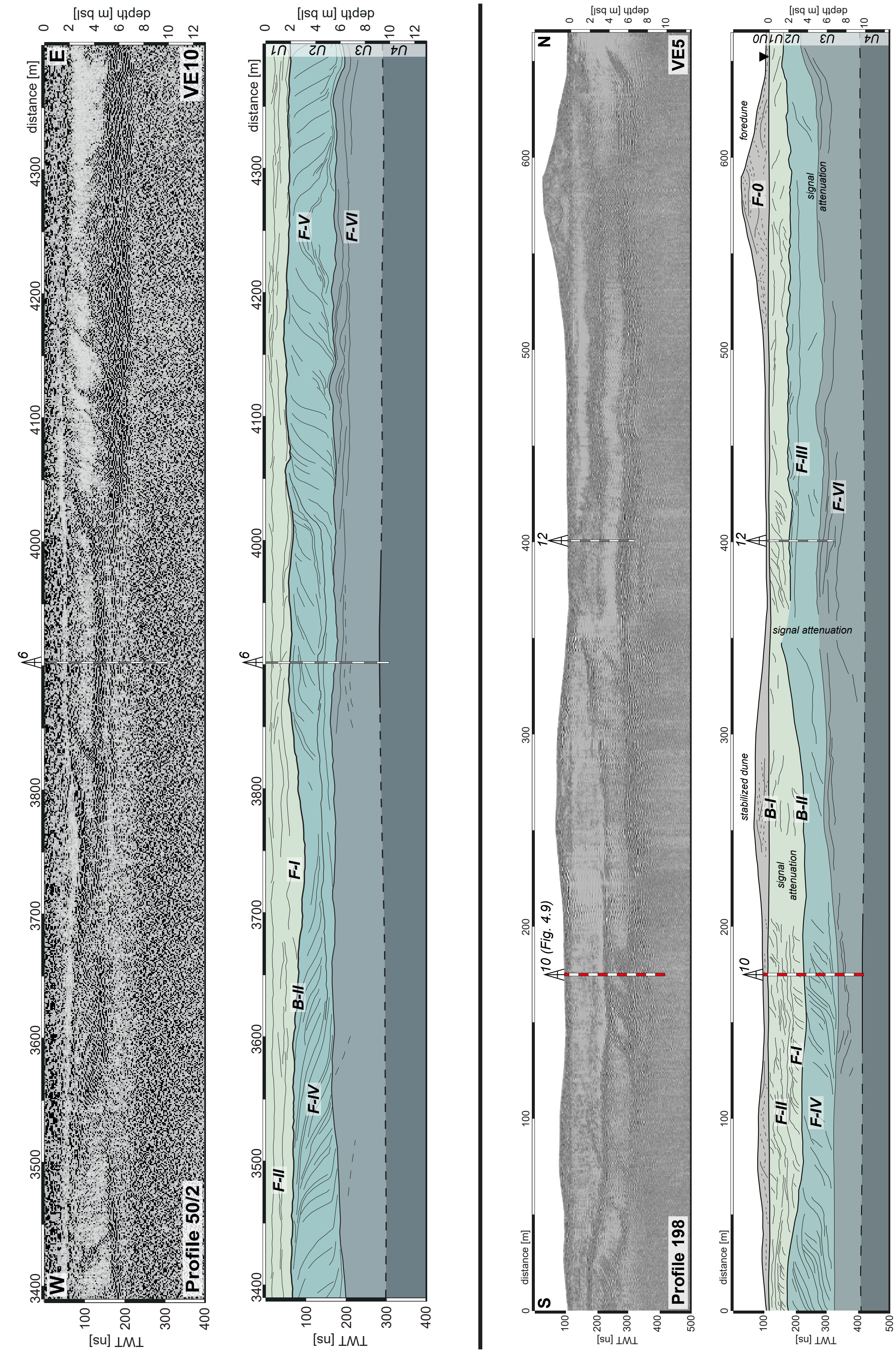
Profile 50/2
VE10
W
E
distance [m]
TWT [ns]
depth [m bsl]
U1
U2
U3
U4
F-I
F-II
F-IV
F-V
F-VI
B-II
Profile 198
VE5
S
N
U0
foredune
stabilized dune
signal attenuation
F-0
F-III
B-I
10 (Fig. 4.9)
12
6

Unit 1 shows sub-horizontal to wavy reflections (F-II), that bound south-east (5° to 15°) inclined reflections into 1.2 m thick sediment packages (F-I) (Figs. 4.4, 4.7). Landward dipping reflections of high amplitude partly truncate this reflection configuration (Fig. 4.8). Sands of U1 are medium-grained, well sorted and slightly negatively skewed. Light brown fibre remains occur between 1.50 m and 1.80 m bsl. Remains of wood and reed occur throughout the entire sedimentary succession of the spit, but predominate in U1. A horizontal high amplitude surface (B-I) terminates U1 on top. Overlying sediments of unit U0 show eastward-inclined and sub-horizontal reflections (F-0).

Out of core 10 three shells (*Cerastoderma glaucum* at 8.72 m bsl, *Valvata piscinalis* at 5.87 m bsl and *Valvata piscinalis* at 3.76 m bsl) and sediments from two organic-rich horizons (depths 9.91 and 3.38 m bsl) were dated using AMS ^{14}C (Tab. 4.1).

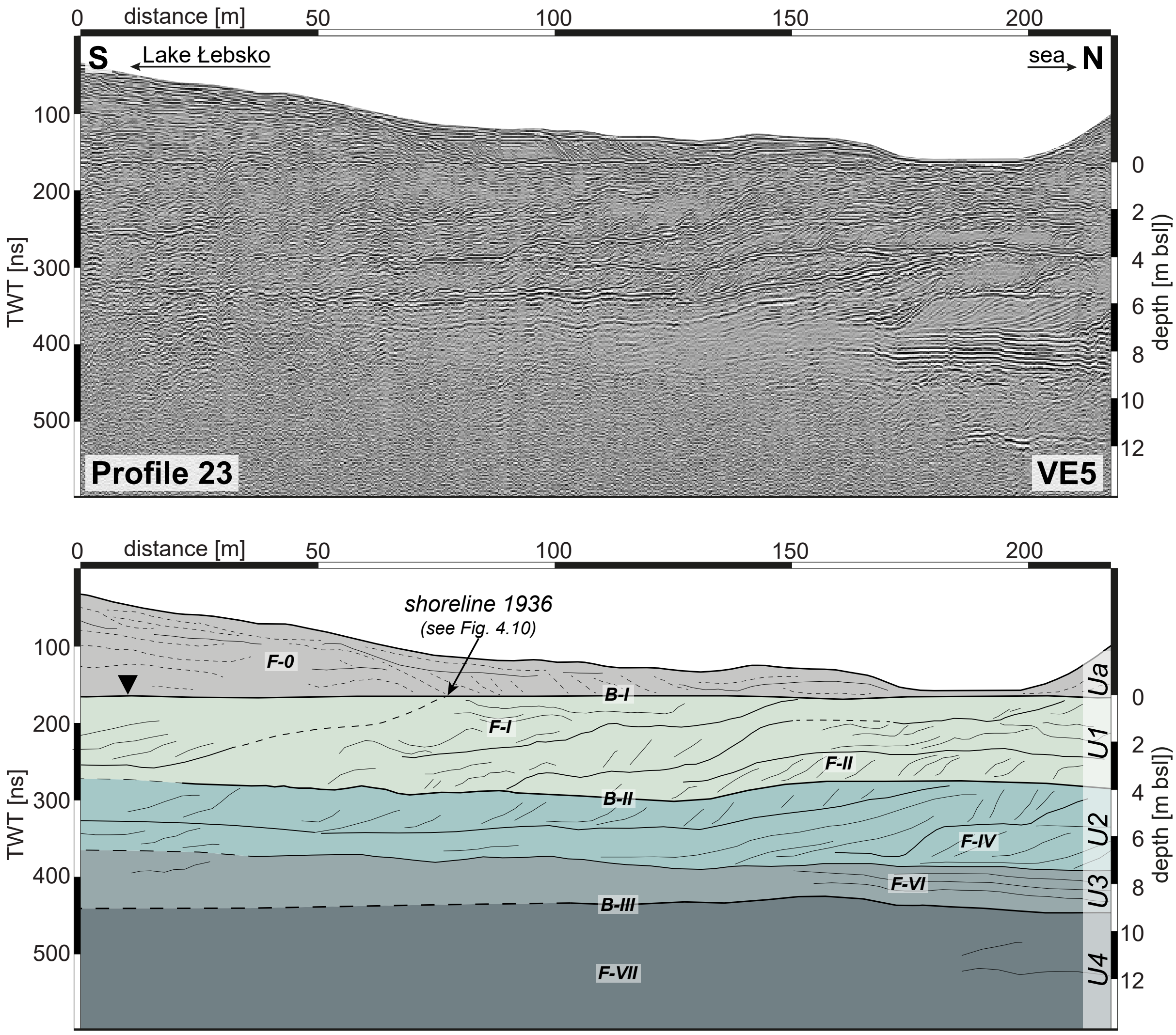

Fig. 4.8: The shore-perpendicular aligned GPR profile 23 shows southward dipping foresets of distal washover and foresets of preserved dune bottom sets. To the south inclined surfaces in U1 truncate foresets and indicate a stabilized shoreline of the lagoon at time periods without aeolian sediment influx into the lagoon.

4.4.2 Geomorphology

Figure 4.10 A shows the location of the barrier coastline in the years 1936 and 2012. The shoreline facing the sea retreated, whereas the position of the lake shoreline moved towards the south. In the area shown, the barrier experienced a net-growth of about 1.06 km² (8.8 %) between 1936 and 2012, whereby a loss of 0.474 km² towards the open sea contrasted with a growth of 1.535 km² towards the lagoon. Barrier growth towards the south shows a lateral variability and is highest close to the present active dune field (Figs. 4.1, 4.10).

The coastline of the Gardno-Łeba coastal plain strikes SW-NE in its western part (C1) and WSW-ENE in the east (C2) (Fig. 4.10 B). The active dune field is located along the C2 coastline. Transgressive dunes further to the east (downwind) and west (upwind) are stabilized. Vegetated dune arms strike parallel to the prevailing wind direction coming from the west and indicate a migration direction of the transgressive dunes towards the east, an observation which is corroborated by the internal geometries. Vegetated dune arms along C1 have an oblique orientation to the coastline, whereas dune arms along C2 are almost coast-parallel oriented.

4.5 Discussion

The sedimentary architecture of the Łeba barrier is presented in figure 4.3. Barrier development through time comprises four stages and is presented in figure 4.11.

4.5.1 Sedimentary architecture

4.5.1.1 Unit 4 (glacio-fluvial sediments)

Sediments of U4 are interpreted as glacio-fluvial sediments, accumulated prior to the Littorina transgression. This interpretation is in line with Rotnicki et al. (2009), who attributed sands below 8.40 m bsl to a glacio-fluvial environment of the Late Vistulian (13-11.7 ka BP). Glacio-fluvial deposits of U4 are unconformably overlain by a palaeosol, dated to 11.2 ka cal BP (Fig. 4.9, Tab. 4.1). Such horizons of organic-enriched sands are a general feature before Holocene sediments of the Gardno-Łeba coastal plain developed (Tomczak, 1995a; Rotnicki et al., 2009).

4.5.1.2 Unit 3 (marine, lagoonal sediments)

Sediments of the Pre-Littorina phase (U4) are covered by very fine grained, poorly sorted and positively skewed sands (U3) (Fig. 4.9). These characteristics indicate a sediment accumulation in a low-energy depositional environment, most likely a lagoon (Avramidis et al., 2008; Lima et al., 2013). In this context, the poor sorting demonstrates a short transport distance (Avramidis et al., 2008). The positive skewness is seen as an indicator for the absence of winnowing, which would be indicative for waves or currents (Friedman, 1961; Duane, 1964; Martins, 2003). The interpretation of U3 as lagoonal deposits is further corroborated by the well-stratified and horizontal sedimentary bedding of these sediments (Figs. 4.4, 4.6, 4.7, 4.8). The marine macro fossil *Cerastoderma glaucum* indicates a permanent water exchange between the Baltic Sea and the lagoon. The described conditions are best matched by a lagoonal system sheltered by sandy shoals or an incomplete barrier located further seaward. This facies interpretation is supported by comparable transgressive barrier systems elsewhere (e.g. Davis Jr. et al., 2003; Hein et al., 2012; Lima et al., 2013).

Beds composed of coarse grained sand are intercalated in the fine grained lagoonal deposits. These sediments are indicative for the mobilization of barrier sand during ephemeral periods of increased wave energy, most likely during storms (Fig. 4.8). Comparable deposits in the northern part of the barrier were interpreted as overflows of marine waters during storms and periods the lagoon had a better connection to the sea (Rotnicki et al., 2009). Thickness of U3 sediments decreases from north to south from 4 m to a few centimeters, further indicating a N-S directed sediment transport.

4.5.1.3 Unit 2 (freshwater, washover sediments)

Lagoonal sediments of U3 are conformable overlain by sediments of U2. The internal sedimentary architecture of U2 varies from north to south. A sub-parallel and low-inclined bedding in the northern part of the barrier (Figs. 4.4, 4.6) contrasts with 2° to 15° landward-dipping concave or convex curved beds in the southern part (Figs. 4.4, 4.5, 4.6, 4.7).

Sediments of U2 are interpreted as washover fans. Aggrading parallel-bedded sediments close to the present day sea are interpreted as the proximal part of washover fans, whereas steep landward- (south-) inclined foresets in the southern part of the barrier represent the associated distal deposits. The sigmoidal shape of distal washover sediments is the result of sediment input into a standing water body, the lagoon, and the subsequent generation of a subaqueous washover delta (Wang and Horwitz, 2007). Comparable proximal to distal successions of washover deposits were described from transgressive barriers worldwide (e.g. Schwartz, 1982; Héquette and Ruz, 1991; Davidson-Arnott and Fisher, 1992; Møller & Anthony, 2003; Neal et al., 2003; Horwitz and Wang, 2005; Costas et al., 2006; Garrsison Jr. et al., 2010). In shore-parallel GPR lines, distal washover foresets are associated with mound-shaped bedding patterns (Fig. 4.6). These are interpreted as the central part of washover fans. In the study area, eastward-dipping foresets dominate. This is attributed to the prevailing westerly winds which control the direction of near-surface currents. Unconformities imaged by GPR are characterized by a different dipping of washover foresets above or below and are interpreted to separate two different washover generations. The switch

sample ID	material	core depth [m]	depth bsl [m]	^{14}C age [ka BP]	$^{12}C/^{13}C$ [o/oo]	calibrated age [2-sigma range] calib curve (Reimer et al., 2013)	range [ka cal BP]	rel. area u. distribution	median probability [ka cal BP]	reservoir Δ R [years]
LEBA-10_438	plant material	4.38	3.28	0.49 ± 0.03	-26.5	Intcal13	5.01 - 5.45	1	0.52 ± 44	0
LEBA-10_476	shell	4.76	3.66	4.23 ± 0.03	-4.6	Intcal13	4.81 - 4.86	0.577	4.83 ± 50	0
LEBA-10_687	shell	6.87	5.77	4.40 ± 0.03	-6.1	Intcal13	4.87 - 5.05	0.991	4.96 ± 181	0
LEBA-10_972	shell	9.72	8.62	5.39 ± 0.03	-2.7	Marine13	5.31 - 6.21	1	5.76 ± 891	-200
LEBA-10_1091	organic sediment	10.91	9.81	9.71 ± 0.03	-29.0	Intcal13	11.10 - 11.22	1	11.16 ± 121	0

Tab. 4.1: Results of radiocarbon dating. Local reservoir correction of ΔR = -200 years only for the marine sample.

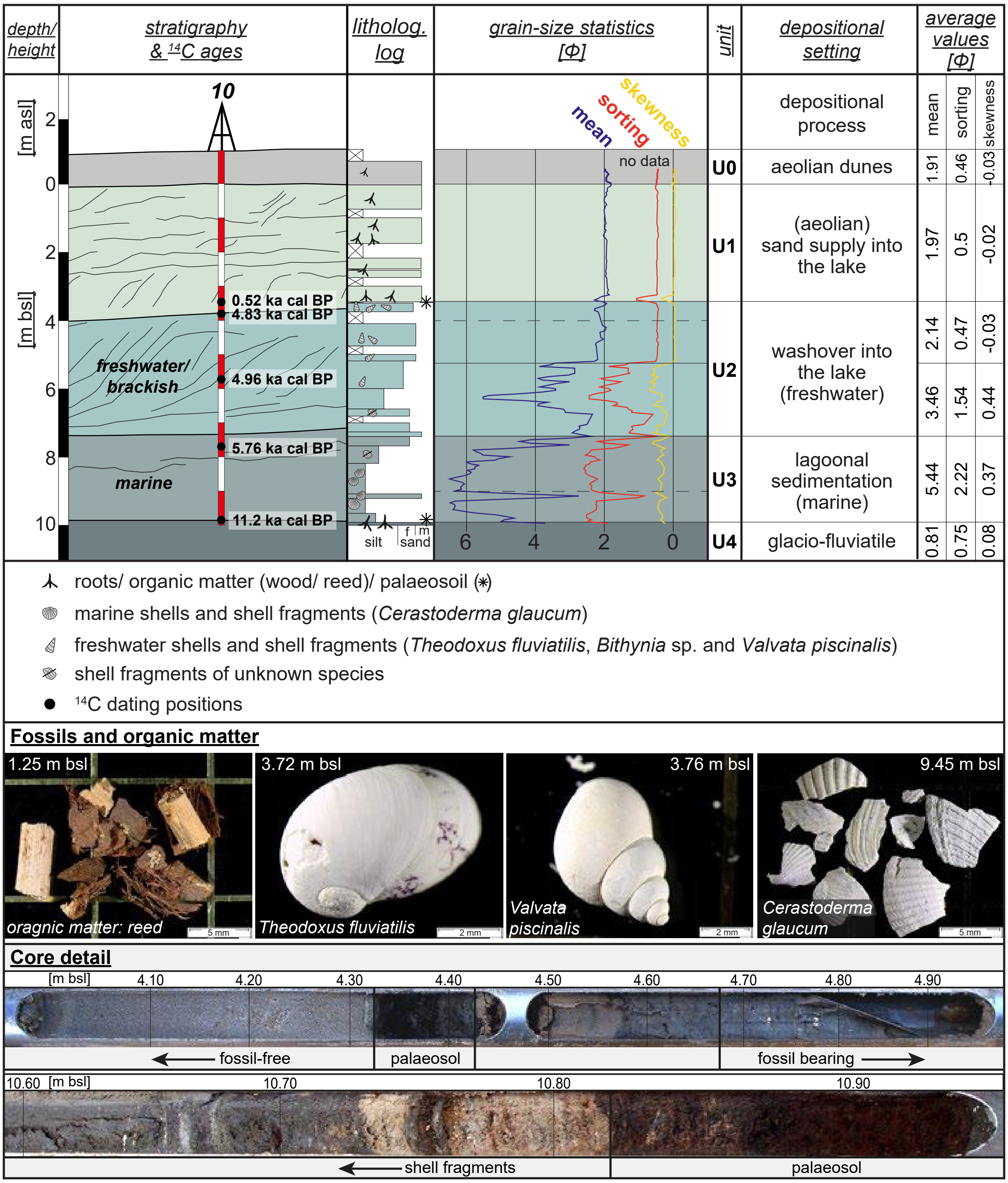

Fig. 4.9: Sedimentological results of core 10. In the upper part, the depositional setting of each unit is based on GPR-based barrier stratigraphy linked to sedimentological characteristics. Note that phi-values given at the right partly average strongly varying single values. Ages given are based on radiocarbon dated shells and soils (see Tab. 4.1). The change from marine (U3) to freshwater (U2) shells indicate changed environmental conditions. In the lower part, core details are shown.

from one generation to the other is either attributed to a shift of the overwash throat location or calm periods accompanied by a stabilization of the shoreline.

Washover sediments represent a major building block of the Łeba barrier. This is comparable to numerous transgressive barrier systems elsewhere, where washover sediments were described as significant contributor to the sediment budget of barrier islands and important factor in maintain the barrier width during landward migration (e.g. Schwartz, 1982; Leatherman and Zaremba, 1987; Davidson-Arnott and Fisher, 1992; Roy et al., 1994; Morton, 2002; Buynevich and Donnelly, 2006; Donnelly and Sallenger, 2007; Wang and Horwitz, 2007; Matias et al., 2008).

Sediments of the distal parts of the washover fans vary in grain size (core 10, Fig. 4.9). The lower part of U2 (8.40 m to 6.20 m core depth), representing the bottom-sets of the washover foresets, is dominated by medium to fine grained sands. This grain-size spectrum is interpreted to result from an alternating accumulation of lagoonal fine grained background sedimentation and the input of medium grained sands by overwash. The positive skewness indicates absence of waves or currents, comparable with deposits of U3. By contrast, the upper part of U2 (6.20 m to 4.40 m), representing the steep inclined foresets, are composed of medium-grained and well-sorted sands. The better sorting is directly linked to the steep inclination of the foresets, as good sorting is associated with step gradients (McLean and Kirk, 1969). The freshwater macro-fauna preserved in U2 shows that the lagoon was isolated from the sea, probably as the result of barrier stabilization (Figs. 4.9, 4.11 stage C). Shell layers that occur in core 10 are interpreted as the result of phases of sediment starvation due to reduced sediment input from the sea (Sedgwick and Davis Jr., 2003).

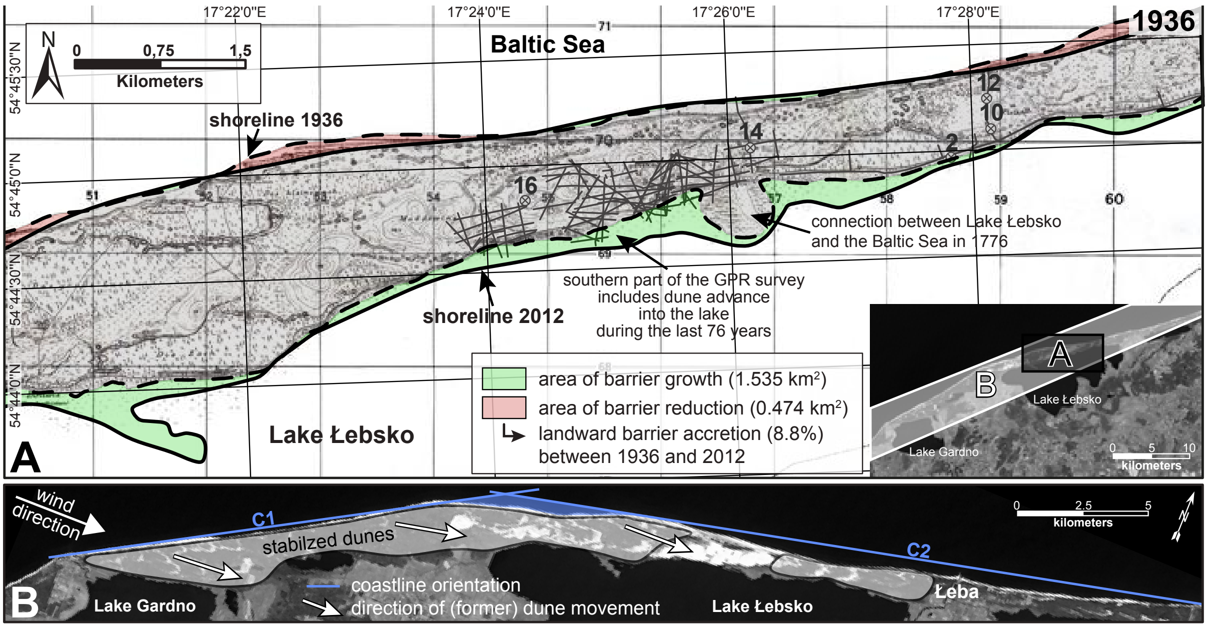

Fig. 4.10: A) Topographic map showing the barrier in 1936. Differences in the coast- and shoreline position between 1936 and 2012 illustrate erosion at the seaward facing part of the barrier and barrier growth towards the south; **B)** The orientation of the coast varies being SW-NE in the west (C1) and WSW-ENE in the east (C2) of the Gardno-Łeba plain. Dune movement on top of the barrier is parallel to the prevailing wind direction.

The thickness of U2 increases towards the south which is seen as the result of thickness variations of the underlying U3. Unit 2 is bounded on top (between 2 m and 4 m bsl) by a 10 cm to 30 cm thick organic-enriched sand layer. Palaeosols in comparable depths were dated to 3 ka and 1.7 ka BP and interpreted as the result of a temporal sea-level lowering by Rotnicki et al. (2009).

4.5.1.4 Unit 1 and U0 (dune sediments)

Sediments of unit U1 show landward inclined foresets bundled into up to 1.2 m thick sediment packages (Figs. 4.4, 4.5, 4.7, 4.8). These sediment packages are interpreted as the lowermost parts of the foresets of subaerial dunes; preserved as the dunes migrated into the lagoon, comparable to the active dunes nowadays (Fig. 4.1 D). Present active dunes are internally characterized by east/southeast dipping foresets due to the prevalence of westerly winds in the study area (see chapter 5) (U0). The direct coupling of aeolian sedimentation and landward growth of the barrier surface by subaquatic trapping of aeolian deposits is comparable to systems described e.g. from Brazil and Lithuania (Buynevich et al., 2007a, 2011; Barboza et al., 2011; Dobrotin et al., 2013; Lima et al., 2013).

Foreset packages are bounded by sub-horizontal beds that represent sand sheets, interpreted to reflect time periods when the active dune field is separated from the lake shoreline by e.g. vegetation and when sand is blown into the lagoon only by strong winds. This is common for aeolian sand sheets that accumulated during stormier conditions in depression behind a barrier (Rodriguez et al., 2013). Both processes – migration of dunes into the lagoon and sediment input during strong onshore winds – show that migrating dunes on top of the barrier contribute significantly to a landward-directed barrier migration.

The described facies association of landward dipping dune foresets and sub-horizontal beds are bounded by less, landward-inclined surfaces (Figs. 4.8, 4.10 A). Development of these surfaces is attributed to time periods of reduced aeolian sediment input or sediment starvation most likely as the result of a temporal stabilization of the dune field, or, the absence of dunes nearby. This alternation of enhanced aeolian activity and shoreline stabilization was previously described as a characteristic process of the Łeba barrier (Borówka 1990; 1995) and illustrates the successive landward progradation of the Łeba barrier.

4.5.2 Evolution of the Łeba barrier system

4.5.2.1 Glacio-fluviatile (>6 ka BP)

At the beginning of the Holocene the sea level was 60 m lower than today and the Łeba river discharged further north into the Baltic Sea basin (Rotnicki and Borówka, 1995; Tomczak, 1995a). The lowering in base level resulted in incision of fluvial channels into the late glacial sediments (Fig. 4.11, stage A). These Pre-Littorina sediments are covered by a palaeosol, 11.2 ka cal BP old, that developed in a vegetated paralic environment as the sea level began to rise. Palaeosols determine the onset of a groundwater-table rise as the result of the beginning transgression (Hoffmann et al., 2005; Lima et al., 2013).

4.5.2.2 Lagoonal (~6 – 5 ka BP)

Stage B is characterized by the development of a lagoon sheltered by an early barrier system (Fig. 4.11). Marine shells indicate an age of 5.97 ka cal BP for the associated lagoonal sediments (Fig. 4.9, Tab. 4.1). The comparison with published local sea-level curves indicates a sea level position of about 5 m bsl for this time period (Fig. 4.11) and a decline in the rate of sea-level rise (Uścinowicz, 2006). The deposition of the lagoonal sediments is therefore attributed to the "Littorina" Baltic stage (7.5 ka to 4 ka BP), which is characterized by the predominance of *Cerastoderma glaucum* (Wojciechewski, 2011).

4.5.2.3 Barrier growth and landward migration (~5 – ~3 ka BP)

Washover fans are the major building block of the Łeba barrier (Fig. 4.3). This indicates that the initial growth of the barrier took place at a more seaward position compared to today. Washover in the southern part of the barrier were deposited during the early Subboreal as indicated by radiocarbon ages of shells (4.5-5.0 ka BP) (Figs. 4.9, 4.11 stage C; Tab. 4.1). Sea level at that time was 2.5 m lower than today (Uścinowicz, 2006). The previous decline in the rate of sea-level rise is seen as prerequisite of barrier stabilization (Hoffmann et al., 2005; Uścinowicz, 2006). Establishment of a permanent barrier and freshwater conditions in the lagoon are documented by the presence of shells of freshwater mollusks (Fig. 4.9). A decline in the rate of sea-level rise results in increasing storm impact on barrier development, especially in non-tidal settings (Hünicke et al., 2015), and causes an amplified vertical barrier growth (Wang and Horwitz, 2007). The large lateral extend of the washover deposits indicates a flat barrier morphology, most likely without transgressive dunes and only incipient foredunes, for this time interval.

4.5.2.4 Dune development (~3 - 0 ka BP)

Barrier stabilization since 3 ka BP is interpreted to correlate with a nearly stable sea level, close to the present sea level (Fig. 4.11 stage D) (Uścinowicz, 2006). Four phases of dune activity occurred during the younger Holocene (Borówka, 1975, 1990, 1995). First foredunes established around 4 ka BP ago, migrating dunes appeared around 3.3 ka BP. The appearance of migrating dunes coincides with the deposition of dune foresets in a subaquatic setting in the northern part of the barrier. Further to the south, dune sediments overlie a 0.52 ka cal BP old palaeosol, which indicates a later onset of dune activity in this area (Figs. 4.1 D, 4.9).

Four phases of dune activity (5.8 - 4.5 ka BP; 3.9 - 3.1 ka BP; 2.6 - 2.4 ka BP and since 0.05 ka BP) were also reported from the Curonian spit further to the east (Dobrotin et al., 2013). These intervals only partially overlap with the periods of dune activity observed for the Łeba barrier. This implies that aeolian activity not necessarily reflects large scale climate patters but more depends on local factors.

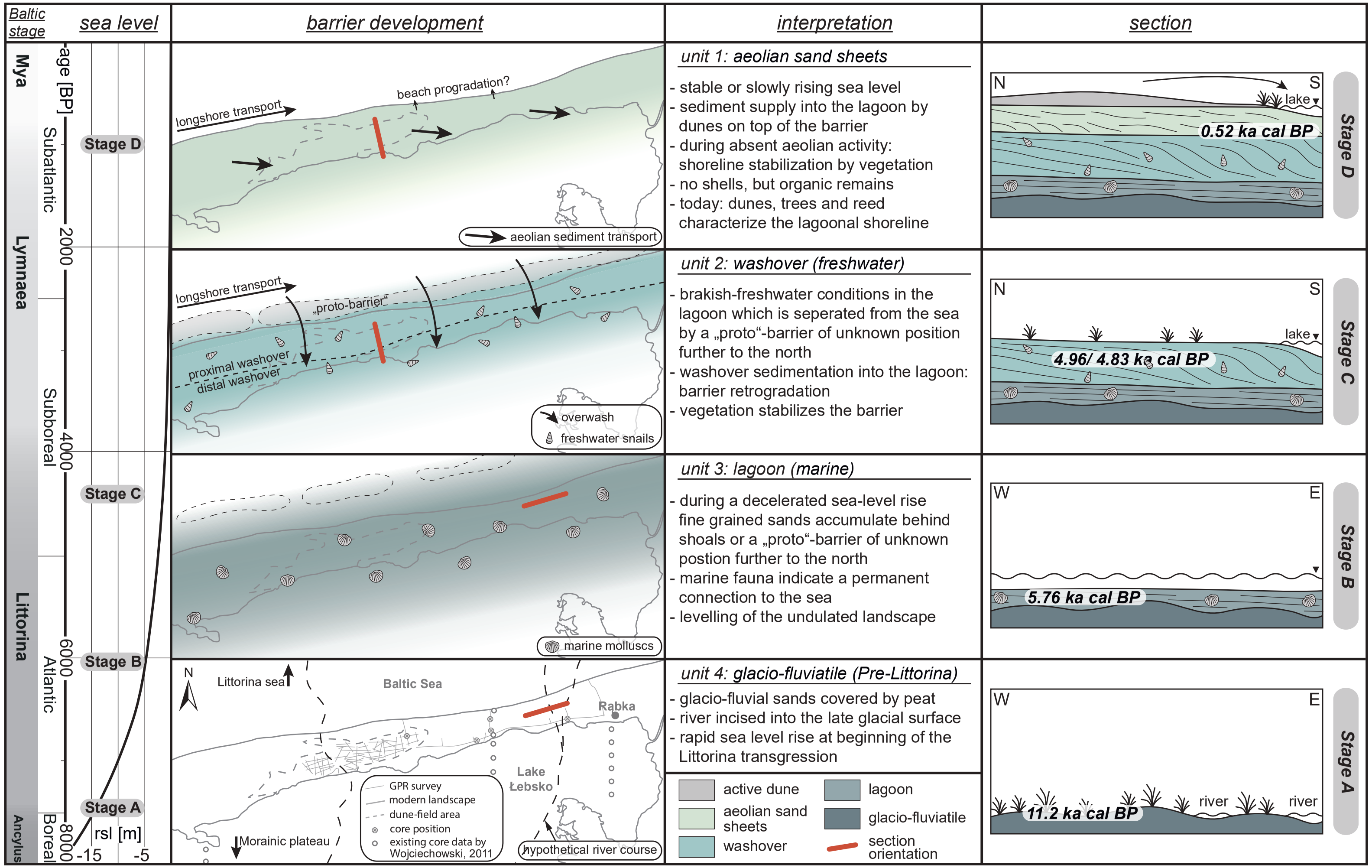

sea level curve for Łeba area after Uścinowicz, 2006

Fig. 4.11: Evolutionary model of the Łeba barrier presented in four steps. Pleistocene glacio-fluvial sediments (stage A) are covered by lagoonal sediments deposited under marine conditions during a decelerating sea-level rise (stage B). The development of a proto-barrier allows for washover sedimentation under freshwater conditions during the early Subboreal (stage C). Dune activity since the late Subboreal and early Subatlantic prevents overwash sedimentation, but also maintains the landward barrier migration by dune migration into the lagoon. Age assignment is based on dated shells and soils (see Tab. 4.1, Fig. 4.9).

4.5.3. Barrier morphology

Based on their net-landward directed migration, the Łeba barrier is classified as a transgressive system. The landward migration of the barrier during its earlier development resulted from a negative sediment budget at the seaward side (north) due to erosion and a positive sediment budget at the landward side (south) due to overwash sedimentation. Since establishment of a stabilized barrier covered by aeolian dunes, the increased height of the Łeba barrier restricted the overwash sedimentation but added aeolian input into the lagoon as a process to maintain the transgressive behaviour of the barrier (Fig. 4.10). At present, the seaward shore of the barrier is still subjected to erosion, but the eroded material is no longer transported into the lagoon but distributed alongshore and offshore. Coastal erosion is indicated by fossil tree trunks and palaeosols cropping out at the beach (Borówka and Rotnicki, 1995b). As a result, shoreline retreat and landward migration of the barrier are decoupled since establishment of aeolian dunes on top of the Łeba barrier.

The migration direction of the dunes on top of the Gardno-Łeba coastal plain is parallel to the prevailing wind direction (Figs. 4.1, 4.10 B). Dunes are either stabilized (along C1, C2) or active (along C2). Along the ENE-WSW striking coastline segment C1 dune migration is oblique to the coast which indicates that dunes evolve directly from the beach or their development may be initiated by the destabilization of foredunes. Both mechanisms are described from dunes worldwide (Hesp, 2013). By contrast, dunes migrating along the coastal segment C2 were not supplied anymore with sediment from the adjacent beach or foredunes. The coastline towards the west of the present active dune field, the segment C1, is regressive. The material released from this coastal segment is therefore seen as the potential source for the dunes along the C2 segment of the coast. Differences in the coastline between both segments, C1 and C2, may be attributed to result from a higher impact of the prevailing westerly winds along the C1 segment as sediment is mobilized and transported towards the east.

4.6 Conclusion

This study shows that the landward migration of transgressive barrier systems can be the result of both, marine- (overwash-) as well as aeolian processes. It demonstrates that barrier morphology, controlled by the presence of aeolian dunes, plays a major role in controlling sediment input into the lagoon. Increasing aeolian activity by the one hand leads to a reduction of overwash sedimentation but, on the other hand, increases the volume of aeolian sediment input into the lagoon, maintaining the transgressive character of the barrier. This underlines the importance of aeolian sediment transport in barrier evolution.

Chapter 5

Annual wind climate reconstructed from coastal dunes (Łeba, Poland)

Abstract

It is shown that coastal dunes bear an archive of annual wind intensity. Active dunes at the Polish coast near Łeba consist of two genetic units: primary dunes with up to 18 m high eastward-dipping foresets, which are temporarily superimposed by smaller secondary dunes. Ground-penetrating radar (GPR) data reveal that the foresets of the primary dunes are bundled into alternating packages imaged as either low- or high-amplitude reflections. High-amplitude packages are composed of quartz sand with intercalated heavy-mineral layers. Low-amplitude packages lack these heavy-mineral concentrations. Dune net-progradation is towards the east, reflecting the prevalence of westerly winds in the study area. Winds blowing parallel to the dune crest (i.e. from northerly or southerly directions) winnow the lee slope, leaving layers enriched in heavy minerals. Sediment transport to the slip face of the dunes is enhanced during the winter and spring months, whereas winnowing predominantly takes place during summer. As a consequence of this seasonal shift, the sedimentary record of one year comprises one low- and one high-amplitude GPR reflection interval. This sedimentary pattern is a persistent feature of the Łeba dunes and resembles a sedimentary "bar code". To overcome hiatuses in the bar code of individual dunes and dune-to-dune variations in bar-code quality, dendrochronological methods were adopted to compile a composite bar code from several dunes in the study area. The resulting data series shows annual variations in west-wind intensity for the time period 1987 to 2012. This is validated by comparison with instrumental based weather observations.

This chapter is based on a manuscript submitted to Aeolian Research: Ludwig, J., Lindhorst, S., Betzler, C., Bierstedt, S.E., Borówka, R.K., 2016. Annual wind climate reconstructed from coastal dunes (Łeba, Poland)

5.1 Introduction

Proxy-based reconstructions allow tracing of environmental and climatic conditions for areas and periods without instrumental observations. Such reconstructions are often based on sedimentary archives which provide a limited resolution and – especially in the continental realm – may be discontinuous due to erosion or non-deposition.

Wind is the main driver of sedimentological processes acting on continental dunes, making them a potential archive of wind-field variations. Consequently, shape and architecture of aeolian dunes were used in numerous studies to reconstruct phases of increased storminess (Clemmensen and Murray, 2006; Clemmensen et al., 2001a, b, 2007, 2014; Costas et al., 2012a, 2013, 2016; Havholm et al., 2004; Orford et al., 2000; Reimann et al, 2011; Wilson et al., 2001) or changes of the prevailing wind direction (Bristow et al., 2005, 2010; Lancaster et al., 2002a). Attempts to reconstruct past wind strengths from aeolian dunes focuses on sediment grain-size or dune migration velocity (Bristow et al., 2005; Costas et al., 2012b; Forman et al., 2008; Lancaster et al., 2002b; Tsoar et al., 2004; Yao et al., 2007).

Successful reconstructions of wind-field variations act on time scales of decades to millennia. Reconstructions on annual to sub-decadal time scales are missing, so far. This study fills this gap. Integrating geophysical and sedimentological data, a proxy-based data-series of annual wind intensity at the Polish Baltic coast for the time period 1987 to 2012 is presented and validated against a time series of instrumental based weather observations.

5.2 Study site

The study area is situated at the Polish Baltic coast, 90 km northwest of Gdańsk close to the village Łeba (Fig. 5.1 A, B). Late Holocene barrier beaches are covered by an active dune field consisting of eight barchanoid dunes up to 600 m long and 27 m high (Fig. 5.1 C). Individual dunes consists of primary dunes, superimposed by secondary mesobarchans which are up to 8 m thick and 250 m long (Borówka, 1980, 1990). The primary dunes are regarded as persistent feature of the Łeba dune system, being present since at least 1900, whereas the secondary dunes vary in size on an annual time scale. Dune sands of Łeba are in general composed of 99.5% quartz and less than 1% heavy minerals, including amphiboles, garnets, and small amounts of zircon and ilmenite (Borówka, 1979).

The study area is part of the Słowiński National Park and public access to the dunes is prohibited since the year 1967. The dunes of the Łeba system show a continuous eastward movement parallel to the recent coastline. The annual migration rate is in the range of 10 m to 12 m (Ptak and Rudowski, 2014). Psammophytes and pine trees, planted during the second half of the 19th century AD, border the dune area towards the coast, whereas the lagoonal Lake Łebsko is situated towards the south. The close vegetation cover restricts sand transport from the beach to the dunes (Borówka and Rotnicki, 1995a).

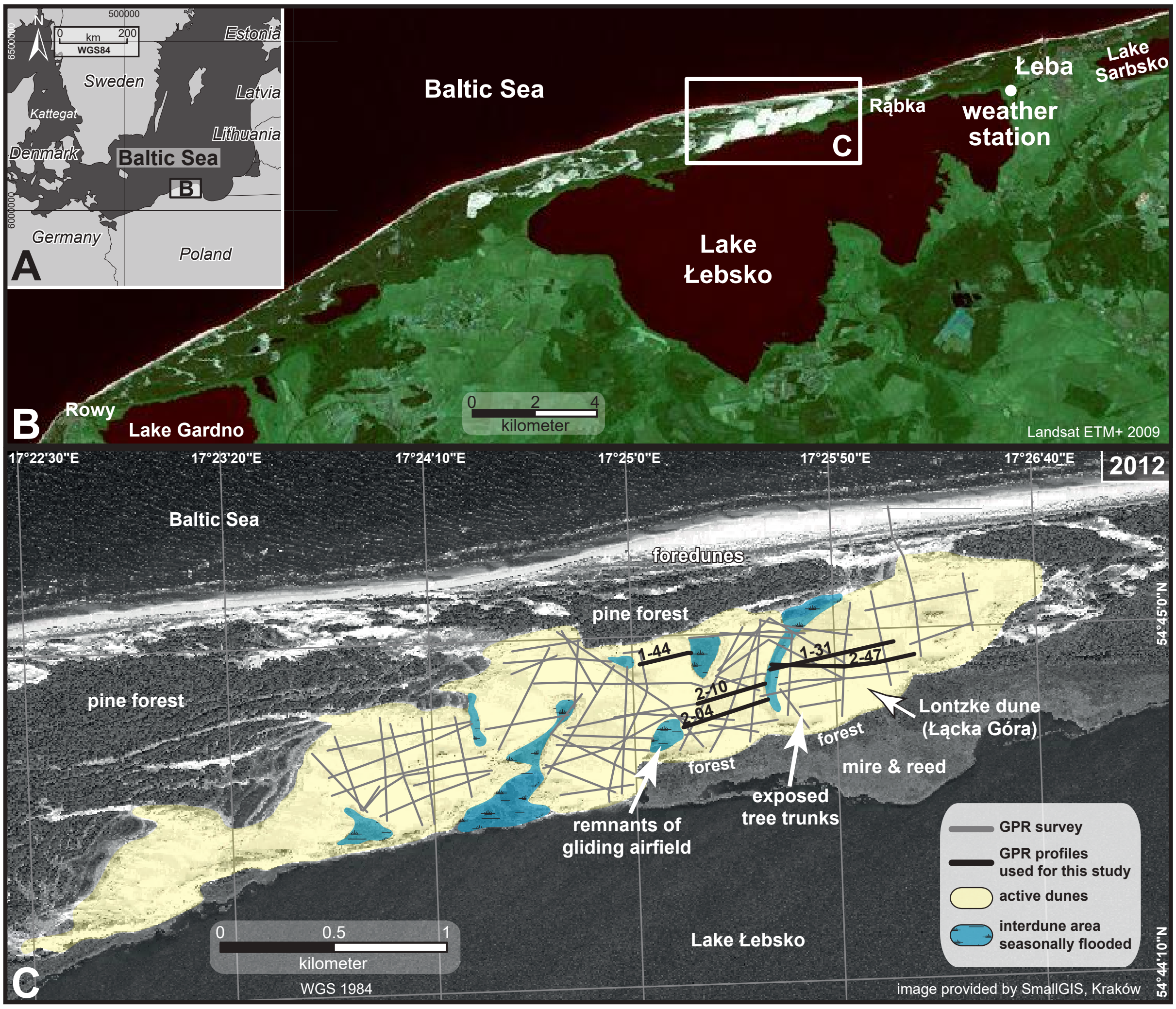

Fig. 5.1: A) Location of the study area; **B)** Łeba barrier with active dunes and position of the weather station southeast of a pine forest; **C)** Aerial image obtained in the year 2012. Profiles used in this study are drawn as thick lines.

Four stages of dune development, interrupted by phases of soil development, are preserved from the younger Holocene (Borówka, 1990, 1995). The oldest soils developed between 4 ka and 3.5 ka BP, stabilizing older foredune ridges and parabolic dunes. The second phase of aeolian acitivity, between 3.3 ka and 2.5 ka BP, was characterized by barchans and parabolic dunes up to several meters high. The third phase, with up to 25 m high barchanoid and parabolic dunes terminated around 1.5 ka BP. Subsequently, there is no evidence for dune development until 0.5 ka BP, when aeolian activity resumed (Borówka, 1990). All palaeo-soils in the Łeba dune system contain charcoal and ceramics, indicating a long history of human settlement in the area (Borówka, 1990).

5.3 Methods and data sets

5.3.1 Ground-penetrating radar

To image the internal sedimentary architecture of the dunes, a Geophysical Survey Systems Inc. (GSSI) SIR-3000 ground-penetrating radar (GPR) equipped with a 200 MHz antenna was used. The survey comprises 32 km of GPR profiles (Fig. 5.1 C). The subsurface radar-wave velocity is 0.13 m ns^{-1} for the dry dune sands and 0.06 m ns^{-1} for the water-saturated barrier deposits underneath, based on the analysis of diffraction hyperbolas. The topography along the survey lines was measured parallel to GPR profiling using a Leica GS09 differential GPS. Accuracy of this system is in the range of 2 cm for all axes (manufacturer specifications). GPR data were processed using ReflexW (Sandmeier, 2013). Processing steps included static correction, dewow, frequency filtering, background removal, topographic migration and gain correction. The interpretation of the GPR data followed the concept of seismic stratigraphy (Mitchum Jr. et al., 1977) and their application to GPR data (Bristow et al., 2000; Lindhorst et al., 2008). The interpretation of radar surfaces is based on the classification of aeolian bounding surfaces (Brookfield, 1977; Kocurek, 1981). Five radar facies (rf) and three radar surfaces (rs) were defined for the Łeba dunes (Fig. 5.2).

GPR reflection pattern	description	interpretation
rf1a 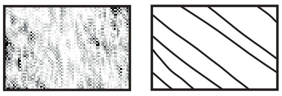 rf1b 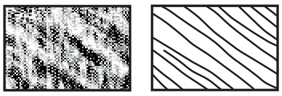	low (a) and high (b) amplitude reflections, moderately to highly continuous, 20 - 27° eastward inclined, parallel - partly disturbed	foresets of primary dune a) quartz-domianted b) with intercalated layers enriched in heavy minerals
rf2 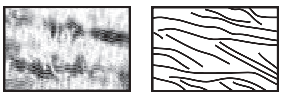	low to high amplitude, moderately to highly continuous, 7 - 16° eastward inclined reflections, truncated by sub-horizontal, high amplitude reflections	foresets of secondary dune
rf3 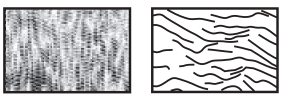	high amplitude, chaotic to (sub-) horizontal refelctions, moderate to discontinuous, numerous diffraction hyperbolas	sediment trapped between tree trunks of buried forests
rf4 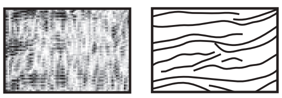	moderate to high amplitude reflections, moderately continuous, (sub-) horizontal to wavy	plane beds, generated by slumping
rs1 	high amplitude reflection, continuous, numerous diffraction hyperbolas, erosive upper termination of rf1, rf3 and rf4	deflation suface
rs2 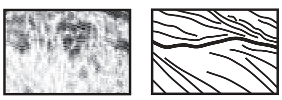	high amplitude reflection, continuous to partly discontiuous, lateral extension > 300 m	bounding surface between primary and secondary dunes and surface of sediment bypass
rs3 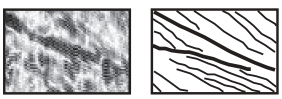	high to medium amplitude reflection, continuous to partly discontiuous	internal bounding surface generated during dune re-organization

Fig. 5.2: Radarfacies (rf) and radar surfaces (rs) as defined for classification of the GPR profiles.

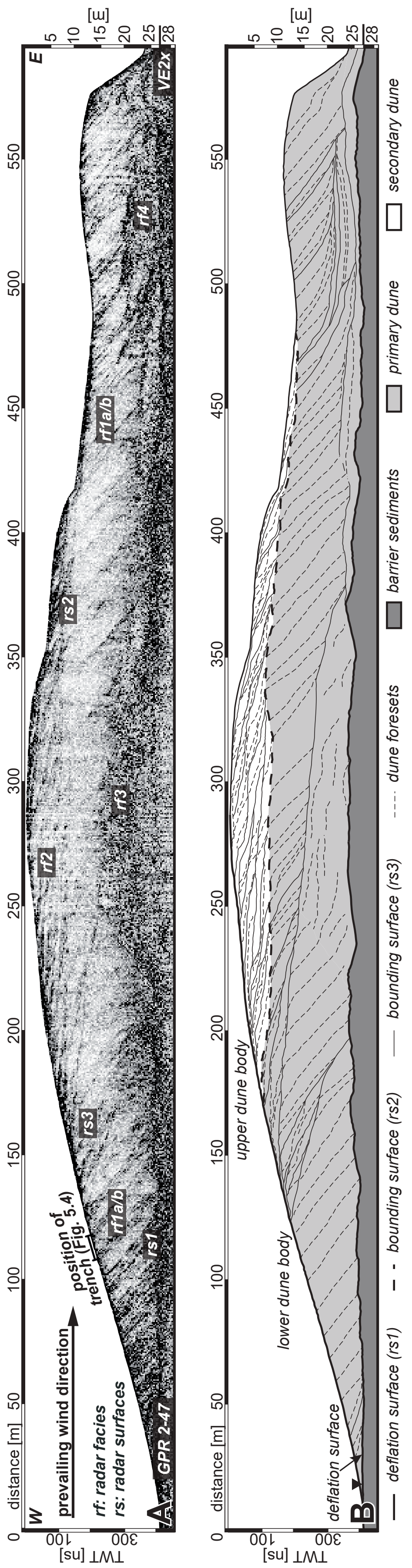

Fig. 5.3: GPR profile 2-47 (see Fig. 5.1 for location); **A)** GPR data and assigned radar facies (rf) and radar surfaces (rs). Note position of trench for sediment sampling; **B)** Interpretation of A). Dunes migrate over the deflation surface and comprise of two genetic units. The upper dune body is characterized by up to 4.5 m thick eastward-dipping foresets. The lower dune body shows eastward-inclined foresets which are imaged by the GPR as alternating low and high-amplitude reflection packages.

5.3.2 Sediment grain size and magnetic susceptibility

Sediments along a 10 m long trench, excavated along the luv side of one dune, were studied to allow for a direct comparison of radar facies with sediment texture and composition (Figs. 5.3, 5.4). Sediment samples (1.5 cm^3 each) were taken equidistantly (each 2 cm) from a depth of 45 cm below the surface. The sediment grain-size distribution was measured using a Sympatec Helos KF Magic laser particle-size analyser. Grain-size statistics were calculated using Gradistat (Blott and Pye, 2001) and are based on the graphical method (Folk and Ward, 1957). Values are given using the logarithmic phi scale. In addition, the magnetic susceptibility along the trench floor was measured using a GF Instruments SM-20 handheld magnetic-susceptibility meter (Fig. 5.4).

5.3.3 Weather data and sand-transport intensity

Meteorological data were provided by the Institute of Meteorology and Water Management (IMGW-PIB) in Warsaw, Poland. These data were continuously recorded since the beginning of the 1970s by the weather station of Łeba (54.7533842 °N, 17.5336994 °E). Wind data comprise wind speed at 10 m above ground and wind direction, both recorded eight times a day (every three hours). Due to the topographic situation of the station, with a forest situated towards the NW, winds from the NW sector might be biased to a certain extend (Mirosław Miętus, University Gdańsk, pers. comm.) (Figs. 5.1, 5.5). For comparison with dune movement, the measured wind directions were divided into an easterly (22.5° to 202.5° azimuth) and a westerly (202.5° to 22.5°) sector based on the averaged dune-crest orientations. To account for even short-time wind events, all wind-speed measurements were considered, without calculating values for daily mean or maximal wind speed (Fig. 5.5). Precipitation data were measured on a daily basis and include convective and large-scale precipitation as well as snow. These data are provided as monthly means over the period 1987 to 2012.

The potential aeolian transport intensity per time unit (ETI) is based on empiric field data from the Łeba dune system and was calculated according to the method described in detail by Borówka (1980, 1990). The ETI gives a measure for the annual sediment volume potentially being transported by winds of a given velocity (Borówka, 1999). Values for ETI provided in this study were calculated for westerly winds and are given as ($kg*10^3 * m^{-1} * a^{-1}$).

5.4 Results

5.4.1 Dune internal architecture and migration rate

GPR profile 2-47 was chosen to exemplarily document the internal sedimentary architecture of the Łeba dunes (Fig. 5.3). The imaged dune is 27 m high and the largest and highest dune of the Łeba system. The dune body overlays the local deflation surface (rs1) and is subdivided by an erosional unconformity (rs2) which dips with 3° towards the east. The lower part of the dune is up to 18 m thick and characterized by eastward inclined (20° - 27°) tabular foresets (rf1a/b) which downlap onto the deflation surface. Internally, these foresets are bundled into packages, characterized by either low- or high-amplitude GPR reflections (Figs. 5.3, 5.4). Along the profile, there are several unconformities (rs3) which interrupt the continuous succession of low- and high-amplitude packages. From profile distance 550 m to 620 m, foresets show a pronounced concave shape with aggrading bottom sets (rf4). The same stacking pattern is assumed for the segment 250 m to 320 m, where the GPR image is masked by interference signals. The upper dune body is up to 7 m thick and characterized by low-angle foresets which have an easterly dip (7° - 16°), and are bundled into maximal 4.5 m thick packages (rf2). Each package is truncated by minor unconformities dipping towards the east with 4° - 10° (rs3).

Other dunes of the Łeba system show a similar internal architecture (Fig. 5.6). This includes, in particular, the bundling of primary-dune foresets into alternating packages characterized by either low- or high-amplitude GPR reflections.

The annual rate of dune movement, based on the comparison of dune positions in aerial images taken in the years 1995 and 2012 is 11.8 m a^{-1} along GPR profile 2-10 and averages to 12 m a^{-1} for the GPR profiles 2-04, -10, -47, -31 and 1-44 (Fig. 5.7). The long-term rate of dune movement is 14 m a^{-1}, based on the positions of dunes and remnants of a gliding airfield which was constructed 82 years ago (in the year 1930) east of the Lontzke dune and is nowadays located about 1.15 km west of the dune front (Figs. 5.1, 5.7).

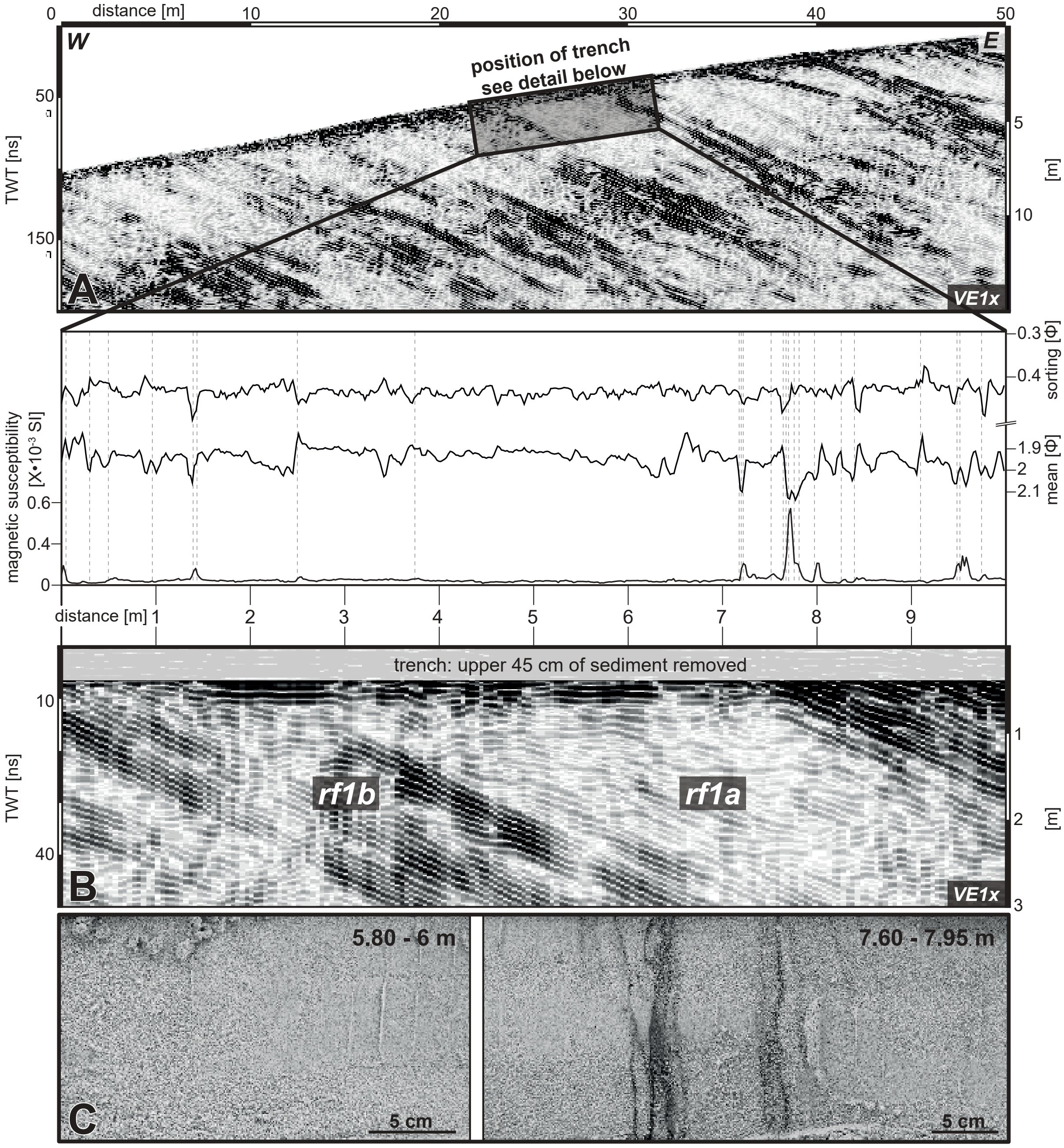

Fig. 5.4: Correlation of GPR- and sediment data; **A)** GPR data and position of trench. The sampled interval covers foresets imaged by the GPR as high or low amplitude reflections, respectively; **B)** Correlation of mean grain size and sorting (both shown with 3 point running average) and magnetic susceptibility with GPR reflections. Dashed lines mark positions of layers enriched in heavy minerals, based on the visual inspection of the trench floor. Low-amplitude reflections correspond to quartz-dominated intervals of medium grain size and low magnetic susceptibility. High-amplitude intervals are characterized by intercalated layers enriched in fine-grained heavy minerals and peaks in the magnetic susceptibility; **C)** Details of the trench floor which illustrates quartz-dominated sediments of low-amplitude intervals (left) and intercalated heavy-mineral layers present in high-amplitude intervals (right).

5.4.2 Sedimentology

The sediment of the Łeba dunes is medium to fine grained (1.76 phi to 2.28 phi with a mean of 1.95 phi) and well sorted (0.35 phi to 0.56 phi) with only minor variations (Fig. 5.4). Along the trench, sediments of the first 2.5 m and the last 3 m are characterized by high-amplitude GPR reflections (rf1b), whereas the sediments in-between are imaged with low amplitudes (rf1a) (Fig. 5.4). Visual inspection of the trench floor showed that high-amplitude intervals contain numerous 1-2 cm thick layers enriched in heavy-mineral grains. Low-amplitude intervals are slightly finer grained and composed of quartz sand with well-distributed heavy-mineral grains. In these intervals, only a few heavy-mineral layers are present.

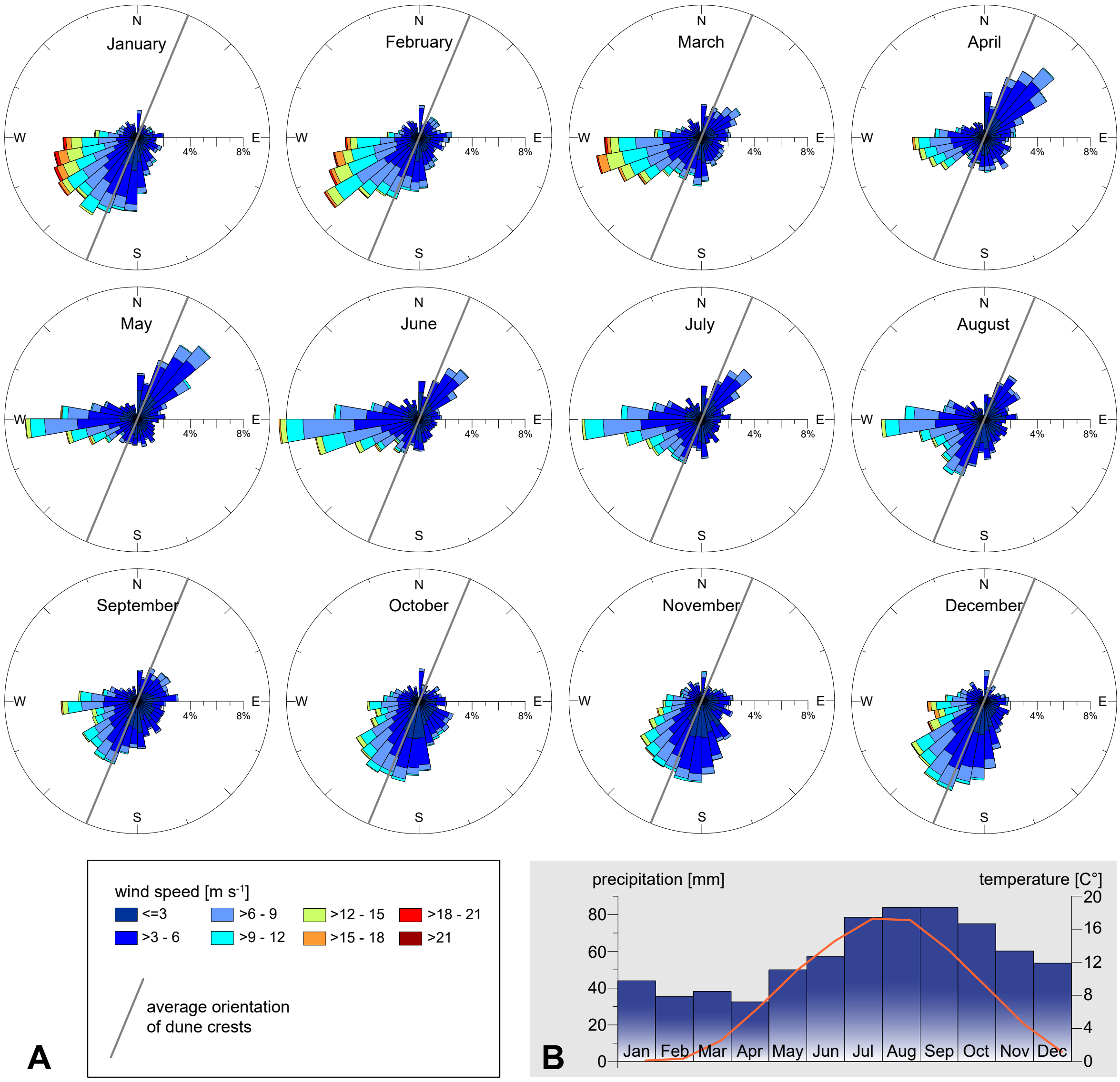

Fig. 5.5: Meteorological data for the time period 1987 to 2012 from the Łeba weather station; **A)** Wind velocity and direction. The NW sector is partly biased in the data (see methods for details). Note average dune crest orientation; **B)** Averaged monthly precipitation and temperature.

The magnetic susceptibility of the sediment in the low-amplitude intervals has a mean value of 0.0510^{-3} SI. Peaks of the magnetic susceptibility (along the trench at 0.1 m, 1.4 m, 2.5 m, 7.2 - 8.1, and 9.45 - 9.6 m) with values of up to 0.610^{-3} SI correspond to visually detected heavy-mineral layers (Fig. 5.4).

5.4.3 Meteorological data

The winter months (November to March) show the highest wind speeds (Fig. 5.5). Westerly winds predominate during the months January to March. In April, the wind field starts to show a bi-directional characteristic with winds blowing from either westerly or north-easterly directions (i.e. oblique to the NNE to SSW dune crest orientation). With mostly moderate wind speeds, this situation lasts during the summer, until September. In autumn and early winter (October to December) the westerly winds calm down and winds blowing from south-westerly directions become predominant. Precipitation varies and is highest during the summer and autumn months, accompanied by high temperatures.

To evaluate the impact of different wind speeds on dune movement, threshold values for the mobilization of the Łeba dune sediments were calculated following the equations of Bagnold (1941) and Dong et al. (2002). Under dry conditions, movement of the smallest grains (1.76 phi) initiates if wind speed exceeds 4.5 m s^{-1}. This value increases to 10 m s^{-1} if the sediment is wet.

5.5 Discussion

5.5.1 Depositional model

A simplified depositional model for the Łeba dunes, linking sedimentological and geophysical data, is shown in Figure 5.8. Dunes migrate over a deflation surface, which in coastal dune systems is determined by the long-term average position of the ground-water table (Lindhorst et al., 2008). The majority of the Łeba dunes consist of two genetic units, a lower, primary dune superimposed by a smaller secondary dune (terminology after Lancaster, 1988). Each unit is characterized by a distinct internal architecture with foreset geometries indicating a net eastward-directed dune progradation (Figs. 5.3, 5.6). Primary and secondary dunes are separated from each other by an erosional unconformity.

Foresets of the primary dunes are bundled into packages imaged as alternating bundles of high- and low-amplitude reflections in the GPR data (Figs. 5.3, 5.4, 5.6). Intervals characterized by high reflection amplitudes contain thin layers enriched in heavy minerals, which are interpreted to cause enhanced GPR reflections by alteration of the electromagnetic permittivity of the sediment (van Dam and Schlager, 2000; van Dam et al., 2002, 2013; Neal, 2004; Pupienis et al., 2011; Shankar et al., 1996). The thickness of individual heavy-mineral layers is far below the resolution of the GPR signal. GPR reflections from such thin-bedded intervals therefore represent the interference

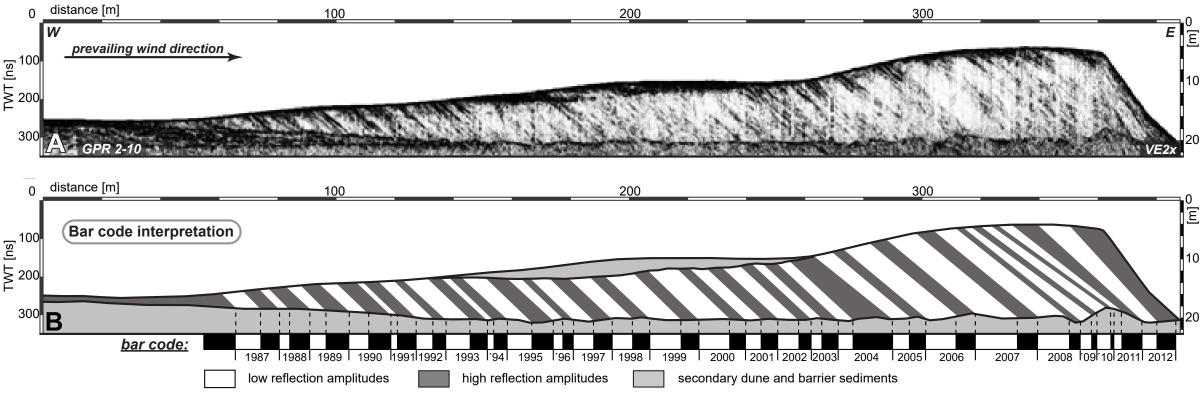

Fig. 5.6: A) GPR profile 2-10 (see Fig. 5.1 for location); **B)** Interpretation of A) with alternating high- and low-amplitude intervals and resulting „sedimentary bar code" covering 26 years (1987 to 2012).

pattern of GPR signal wavelength and the thickness of individual sediment lamina beds (Guha et al., 2005).

Under west-wind conditions, sediment is eroded at the luv side of the primary dune, which serves as a sediment pool, and accumulates near and shortly after the crest, forming the secondary dunes. These dunes develop in time periods when precipitation is low (i.e. during spring) and are eroded during more humid time periods (i.e. during summer; Borówka, 1980, 1990; Fig. 5.5). Sediment reaches the lee slope of the primary dune if westerly winds are strong enough to allow sediment to bypass the secondary dunes (throughout the year with a predominance in winter) or if these superimposed structures become eroded (i.e. during the summer and early autumn). If sediment reaches the lee slope of the primary dunes, quartz-dominated foresets develop, imaged as low-amplitude packages by the GPR.

Foreset packages characterized by high reflection amplitudes result from lee-slope winnowing by winds blowing oblique to the dune crest (i.e. from the NE or SW), a process which is proven by field observations from the Łeba dunes (Borówka, 1979). The formation of high-amplitude foreset packages results from the interplay of eastward-directed sediment re-deposition from the luv

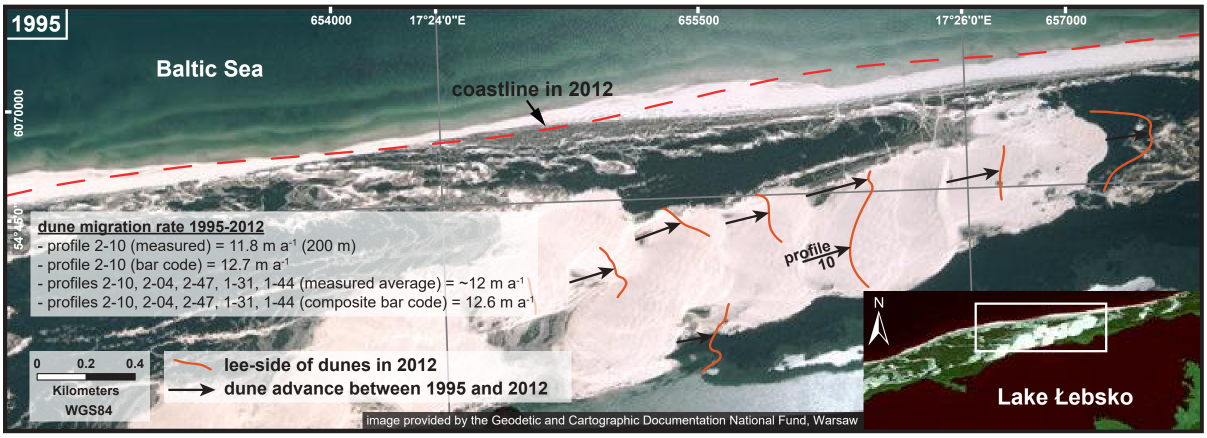

Fig. 5.7: Comparison of dune positions for the years 1995 (this image) and 2012 (red solid lines). Length of arrows indicate total dune advance during this time.

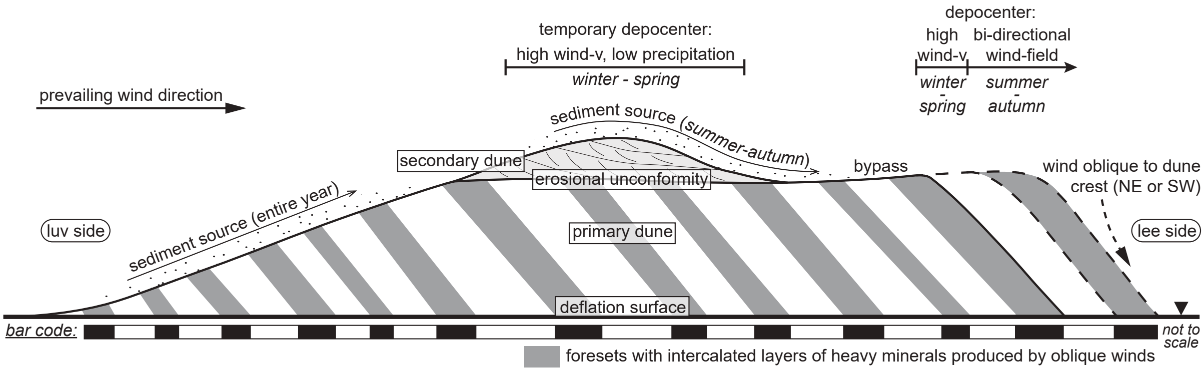

Fig. 5.8: Genetic model for the Łeba dunes. Dunes migrate on top of a deflation surface determined by the long-term average position of the ground-water table. Prevalence of westerly winds results in an overall eastward-directed dune migration. Secondary dunes develop when precipitation is low and winds are strong. Seasonal changes in the wind field result in the deposition of alternating foreset bundles imaged as either low- or high-amplitude reflection package by the GPR.

slope and the secondary dunes, and subsequent episodic winnowing by winds blowing oblique to the lee slope. Such winds occur predominantly during late spring and summer, when the local wind field shows a bi-directional characteristic, and during autumn and early winter when south-westerly winds prevail (Fig. 5.5).

The thickness of paired low- and high-amplitude packages is interpreted to be directly linked to the annual sediment supply to the lee side of the dunes and therefore represents a measure of yearly dune movement, i.e. the intensity of westerly winds (Figs. 5.6, 5.8, 5.9). Package counting allows implementing a chronostratigraphy for the dune sediments with the sedimentary record of one year being composed of one low and one high-amplitude package. The obtained rate of dune movement varies between 6.5 m a^{-1} and 21 m a^{-1} for the time period 1987 to 2012, with a mean of 12.5 m a^{-1} (Fig. 5.9). This value is similar to the mean rate of dune movement deduced from aerial images (11.8 - 12.0 m a^{-1} for the time 1995 to 2012; Fig. 5.7), as well as, to published values (10 - 12 m a^{-1} for 2009 to 2013; Ptak and Rudowski, 2014), and proves that the applied chronostratigraphy is correct. The linkage of foreset bundles, expressed as black and white packages according to the GPR reflection amplitudes, and seasonal changes in the wind field implies that the dunes bear a sort of sedimentary „bar code“ which records yearly changes of west-wind intensity (Figs. 5.6, 5.8, 5.9).

5.5.2 Reconstruction of annual wind intensity

The sedimentary bar code is a persistent feature of the dunes in Łeba. However, bar-code quality may vary from dune to dune or even in one dune due to lateral variations in sediment-supply or the occurrence of hiatuses due to dune re-organization or local erosion (Fig. 5.9). To overcome these local effects and to allow for the compilation of a composite bar code as a data-series of wind intensity, the dendrochronological concepts of replication (introduced by Twinning, 1833 and Babbage, 1838; in Speer, 2010) and crossdating (first summarized by Douglass, 1941) were

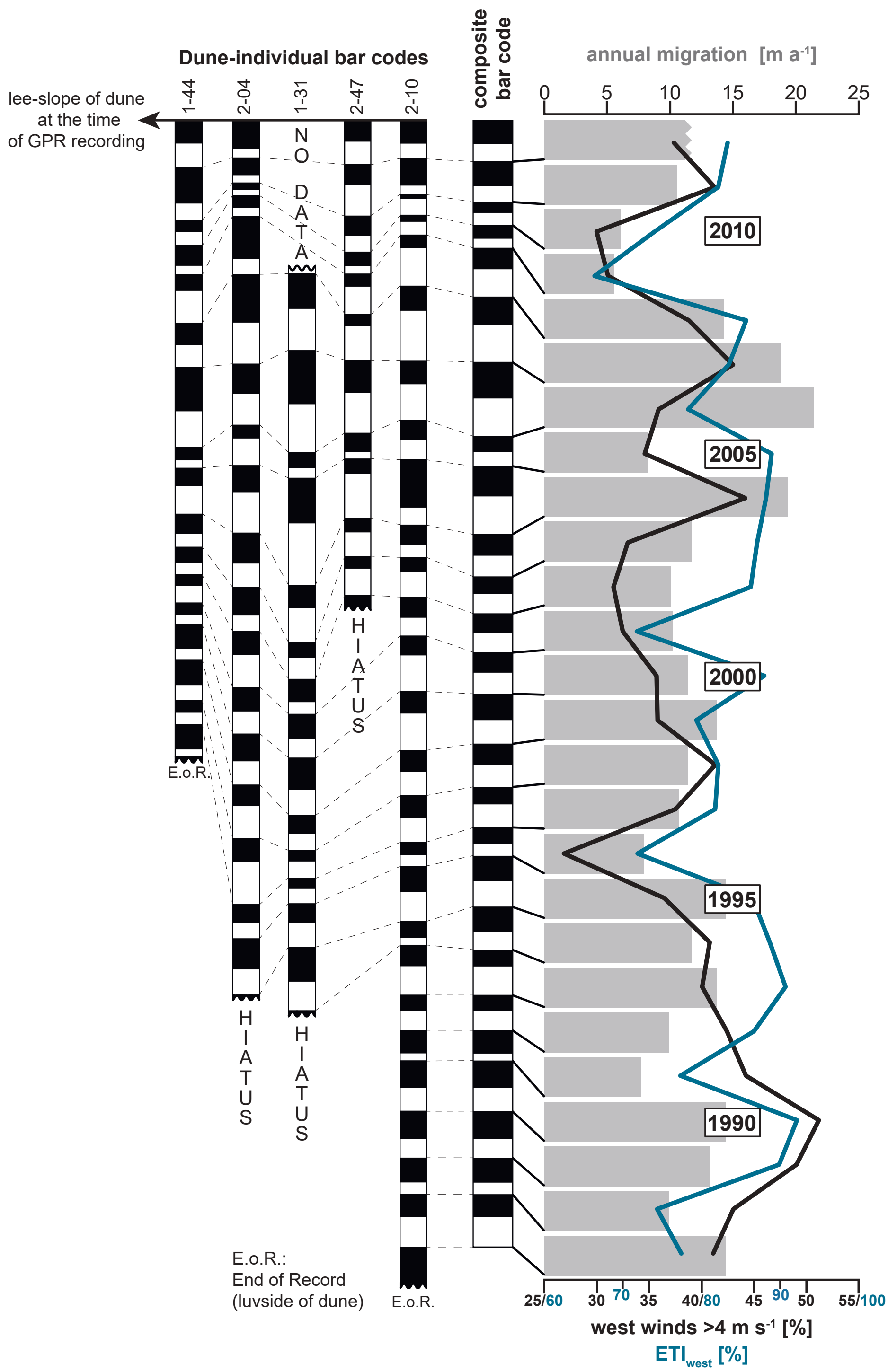
Dune-individual bar codes
lee-slope of dune at the time of GPR recording
1-44
2-04
1-31
2-47
2-10
NO DATA
HIATUS
HIATUS
HIATUS
E.o.R.
E.o.R.
E.o.R.: End of Record (luvside of dune)
composite bar code
annual migration [m a-1]
0 5 10 15 20 25
2010
2005
2000
1995
1990
25/60 30 70 35 40/80 45 90 50 55/100
west winds >4 m s-1 [%]
ETIwest [%]

used in conjunction with the needs of this study. The resulting composite bar code covers the time period 1987 to 2012 (26 years).

The visual comparison of bar-code derived migration rates and instrumental-based wind data shows similar trends (Fig. 5.9). Annual dune migration is fast during years with a high percentage of westerly winds and resulting high aeolian transport intensity (ETI) (e.g. 1990, 2004 and 2007) and vice versa (e.g. 1996, 2005 and 2009 - 2010). The mathematical correlation of wind and dune-migration rate is 0.41 (0.39 for ETI) and decreases to 0.15 if only winds > 10 m s^{-1} are considered (Fig. 5.9). This reflects a limited influence of storms on the long-term dune movement, an interpretation corroborated by measurements on beaches which showed that aeolian sand transport is rather related to continuous moderate winds than to extreme events (Arens, 1996a).

It is concluded that the sedimentary bar code is a record of annual dune migration and as such represents an archive of the intensity of westerly winds. The reconstruction of annual changes in wind intensity is not restricted to the active dunes in Łeba. Similar dune sediments, characterized by intercalated heavy-mineral accumulations, are described e.g. from coastal dunes in Lithuania and Australia (Buynevich et al., 2007b; Hamilton and Collins, 1998), showing that the method proposed herein bears the potential for wind-field reconstructions on a regional scale. Dunes stabilized by vegetation at a certain point in time, on the other hand, may bear a wind record of past time slices. Analysis of such dune archives would require precise dating methods, most likely optical-stimulated luminescence (e.g. Costas et al., 2012b), to determine the onset of the individual records.

5.6 Conclusion

It has been shown that active dunes at the Polish Baltic coast bear a record of annual wind intensity. Net easterly dune migration is attributed to the prevalence of westerly winds during winter and early spring and results in the deposition of quartz-dominated foresets. Winds blowing oblique to the dune crest, especially between late spring and late autumn, winnow the lee slope and left layers enriched in heavy minerals. These periodical changes of the wind field lead to the deposition of foreset bundles imaged by GPR as alternating low- and high-amplitude reflection packages, comparable to a sedimentary bar code. Rates of annual dune migration, deduced from the thickness of distinct bar-code elements, correlate with annual variations in the intensity of westerly wind. The bar code therefore records the natural variability of the wind system in the study area.

Chapter 6

Conclusion and Outlook

6.1 General discussion and conclusion

The purpose and overall aim of this project was the evaluation of barrier and dune sediments, situated along the southern Baltic Sea coast, to access potential archives to reconstruct climate variations, especially changes in the wind field, on a yearly to centennial time scale. The complex sedimentary architecture of the studied barrier and dune systems required careful investigation in order to allow for the reconstruction of possible atmospheric changes within the covered sedimentary succession.

6.1.1 Barrier architecture and development

This study provides a comprehensive look into the architecture of two different barrier systems located off the polish Baltic Sea coast which is based on a broad geophysical and sedimentological data set.

The Wolin barrier system, located in the southern Pomeranian Bight, is comprised of an alongshore-parallel prograding spit and a seaward-attached beach plain, characteristic architectural elements of a regressive barrier system (Figs. 3.1, 3.10). The shift from spit to beach plain deposits is attributed to a limited accommodation space during spit growth and is associated to a change in the predominance of current- or wave-dominated sedimentation. Sediment transport to the spit front caused spit progradation parallel to longshore currents. The wave-related sedimentary succession of the seaward prograding beach plain contains erosional unconformities attributed to severe storm events. The increased sediment erosion of the seaward prograding succession results in a progradation rate of the beach plain being half of the rate of the spit-growth. Prograding barrier systems are often associated with a well-developed foredune ridge plain on top of the barrier. The foredune crest orientation indicates the former and recent barrier progradation direction as a result of the shoreline-parallel growth of foredunes. Internally, foredunes of the Wolin barrier show aggrading and prograding sediment accretion patterns. The change from aggradation to progradation is the result of increasing foredune height which is controlled by the beach progradation rate and the potential aeolian sediment transport rate.

Near-subsurface investigation of the transgressive Łeba barrier showed that not only washover, but also aeolian sediments contributed significantly to a landward barrier migration (Figs. 4.1, 4.3). Transgressive barriers are characterized by a landward shift of the coastline due to erosion along the coast and subsequent sediment transport across the barrier by overwash or sediment redistribution alongshore. Overwash processes are linked to a flat barrier topography without (fore-) dunes or their degradation during strong storm surges. Washover deposits are internally characterized by sub-horizontal sand sheets that developed close to the sea and by landward dipping foresets in the distal part of the barrier. Deposits of the central washover fan indicate the position of the overwash throat, where the barrier morphology was low enough to allow for landward sediment transfer. The increasing influence of vegetation and dunes caused barrier stabilization, probably provoked by a nearly stable sea level, and prevented further overwash. In this study the landward movement of the lagoon shoreline is maintained by dunes atop the barrier migrating into the lagoon. The upper most unit of the Łeba barrier is characterized by foresets bounded by sub-horizontal sand sheets. Foresets are preserved bottom-sets of dunes that migrated into the lagoon. Sand sheets developed at time periods when dunes were separated from the lagoon and strong onshore winds blew sediment into the lagoon. Gaps in sedimentation, e.g. due to a vegetated dune field, stabilized the lagoon shoreline. This alternation of dune migration into the lagoon and dune stabilization provokes a successive landward barrier growth.

The development of transgressive (Łeba) and regressive (Wolin) barrier systems along the southern Baltic Sea coast depends on the complex interaction of several factors with sea level, sediment input and wave energy being the most important (Fig. 6.1 A, B). Barrier systems along the southern Baltic Sea coast developed under the circumstances of a decelerating sea-level rise of the Littorina trangression (Hoffmann et al., 2005; Rotnicki et al., 2009; Lampe et al., 2011). As the result of regional variation in post-glacial isostatic adjustment, the sea level in the Łeba area showed a constant rise (Uścinowicz, 2006) (Fig. 4.11), whereas the sea level at the position of the Wolin system stabilized between 6.5 ka and 3 ka BP (Hoffmann et al., 2009) (Fig. 3.11). Local differences in sea-level evolution are hence seen as major factors controlling barrier behaviour through time, as the landward migration of transgressive systems is attributed to a rising sea

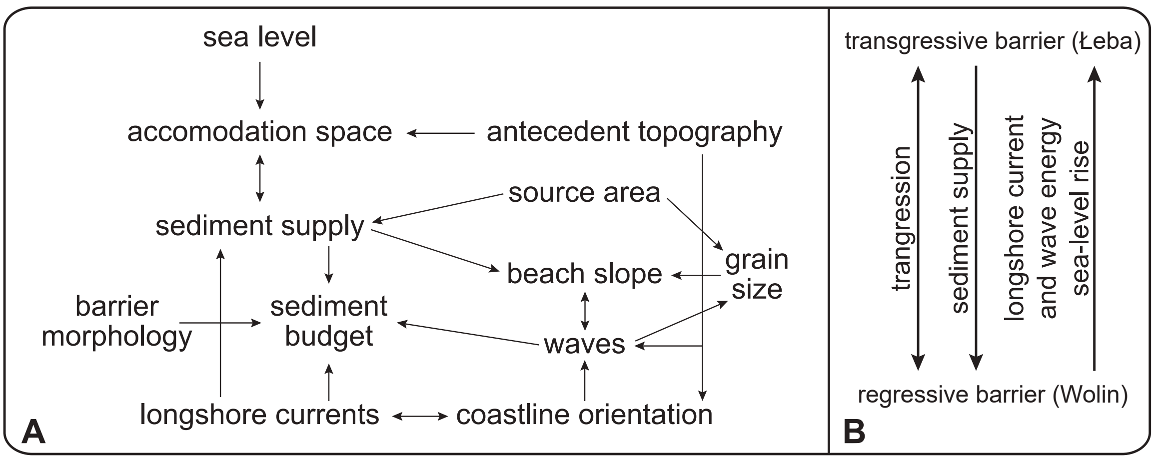

Fig. 6.1: Compilation of interacting controlling factors affacting the barrier geometry in micro-/ non-tidal settings.

level, subsequently increasing accommodation space, whereas regressive barriers correlate with a stable sea level (e.g. Thom, 1984; Kraft and Chrzastowski, 1985; Davis Jr., 1994; Cattaneo and Steel, 2003; de Oliveira Caldas et al., 2006). The accommodation space is mainly controlled by the sea level and antecedent topography and is directly linked to the rate of sediment supply (Roy et al., 1994; FitzGerald and Heteren, 1999; Storms et al., 2002). A sediment supply rate exceeding the rate of accommodation space, leads to a positive sediment budget for regressive systems, whereas transgressive barriers are linked to a constant or negative sediment budget (Lessa et al., 2000; Timmons et al., 2010). Differences in the sediment supply are controlled along the southern Baltic Sea coast by variations in the abrasion rates of barrier adjacent moraine cliffs, indicating a higher sediment supply to the Wolin barrier than to the Łeba barrier (Rotnicki and Rotnicka, 2010) (Figs. 4.1, 6.1 B).

According to Martinho et al., (2009) and others (Dillenburg and Barboza, 2009; Barboza et al., 2011; Lima et al., 2013) the impact of longshore currents and wave energy on the barrier depends on the position of the barrier along the coast (coastline orientation). Regressive barriers, such as the Wolin barrier, develop in coastal embayments that are sheltered from high wave energy throughout the year. Transgressive barriers, such as the Łeba barrier, develop where the wave impact is high, as the result of their exposed position along the coastline (Fig. 6.1 B).

Factors like the source area, grain size distribution and antecedent topography are seen to be similar along the southern Baltic Sea coast and are interpreted to be negligible in dominating the barrier geometry. The barrier topography controls, amongst others, the sediment budget in transgressive barrier systems. A well-developed barrier topography has a negative impact on overwash processes. However, migrating dunes on top of the barrier, e.g. on the Łeba barrier, still contribute to a landward barrier migration and maintain or increase the barrier width by aeolian sediment supply into the lagoon.

6.1.2 Dunes as climate archives

The migrating dunes on top of the Łeba barrier provide an extraordinary example of a wet aeolian system and bear a record of the annual wind intensity (Fig. 5.9). In temperate climates, aeolian processes are controlled by wind and humidity-related vegetation. The transgressive dunes in Łeba are free of vegetation, but precipitation plays an important role during dune movement. The up to 18 m high primary dune is superimposed by a smaller secondary dune, seasonally varying in size and volume as a result of wind-intensity and precipitation-rate variations.

Sediments of the primary dunes are characterized by an alternation of foreset intervals dominated by quartz sands and intervals with layers enriched in heavy minerals; in GPR data imaged by low and high amplitude packages. Sub-yearly changes of the wind field results in the deposition of either quartz-dominated intervals or the development of layers enriched in heavy minerals. This sediment-based log resembles a sedimentary “bar code” in GPR data, which provides the record of annual wind-intensity variations. The yearly thickness variation of a paired low- and high amplitude package is the result of an annual changing net sediment transfer to the lee-side of the dune. The annual dune migration rate and is directly linked to variations in the wind intensity. The generation of a proxy-based record of yearly variations in the wind intensity is thus achieved by bar code thickness variations which was tested and verified by meteorological data. The presented dune bar code is a new approach to provide a time-based proxy record of wind variations on a yearly resolution, especially for instrumental data sparse areas and time periods.

6.2 Outlook

A major outcome of this study is the potential of dunes to serve as archives recording wind-intensity variations on an annual resolution. The sedimentary record provided in this study comprises the time span 1987 to 2012, a time period meteorological data is available. The new approach allows developing a proxy record of annual wind-intensity variations for time periods beyond the instrumental weather record and for areas without an existing meteorological data set. Possible targets to be investigated are dunes, stabilized by vegetation or active, with similar sedimentary properties.

The formation of either regressive or transgressive barriers along the southern Baltic Sea coast is seen to result from local differences in the sea level and from the barrier position along the coast. A more detailed focus on controlling factors was beyond the scope of this study but would improve the understanding between interacting processes.

Washover deposits of the Łeba barrier contain shell layers that were interpreted to result from time periods of less overwash activity. A precise age dating of the sediment by either radiocarbon or OSL may allow for determining gaps in overwash sedimentation indicating time periods with less stormy conditions.

Unconformities in the seaward prograding beach plain of the Wolin barrier were attributed to storm-induced wave erosion. The lateral distribution of single unconformities by a dense grid of GPR lines in combination with precise age dating would make this record accessible to reconstruct the storm intensity and frequency within the last centuries. An increasing or decreasing amount of unconformities within the sedimentary record may indicate a more or less frequent storm activity along the coast of the Pomeranian Bight.

Reference List

Aagaard, T., Orford, J. and Murray, A.S., 2007. Environmental controls on coastal dune formation; Skallingen Spit, Denmark: Geomorphology, 83, p. 29–47.

Andrén, T., Björck, S., Andrén, E., Conley, D., Zillén, L. and Anjar, J., 2011. The Development of the Baltic Sea Basin during the last 130 ka. In: The Baltic Sea Basin (Harff, J., Björck, S., and Hoth, P., eds.) Springer Berlin Heidelberg, Berlin, Heidelberg, p. 75–97.

Arens, S.M., 1996a. Pattens of sand transport on vegetated foredunes: Geomorphology, 17, p. 339–350.

Arens, S.M., 1996b. Rates of aeolian transport on a beach in a temperate humid climate: Geomorphology, 17, p. 3–18.

Arens, S.M., van Boxel, J.H. and Abuodha, J.O.Z., 2002. Changes in grain size of sand in transport over a foredune: Earth Surface Processes and Landforms, 27, p. 1163–1175.

Avramidis, P., Bouzos, D., Antoniou, V. and Kontopoulos, N., 2008. Application of grain-size trend analysis and spatio-temporal changes of sedimentation, as a tool for lagoon management. Case study: the Kotychi lagoon (western Greece): Geologica Carpathica - Bratislava, 59, p. 261–268.

Babbage, C., 1838. Note M: On the age of strata, as inferred from the rings of trees embedded in them. In: The Ninth Bridgewater Treatise, a Fragment (Murray, J., ed.) London, p. 256–264.

Bagnold, R.A., 1941. The physics of blown sand and desert dunes: Methuen, London.

Bailey, S. and Bristow, C.S., 2000. Structure of coastal dunes: observations from ground penetrating radar (GPR) surveys: Eighth International Conference on Ground Penetrating Radar, 4084, 660-665.

Bailey, S.D. and Bristow, C.S., 2004. Migration of parabolic dunes at Aberffraw, Anglesey, north Wales: Geomorphology, 59, p. 165–174.

Baker, P.L., 1991. Response of ground-penetrating radar to bounding surfaces and lithofacies variations in sand barrier sequences: Exploration Geophysics, 22, p. 19–22.

Barboza, E.G., Dillenburg, S.R., Rosa, M.L.C.C., Tomazelli, L.J. and Hesp, P.A., 2009. Ground-penetrating radar profiles of two Holocene regressive barriers in southern Brazil: Journal of Coastal Research, Special Issue, 56, p. 579–583.

Barboza, E.G., Rosa, M., Hesp, P.A., Dillenburg, S.R., Tomazelli, L.J. and Ayup-Zouain, R.N., 2011. Evolution of the Holocene Coastal Barrier of Pelotas Basin (Southern Brazil)-a new approach with GPR data: Journal of Coastal Research, Special Issue, 64, p. 646–650.

Barboza, E.G., Rosa, M., Dillenburg, S.R. and Tomazelli, L.J., 2013. Preservation potential of foredunes in the stratigraphic record: Journal of Coastal Research, 65, p. 1265–1270.

Björck, S., 1995. A review of the history of the Baltic Sea, 13.0-8.0 ka BP: Quaternary Research, 27, p. 19–40.

Blott, S.J. and Pye, K., 2001. GRADISTAT: A grain size distribution and statistics package for the analysis of unconsolidated sediments: Earth Surface Processes and Landforms, 26, p. 1237–1248.

Bobertz, B. and Harff, J., 2004. Sediment facies and hydrodynamic setting: a study in the south western Baltic Sea: Ocean Dynamics, 54, p. 39–48.

Borówka, R.K., 1975. Problem of the morphology of fossil dune forms on the Łeba bar: Quaestiones geographicae, 2, p. 39–51.

Borówka, R.K., 1979. Accumulation and redeposition of eolian sands on the lee slope of dunes and their influence on formation of sedimentary structures: Quaestiones geographicae, 5, p. 5–22.

Borówka, R.K., 1980. Present day dune processes and dune morphology on the Łeba barrier, polish coast of the Baltic: Geografiska Annaler, 62 A, p. 75–82.

Borówka, R.K., 1990. The Holocene development and present morphology of the Łeba Dunes, Baltic coast of Poland. In: Coastal Dunes: Form and process, Chapter Thirteen (Nordstrom, K.F., Psuty, N.P., and Carter, R.W.G., eds.) John Wiley and Sons Ltd., p. 289–313.

Borówka, R.K., 1995. Dunes on the Łeba Barrier - their history and dynamics of present-day aeolian processes. In: Polish Coast: Past, Present and Future (Rotnicki, K., ed.) Journal of Coastal Research, 22, p. 247–251.

Borówka, R.K. and Rotnicki, K., 1995a. Balance of the aeolian sand transport on the beach and the problem of sand nourishment of the active dune field on the Łeba Barrier. In: Polish Coast: Past, Present and Future (Rotnicki, K., ed.) Journal of Coastal Research, 22, p. 257–265.

Borówka, R.K. and Rotnicki, K., 1995b. Shoreline changes of the Łeba Barrier in modern time. In: Polish Coast: Past, Present and Future (Rotnicki, K., ed.) Journal of Coastal Research, 22, p. 271–274.

Borówka, R.K., 1999. Multi-year trends of change in the intensity of potential aeolian transport on the West Pomeranian coast of the Baltic in the context of the morphology and present-day development of coastal dunes: Quaternary Studies in Poland, Special Issue, p. 67–75.

Borówka, R.K., Osadczuk, A., Witkowski, A., Wawrzyniak-Wydrowska, B. and Duda, T., 2005. Late Glacial and Holocene depositional history in the eastern part of the Szczecin Lagoon (Great Lagoon) basin - NW Poland: Quaternary International, 130, p. 87–96.

Bristow, C.S., 1995. Facies analysis in the Lower Greensand using ground-penetrating radar: Journal of the Geological Society, 152, p. 591–598.

Bristow, C.S., Chroston, P.N. and Bailey, S.D., 2000. The structure and development of foredunes on a locally prograding coast: insights from ground-penetrating radar surveys, Norfolk, UK: Sedimentology, 47, p. 923–944.

Bristow, C.S., Lancaster, N. and Duller, G.A.T., 2005. Combining ground penetrating radar surveys and optical dating to determine dune migration in Namibia: Journal of the Geological Society, 162, p. 315–321.

Bristow, C.S. and Pucillo, K., 2006. Quantifying rates of coastal progradation from sediment volume using GPR and OSL: the Holocene fill of Guichen Bay, south-east South Australia: Sedimentology, 53, p. 769–788.

Bristow, C.S., Augustinus, P.C., Wallis, I.C., Jol, H.M. and Rhodes, E.J., 2010. Investigation of the age and migration of reversing dunes in Antarctica using GPR and OSL, with implications for GPR on Mars: Earth and Planetary Science Letters, 289, p. 30–42.

Bristow, C.S., Augustinus, P., Rhodes, E.J., Wallis, I.C. and Jol, H.M., 2011. Is climate change affecting rates of dune migration in Antarctica? Geology, 39, p. 831–834.

Brookfield, M.E., 1977. Origin of bounding surfaces in ancient aeolian sandstones: Sedimentology, 24, p. 303–332.

Buynevich, I.V. and FitzGerald, D.M., 2003. High-resolution subsurface (GPR) imaging and sedimentology of coastal ponds, Maine, USA: Implications for Holocene back-barrier evolution: Journal of Sedimentary Research, 73, p. 559–571.

Buynevich, I.V., FitzGerald, D.M. and van Heteren, S., 2004. Sedimentary records of intense storms in Holocene barrier sequences, Maine, USA: Marine Geology, 210, p. 135–148.

Buynevich, I.V., 2006. Coastal environmental changes revealed in geophysical images of Nantucket Island, Massachusetts, USA: Environmental & Engineering Geoscience, 12, p. 227–234.

Buynevich, I.V. and Donnelly, J.P., 2006. Geological Signatures of Barrier Breaching and Overwash, Southern Massachusetts, USA: Journal of Coastal Research, Special Issue, 39, p. 112–116.

Buynevich, I.V., Bitinas, A. and Pupienis, D., 2007a. Lithological anomalies in a relict coastal dune: Geophysical and paleoenvironmental markers: Geophysical Research Letters, 34.

Buynevich, I.B., Bitinas, A. and Pupienis, D., 2007b. Reactivation of coastal dunes documented by subsurface imaging of the Great Dune Ridge, Lithuania: Journal of Coastal Research, Special Issue, 50, p. 226–230.

Buynevich, I.V., Bitinas, A., Souza, P.W.M., Pupienis, D., Asp, N.E., Goble, R.J. and Kerber, L.E., 2011. Rapid coastal dune migration into temperate and equatorial forests: Optical chronology of imaged upper slipface Strata: Journal of Coastal Research, Special Issue, 64, p. 726–730.

Cattaneo, A. and Steel, R.J., 2003. Transgressive deposits: a review of their variability: Earth-Science Reviews, 62, p. 187–228.

Chappel, J., 1967. Recognizing fossil strand-lines from grain-size analysis: Journal of Sedimentary Petrology, 37, p. 157–165.

Choi, K.H., Choi, J.-H. and Kim, J.W., 2014. Reconstruction of Holocene coastal progradation on the east coast of Korea based on OSL dating and GPR surveys of beach-foredune ridges: The Holocene, 24, p. 24–34.

Cieślak, A., 1995. Contemporary coastal transformation - The coastal management and protection aspect. In: Polish Coast: Past, Present and Future (Rotnicki, K., ed.) Journal of Coastal Research, 22, p. 63–71.

Clemmensen, L.B., Murray, A.S., Beck, J.H. and Clausen, A., 2001a. Large-scale aeolian sand movement on the west coast of Jutland, Denmark in late Subboreal to early Subatlantic time - a record of climate change or cultural impact? Gff, 123, p. 193–203.

Clemmensen, L.B., Pye, K., Murray, A. and Heinemeier, J., 2001b. Sedimentology, stratigraphy and landscape evolution of a Holocene coastal dune system, Lodbjerg, NW Jutland, Denmark: Sedimentology, 48, p. 3–27.

Clemmensen, L.B. and Murray, A., 2006. The termination of the last major phase of aeolian sand movement, coastal dunefields, Denmark: Earth Surface Processes and Landforms, 31, p. 795–808.

Clemmensen, L.B., Bjornsen, M., Murray, A. and Pedersen, K., 2007. Formation of aeolian dunes on Anholt, Denmark since AD 1560: A record of deforestation and increased storminess: Sedimentary Geology, 199, p. 171–187.

Clemmensen, L.B. and Nielsen, L., 2010. Internal architecture of a raised beach ridge system (Anholt, Denmark) resolved by ground-penetrating radar investigations: Sedimentary Geology, 223, p. 281–290.

Clemmensen, L.B., Hansen, K.W.T. and Kroon, A., 2014. Storminess variation at Skagen, northern Denmark since AD 1860: Relations to climate change and implications for coastal dunes: Aeolian Research, 15, p. 101–112.

Costas, S., Alejo, I., Rial, F., Lorenzo, H. and Nombela, M.A., 2006. Cyclical evolution of a modern transgressive sand barrier in northwestern Spain elucidated by GPR and aerial photos: Journal of Sedimentary Research, 76, p. 1077–1092.

Costas, S., Jerez, S., Trigo, R.M., Goble, R. and Rebêlo, L., 2012a. Sand invasion along the Portuguese coast forced by westerly shifts during cold climate events: Quaternary Science Reviews, 42, p. 15–28.

Costas, I., Reimann, T., Tsukamoto, S., Ludwig, J., Lindhorst, S., Frechen, M., Hass, H.C. and Betzler, C., 2012b. Comparison of OSL ages from young dune sediments with a high-resolution independent age model: Quaternary Geochronology, 10, p. 16–23.

Costas, S., Brito, P., Fitzgerald, D. and Globe, R., 2013. Climate-driven episodes of dune mobilization and barrier growth along the central coast of Portugal. In: Sedimentary coastal zones from high to low latitudes: similarities and differences (Martini, I.P., and Wanless, H.R., eds.) Special Publications, Geological Society, London, 388, p. 21.

Costas, S., Naughton, F., Goble, R. and Renssen, H., 2016. Windiness spells in SW Europe since the last glacial maximum: Earth and Planetary Science Letters, 436, p. 82–92.

Daly, J., McGeary, S. and Krantz, D.E., 2002. Ground-penetrating radar investigation of a late Holocene spit complex: Cape Henlopen, Delaware: Journal of Coastal Research, 18 (2), p. 274–286.

Davidson-Arnott, R.G.D. and Fisher, J.D., 1992. Spatial and temporal controls on overwash occurrence on a Great Lakes barrier spit: Canadian Journal of Earth Sciences, 29, p. 102–117.

Davidson-Arnott, R.G.D. and Law, M.N., 1996. Measurement and prediction of long-term sediment supply to coastal foredunes: Journal of Coastal Research, 12 (3), p. 654–663.

Davis, Jr., R., A., 1994. Geology of Holocene Barrier Island Systems: Springer Verlag, Berlin, Heidelberg.

Davis Jr., R.A., Cuffe, C.K., Kowalski, K.A. and Shock, E.J., 2003. Stratigraphic models for microtidal tidal deltas; examples from the Florida Gulf coast: Marine Geology, 200, p. 49–60.

Davis Jr., R.A. and FitzGerald, D.M., 2004. Beaches and Coasts: Blackwell Science.

Deng, J., Zhang, W., Harff, J., Schneider, R., Dudzinska-Nowak, J., Terefenko, P., Giza, A. and Furmanczyk, K., 2014. A numerical approach for approximating the historical morphology of wave-dominated coasts—A case study of the Pomeranian Bight, southern Baltic Sea: Geomorphology, 204, p. 425–443.

Devi, K., Raicy, M.C., Trivedi, D., Srinivasan, P., Murthy, S.G.N., Goble, R.J. and Nair, R.R., 2013. Assessment of coastal dune characteristics using georadar imaging and sedimentological analysis: Odisha and Visakhapatnam, India: Journal of Coastal Conservation, 17, p. 729–742.

de Oliveira Caldas, L.H., Gomes de Oliveira, J., Eugênio de Medeiros, W., Stattegger, K. and Vital, H., 2006. Geometry and evolution of Holocene transgressive and regressive barriers on the semi-arid coast of NE Brazil: Geo-Marine Letters, 26, p. 249–263.

Dickson, M.E., Bristow, C.S., Hicks, D.M., Jol, H., Stapleton, J. and Todd, D., 2009. Beach volume on an eroding sand-gravel coast determined using ground penetrating radar: Journal of Coastal Research, 25 (5), p. 1149–1159.

Dillenburg, S.R., Roy, P.S., Cowell, P.J. and Tomazelli, L.J., 2000. Influence of antecedent topography on coastal evolution as tested by the shoreface translation-barrier model (STM): Journal of Coastal Research, 16 (1), p. 71–81.

Dillenburg, S.R., Tomazelli, L.J. and Barboza, E.G., 2004. Barrier evolution and placer formation at Bujuru southern Brazil: Marine Geology, 203, p. 43–56.

Dillenburg, S.R. and Barboza, E.G., 2009. Long- and short-term progradation of a regressive barrier in southern Brazil: Journal of Coastal Research, Special Issue, 56, p. 599–601.

Dillenburg, S.R., Barboza, E.G., Tomazelli, L.J., Rosa, M. and Maciel, G.S., 2013. Aeolian deposition and barrier stratigraphy of the transition region between a regressive and a transgressive barrier: an example from Southern Brazil: Journal of Coastal Research, Special Issue, 65, p. 464–469.

Dobrotin, N., Bittinas, A., Michelevicius, D., Damusyte, A. and Mazeika, J., 2013. Reconstruction of the Dead (Grey) Dune evolution along the Curonian Spit, Southeastern Baltic: Bulletin of the Geological Society of Finland, 85, p. 53–64.

Dong, Z., 2002. Wind initiation thresholds of the moistened sands: Geophysical Research Letters, 29, p. 25/1-25/3.

Donnelly, J.P., Butler, J., Roll, S., Wengren, M. and Webb, T., 2004. A backbarrier overwash record of intense storms from Brigantine, New Jersey: Marine Geology, 210, p. 107–121.

Donnelly, C. and Sallenger, A.H., 2007. Characterization and Modeling of Washover Fans. In: Coastal Sediments ’07 (Kraus, N.C., and Dean Rosati, J., eds.) American Society of Civil Engineers, New Orleans, United States, p. 2061–2073.

Dougherty, A.J., FitzGerald, D.M. and Buynevich, I.V., 2004. Evidence for storm-dominated early progradation of Castle Neck barrier, Massachusetts, USA: Marine Geology, 210, p. 123–134.

Doughty, S.D., Cleary, W.J. and McGinnis, B.A., 2006. The recent evolution of storm-influenced retrograding barriers in southeastern North Carolina, USA: Journal of Coastal Research, Special Issue, 39, p. 122–126.

Douglass, A.E., 1941. Crossdating in dendrochronology: Journal of Forestry, 39 (10), p. 825–831.

Duane, D.B., 1964. Significance Of Skewness In Recent Sediments, Western Pamlico Sound, North Carolina: Journal of Sedimentary Petrology, 34, p. 864–874.

Emeis, K., Christiansen, C., Edelvang, K., Jahmlich, S., Kozuch, J., Laima, M., Leipe, T., Loffler, A., Lund-Hansen, L.C., Miltner, A., Pazdro, K., Pempkowiak, J., Pollehne, F., Shimmield, T., Voss, M. and Witt, G., 2002. Material transport from the near shore to the basinal environment in the southern Baltic Sea - II: Synthesis of data on origin and properties of material: Journal of Marine Systems, 35, p. 151–168.

Emeis, K.-C., Struck, U., Blanz, T., Kohly, A. and Voβ, M., 2003. Salinity changes in the central Baltic Sea (NW Europe) over the last 10000 years: The Holocene, 13, p. 411–421.

Engels, S. and Roberts, M.C., 2005. The architecture of prograding sandy-gravel beach ridges formed during the last Holocene highstand: southwestern British Columbia, Canada: Journal of Sedimentary Research, 75, p. 1052–1064.

Falqués, A., 2006. Wave driven alongshore sediment transport and stability of the Dutch coastline: Coastal Engineering, 53, p. 243–254.

Fitzgerald, D.M. and van Heteren, S., 1999. Classification of paraglacial barrier systems: coastal New England, USA: Sedimentology, 46, p. 1083–1108.

Folk, R.L. and Ward, W.C., 1957. Brazos River bar: a study in the significance of grain size parameters: Journal of Sedimentary Petrology, 27, p. 3–26.

Forbes, D.L., Orford, J.D., Carter, R.W.G., Shaw, J. and Jennings, S.C., 1995. Morphodynamic evolution, self-organisation, and instability of coarse-clastic barriers on paraglacial coasts: Marine Geology, 126, p. 63–85.

Forbes, D.L., Parkes, G.S., Manson, G.K. and Ketch, L.A., 2004. Storms and shoreline retreat in the southern Gulf of St. Lawrence: Marine Geology, 210, p. 169–204.

Forman, S.L., Oglesby, R. and Webb, R.S., 2001. Temporal and spatial patterns of Holocene dune activity on the Great Plains of North America: megadroughts and climate links: Global and Planetary Change, 29, p. 1–29.

Forman, S.L., Sagintayev, Z., Sultan, M., Smith, S., Becker, R., Kendall, M. and Marin, L., 2008. The twentieth-century migration of parabolic dunes and wetland formation at Cape Cod

National Sea Shore, Massachusetts, USA: landscape response to a legacy of environmental disturbance: Holocene, 18, p. 765–774.

Friedman, G.M., 1961. Distinction between dune, beach and river sands from their textural characteristics: Journal of Sedimentary Petrology, 31, p. 514–529.

Furmańczyk, K.K., Dudzińska-Nowak, J., Furmańczyk, K.A., Paplińska-Swerpel, B. and Brzezowska, N., 2012. Critical storm thresholds for the generation of significant dune erosion at Dziwnow Spit, Poland: Geomorphology, 143, p. 62–68.

Garrison, J.R., Williams, J., Potter Miller, S., Weber, E.T., McMechan, G. and Zeng, X., 2010. Ground-penetrating radar study of North Padre Island: Implications for barrier island internal architecture, model for growth of progradational microtidal barrier islands, and Gulf of Mexico sea-level cyclicity: Journal of Sedimentary Research, 80, p. 303–319.

Gawthorpe, R.L., Li Collier, R.E., Alexander, J., Bridge, J.S. and Leeder, M.R., 1993. Ground penetrating radar: application to sandbody geometry and heterogeneity studies. In: Characterization of Fluvial and Aeolian Reservoirs (North, C.P. and Prosser, D.J., eds.) Special Publications, Geological Society, London, 73, p. 421–432.

Girardi, J.D. and Davis, D.M., 2010. Parabolic dune reactivation and migration at Napeague, NY, USA: Insights from aerial and GPR imagery: Geomorphology, 114, p. 530–541.

Goodwin, I.D., Stables, M.A. and Olley, J.M., 2006. Wave climate, sand budget and shoreline alignment evolution of the Iluka–Woody Bay sand barrier, northern New South Wales, Australia, since 3000 yr BP: Marine Geology, 226, p. 127–144.

Goy, J.L., Zazo, C. and Dabrio, C.J., 2003. A beach-ridge progradation complex reflecting periodical sea-Ievel and climate variability during the Holocene (Gulf of Almería, Western Mediterranean): Geomorphology, 50, p. 251–268.

Guha, S., Kruse, S.E., Wright, E.E. and Kruse, U.E., 2005. Spectral analysis of ground penetrating radar response to thin sedimentary layers: Geophysical Research Letters, 32, p. 1–4.

Hamilton, N.T. and Collins, L.B., 1998. Placer formation in a Holocene barrier system, southwestern Australia: Journal of Coastal Research, 14 (1), p. 240–255.

Hansen, J.M., Aagaard, T. and Binderup, M., 2012. Absolute sea levels and isostatic changes of the eastern North Sea to central Baltic region during the last 900 years: Boreas, 41, p. 180–208.

Harff, J. and Meyer, M., 2011. Coastlines of the Baltic Sea – Zones of Competition Between Geological Processes and a Changing Climate: Examples from the Southern Baltic. In: The Baltic Sea Basin, Central and Eastern European Development Studies (Harff, J., Björck, S., and Hoth, P., eds.) Springer Berlin Heidelberg, Berlin, Heidelberg, p. 149–164.

Havholm, K.G., Ames, D.V., Whittecar, G.R., Wenell, B.A., Riggs, S.R., Jol, H.M., Berger, G.W. and Holmes, M.A., 2004. Stratigraphy of back-barrier coastal dunes, northern North Carolina and Southern Virginia: Journal of Coastal Research, 20 (4), p. 980–999.

Hein, C.J., FitzGerald, D.M., Carruthers, E.A., Stone, B.D., Barnhardt, W.A. and Gontz, A.M., 2012. Refining the model of barrier island formation along a paraglacial coast in the Gulf of Maine: Marine Geology, 307–310, p. 40–57.

Hein, C.J., FitzGerald, D.M., Cleary, W.J., Albernaz, M.B., de Menezes, J.T. and Klein, A.H. da F., 2013. Evidence for a transgressive barrier within a regressive strandplain system: Implications for complex coastal response to environmental change: Sedimentology, 60, p. 469–502.

Héquette, A. and Ruz, M.-H., 1991. Spit and barrier island migration in the southeastern Canadian Beaufort Sea: Journal of Coastal Research, 7 (3), p. 677–698.

Hesp, P.A. and Short, A.D., 1999. Barrier Morphodynamics. In: Handbook of Beach and Shoreface Morphodynamics (Short, A.D., ed.) Wiley, p. 379.

Hesp, P., 2002. Foredunes and blowouts: initiation, geomorphology and dynamics: Geomorphology, 48, p. 245–268.

Hesp, P.A., Dillenburg, S.R., Barboza, E.G., Tomazelli, L.J., Ayup-Zouain, R.N., Esteves, L.S., Gruber, N.L.S., Toldo-Jr., E.E., de A. Tabalara, L.L.C. and Clerot, L.C.P., 2005. Beach ridges, foredunes or transgressive dunefields? Definitions and an examination of the Torres to Tramandaí barrier system, Southern Brazil: Annals of the Brazilian Academy of Sciences, 77, p. 493–508.

Hesp, P.A., 2013. Conceptual models of the evolution of transgressive dune field systems: Geomorphology, 199, p. 138–149.

Hoffmann, G. and Barnasch, J., 2005. Late Glacial to Holocene coastal changes of SE Rügen Island (Baltic Sea, NE Germany): Aquatic Sciences, 67, p. 132–141.

Hoffmann, G., Lampe, R. and Barnasch, J., 2005. Postglacial evolution of coastal barriers along the West Pomeranian coast, NE Germany: Quaternary International, 133, p. 47–59.

Hoffmann, G. and Lampe, R., 2007. Sediment budget calculation to estimate Holocene coastal changes on the southwest Baltic Sea (Germany): Marine Geology, 243, p. 143–156.

Hoffmann, G., Schmedemann, N. and Schafmeister, M.-T., 2009. Relative sea-level curve for SE Rügen and Usedom Island (SW Baltic Sea coast, Germany) using decompacted profiles: Zeitschrift der Deutschen Gesellschaft für Geowissenschaften, 160, p. 69–78.

Horwitz, M.H. and Wang, P., 2005. Sedimentological characteristics and internal architecture of two overwash fans from hurricanes Ivan and Jeanne: Gulf Coast Association of Geological Societies Transactions, 55, p. 342–352.

Houser, C., Hapke, C. and Hamilton, S., 2008. Controls on coastal dune morphology, shoreline erosion and barrier island response to extreme storms: Geomorphology, 100, p. 223–240.

Hugenholtz, C.H., Wolfe, S.A. and Moorman, B.J., 2008. Effects of sand supply on the morphodynamics and stratigraphy of active parabolic dunes, Bigstick Sand Hills, southwestern Saskatchewan: Canadian Journal of Earth Sciences, 45, p. 321–335.

Hugenholtz, C.H., Wolfe, S.A., Walker, I.J. and Moorman, B.J., 2009. Spatial and temporal patterns of aeolian sediment transport on an inland parabolic dune, Bigstick Sand Hills, Saskatchewan, Canada: Geomorphology, 105, p. 158–170.

Hünicke, B., Zorita, E., Soomere, T., Madsen, K.S., Johansson, M. and Suursaar, Ü., 2015. Recent Change—Sea Level and Wind Waves. In: Second Assessment of Climate Change for the Baltic Sea Basin (The BACC II Author Team ed.) Springer International Publishing, Cham, p. 155–185.

Hunter, R.E., 1977. Basic types of stratification in small eolian dunes: Sedimentology, 24, p. 361–387.

Hunter, R.E., Richmond, B.M. and Alpha, T.R., 1983. Storm-controlled oblique dunes of the Oregon coast: Geological Society of America Bulletin, 94, p. 1450–1465.

Jol, H.M., Lawton, D.C. and Smith, D.G., 2002. Ground penetrating radar: 2-D and 3-D subsurface imaging of a coastal barrier spit, Long Beach, WA, USA: Geomorphology, 53, p. 165–181.

Kahn, J.H. and Roberts, H.H., 1982. Variations in storm response along a microtidal transgressive barrier-island arc: Sedimentary Geology, 33, p. 129–146.

Keilhack, K., 1914. Die Verlandung der Swinepforte: Jahrbuch der Königlich Preußischen Geologischen Landesanstalt, 32, p. 209–244.

Kliewe, H. and Janke, W., 1982. Der holozäne Wasserspiegelanstieg der Ostsee im nordöstlichen Küstengebiet der DDR: Petermanns Geographische Mitteilungen, 126, p. 65–74.

Kocurek, G., 1981. Significance of interdune deposits and bounding surfaces in aeolian dune sands: Sedimentology, 28, p. 753–780.

Kowalczyk, K., 2006. New model of the vertical crustal movements in the area of Poland: Geodezija ir kartografija, 32, p. 83–87.

Kraft, J.C. and Chrzastowski, M.J., 1985. Coastal stratigraphic sequences. In: Coastal Sedimentary Environments (Davis Jr., R.A., ed.) Springer Verlag, New York Berlin Heidelberg Tokyo, p. 625–663.

Łabuz, T.A., 2005. Present-day dune environment dynamics on the coast of the Swina Gate Sandbar (Polish West coast): Estuarine Coastal and Shelf Science, 62, p. 507–520.

Łabuz, T.A., 2013. Polish coastal dunes–affecting factors and morphology: Landform Analysis, 22, p. 33–59.

Lampe, R., Ziekur, R., Schuricht, R. and Hoffmann, G., 2004. Georadaruntersuchungen zur Erkundung der Faziesarchitektur im Küstenholozän NE-Deutschlands unter Einbeziehung von Rammkernsondierungen und geoelektrischen Messungen: Zeitschrift für Geologische Wissenschaften, 32, p. 97–112.

Lampe, R., 2005. Lateglacial and Holocene water-level variations along the NE German Baltic Sea coast: review and new results: Quaternary International, 133, p. 121–136.

Lampe, R., Endtmann, E., Janke, W. and Meyer, H., 2010. Relative sea-level development and isostasy along the NE German Baltic Sea coast during the past 9 ka.: Quaternary Science Journal, 59, p. 3–20.

Lampe, R., Naumann, M., Meyer, H., Janke, W. and Ziekur, R., 2011. Holocene evolution of the southern Baltic Sea coast and interplay of sea-level variation, isostasy, accomodation and sediment supply. In: The Baltic Sea Basin, Central and Eastern European Development Studies (Harff, J.,, Björck, S., and Hoth, P., eds.) Springer Berlin Heidelberg, Berlin, Heidelberg, p. 233–251.

Lancaster, N., 1988. Controls of eolian dune size and spacing: Geology, 16, p. 972–975.

Lancaster, N., Kocurek, G., Singhvi, A., Pandey, V., Deynoux, M., Ghienne, J.F. and Lo, K., 2002a. Late Pleistocene and Holocene dune activity and wind regimes in the western Sahara Desert of Mauritania: Geology, 30, p. 991–994.

Lancaster, N., Nickling, W.G. and Neuman, C.M., 2002b. Particle size and sorting characteristics of sand in transport on the stoss slope of a small reversing dune: Geomorphology, 43, p. 233–242.

Lass, H.U., Mohrholz, V. and Seifert, T., 2001. On the dynamics of the Pomeranian bight: Continental Shelf Research, 21, p. 1237–1261.

Leatherman, S.P. and Zaremba, R.E., 1987. Overwash and aeolian processes on a US northeast coast barrier: Sedimentary Geology, 52, p. 183–206.

Lehmann, F. and Green, A.G., 2000. Topographic migration of georadar data: Implications for acquisition and processing: Geophysics, 65, p. 836–848.

Leppäranta, M. and Myrberg, K., 2009. Physical Oceanography of the Baltic Sea: Springer.

Lessa, G.C., Angulo, R.J., Giannini, P.C. and Araújo, A. de, 2000. Stratigraphy and Holocene evolution of a regressive barrier in south Brazil: Marine Geology, 165, p. 87–108.

Lima, L.G., Dillenburg, S.R., Medeanic, S., Barboza, E.G., Rosa, M.L.C.C., Tomazelli, L.J., Dehnhardt, B.A. and Caron, F., 2013. Sea-level rise and sediment budget controlling the evolution of a transgressive barrier in southern Brazil: Journal of South American Earth Sciences, 42, p. 27–38.

Lindhorst, S., Betzler, C. and Hass, H.C., 2008. The sedimentary architecture of a Holocene barrier spit (Sylt, German Bight): Swash-bar accretion and storm erosion: Sedimentary Geology, 206, p. 1–16.

Lindhorst, S., Furstenau, J., Hass, H.C. and Betzler, C., 2010. Anatomy and sedimentary model of a hooked spit (Sylt, southern North Sea): Sedimentology, 57, p. 935–955.

Lindhorst, S., Betzler, C. and Hass, C.H., 2013. Large scale architecture of a stacked Holocene spit – the stratigraphy of northern Sylt (southern North Sea): Zeitschrift der Deutschen Gesellschaft für Geowissenschaften, 164, p. 63–79.

Lindhorst, S. and Schutter, I., 2014. Polar gravel beach-ridge systems: Sedimentary architecture, genesis, and implications for climate reconstructions (South Shetland Islands/Western Antarctic Peninsula): Geomorphology, 221, p. 187–203.

Lindhorst, S. and Betzler, C., 2016. The climate-archive dune: Sedimentary record of annual wind intensity: Geology, in press, p. G38093.1, doi: 10.1130/G38093.1.

Lougheed, B.C., Filipsson, H.L. and Snowball, I., 2013. Large spatial variations in coastal 14C reservoir age - a case study from the Baltic Sea: Climate of the Past, 9, p. 1015–1028.

Lurton, X., 2010. An Introduction to Underwater Acoustics: Principles and Applications: Springer Berlin Heidelberg.

Maio, C.V., Gontz, A.M., Weidman, C.R. and Donnelly, J.P., 2014. Late Holocene marine transgression and the drowning of a coastal forest: Lessons from the past, Cape Cod, Massachusetts, USA: Palaeogeography, Palaeoclimatology, Palaeoecology, 393, p. 146–158.

Mäkinen, J. and Räsänen, M., 2003. Early Holocene regressive spit-platform and nearshore sedimentation on a glaciofluvial complex during the Yoldia Sea and the Ancylus Lake phases of the Baltic Basin, SW Finland: Sedimentary Geology, 158, p. 25–56.

Martinho, C.T., Dillenburg, S.R. and Hesp, P., 2009. Wave energy and longshore sediment transport gradients controlling barrier evolution in Rio Grande do Sul, Brazil: Journal of Coastal Research, 25 (2), p. 285–293.

Martins, L.R., 2003. Recent sediments and grain-size analysis: Gravel, 1, p. 90–105.

Matias, A., Ferreira, Ó., Vila-Concejo, A., Garcia, T. and Dias, J.A., 2008. Classification of washover dynamics in barrier islands: Geomorphology, 97, p. 655–674.

McCubbin, D.G., 1982. Barrier-island and strand-plain facies. In: Sandstone Depositional Environments (Scholle, P.A., and Spearing, D., eds.) The American Association of Petroleum Geologists, Tulsa, Oklahoma, p. 247–279.

McKee, E.D., 1966. Structures of dunes at White Sands National Monument, New Mexico (and a comparison with structures of dunes from other selected areas): Sedimentology, 7, p. 3–69.

McKee, E.D. and Bigarella, J.J., 1972. Deformational structures in Brazilian Coastal Dunes: Journal of Sedimentary Petrology, 42, p. 670–681.

McLean, R.F. and Kirk, R.M., 1969. Relationships between grain size, size-sorting, and foreshore slope on mixed sand - shingle beaches: New Zealand Journal of Geology and Geophysics, 12, p. 138–155.

Mitchum Jr., R.M., Vail, P.R. and Sangree, J.B., 1977. Seismic stratigraphy and global changes of sea level: Part 6. Stratigraphic interpretation of seismic reflection patterns in depositional sequences. In: Seismic Stratigraphy--Applications to Hydrocarbon Exploration, AAPG Memoir 26 (Pyton, C.E., ed.) p. 117–133.

Møller, I. and Anthony, D., 2003. A GPR study of sedimentary structures within a transgressive coastal barrier along the Danish North Sea coast. In: Ground Penetrating Radar in Sediments (Bristow, C.S., and Jol, H., eds.) Special Publications, Geological Society, London, 211, p. 55–65.

Moore, L.J., Jol, H.M., Kruse, S., Vanderburgh, S. and Kaminsky, G.M., 2004. Annual layers revealed by GPR in the subsurface of a prograding coastal barrier, southwest Washington, USA: Journal of Sedimentary Research, 74, p. 690–696.

Morton, R.A., 2002. Factors controlling storm impacts on coastal barriers and beaches: A preliminary basis for near real-time forecasting: Journal of Coastal Research, 18 (3), p. 486–501.

Morton, R.A. and Sallenger Jr, A.H., 2003. Morphological impacts of extreme storms on sandy beaches and barriers: Journal of Coastal Research, 19 (3), p. 560–573.

Morton, R.A., Gelfenbaum, G. and Jaffe, B.E., 2007. Physical criteria for distinguishing sandy tsunami and storm deposits using modern examples: Sedimentary Geology, 200, p. 184–207.

Moulton, M., Oliveira Filho, S., Rocha, T.B. and Fernandez, G.B., 2013. Foredunes of Rio de Janeiro coast: genesis, structure and morphology: Journal of Coastal Research, Special Issue, 65, p. 1319–1324.

Musielak, S. and Osadczuk, K., 1995. Evolution of the Świna Gate. In: Polish Coast: Past, Present and Future (Rotnicki, K., ed.) Journal of Coastal Research, 22, p. 305–308.

Neal, A., Pontee, N.I., Pye, K. and Richards, J., 2002. Internal structure of mixed-sand-and-gravel beach deposits revealed using ground-penetrating radar: Sedimentology, 49, p. 789–804.

Neal, A., Richards, J. and Pye, K., 2003. Sedimentology of coarse-clastic beach-ridge deposits, Essex, southeast England: Sedimentary Geology, 162, p. 167–198.

Neal, A., 2004. Ground-penetrating radar and its use in sedimentology: principles, problems and progress: Earth-Science Reviews, 66, p. 261–330.

Nielsen, L.H., Johannessen, P.N. and Surlyk, F., 1988. A Late Pleistocene coarse-grained spit-platform sequence in northern Jylland, Denmark: Sedimentology, 35, p. 915–937.

Nielsen, L. and Clemmensen, L.B., 2009. Sea-level markers identified in ground-penetrating radar data collected across a modern beach ridge system in a microtidal regime: Terra Nova, 21, p. 474–479.

Nielsen, L.H. and Johannessen, P.N., 2009. Facies architecture and depositional processes of the Holocene-Recent accretionary forced regressive Skagen spit system, Denmark: Sedimentology, 56, p. 935–968.

Oliveira Jr, J.G., Medeiros, W.E., Tabosa, W.F. and Vital, H., 2008. From barchan to domic shape: evolution of a coastal sand dune in northeastern Brazil based on GPR survey: Revista Brasileira de Geofísica, 26, p. 5–20.

Ollerhead, J. and Davidson-Arnott, R.G.D., 1995. The evolution of Buctouche Spit, New Brunswick, Canada: Marine Geology, 124, p. 215–236.

Ollerhead, J., Davidson-Arnott, R., Walker, I.J. and Mathew, S., 2013. Annual to decadal morphodynamics of the foredune system at Greenwich Dunes, Prince Edward Island, Canada: Earth Surface Processes and Landforms, 38, p. 284–298.

Orford, J.D., Wilson, P., Wintle, A.G., Knight, J. and Braley, S., 2000. Holocene coastal dune initiation in Northumberland and Norfolk, eastern UK: climate and sea-level changes as possible forcing agents for dune initiation. In: Holocene coastal dune initiation in Northumberland and Norfolk, eastern UK (Shennan, I. and Andrews, J., eds) Special Publications , Geological Society, London, 166, p. 197–217.

Osadczuk, K., 2002. Evolution of the Świna barrier spit. In: Greifswalder Geographische Arbeiten (R. Lampe, ed.), 27, p. 119–125.

Osadczuk, A., Musielak, S. and Borówka, R.K., 2007. Why should the Odra River mouth area not be regarded as an estuary? A geologist's point of view: International Journal of Oceanography and Hydrobiology, 36, p. 87–99.

Ostrowski, R. and Pruszak, Z., 2011. Relationships between coastal processes and properties of the nearshore sea bed dynamic layer: Oceanologia, 53, p. 861–880.

Otvos, E.G., 2000. Beach ridges - definitions and significance: Geomorphology, 32, p. 83–108.

Otvos, E.G., 2012. Coastal barriers - Nomenclature, processes, and classification issues: Geomorphology, 139, p. 39–52.

Ptak, A. and Rudowski, S., 2014. Piaskowe giganty: Geodeta (Magazyn geoinformacyjny), 9 (232), p. 22–23.

Pupienis, D., Buynevich, I.V. and Bitinas, A., 2011. Distribution and significance of heavy-mineral concentrations along the southeast Baltic Sea coast: Journal of Coastal Research, Special Issue, 64, p. 1984–1988.

Pye, K., 1983. Coastal dunes: Progress in Physical Geography, 7, p. 531–557.

Reading, H.G. and Collinson, J.D., 2007. Clastic Coasts. In: Sedimentary Environments: Processes, Facies and Stratigraphy (Reading, H.G., ed.) Blackwell Science, p. 688.

Reimann, T., Tsukamoto, S., Harff, J., Osadczuk, K. and Frechen, M., 2011. Reconstruction of Holocene coastal foredune progradation using luminescence dating - An example from the Swina barrier (southern Baltic Sea, NW Poland): Geomorphology, 132, p. 1–16.

Reimer, P.J., Bard, E., Bayliss, A., Beck, J.W., Blackwell, P.G., Bronk Ramsey, C., Buck, C.E., Cheng, H., Edwards, R.L., Friedrich, M. and others, 2013. IntCal13 and Marine13 radiocarbon age calibration curves 0-50,000 years cal BP: Radiocarbon, 55, p. 1869–1887.

Rodriguez, A.B. and Meyer, C.T., 2006. Sea-level variation during the Holocene deduced from the morphologic and stratigraphic evolution of Morgan Peninsula, Alabama, U.S.A.: Journal of Sedimentary Research, 76, p. 257–269.

Rodriguez, A.B., Fegley, S.R., Ridge, J.T., VanDusen, B.M. and Anderson, N., 2013. Contribution of aeolian sand to backbarrier marsh sedimentation: Estuarine, Coastal and Shelf Science, 117, p. 248–259.

Rotnicka, J., 2011. Factors controlling the development of foredunes along the Łeba barrier on the South Baltic Coast of Poland: Journal of Coastal Research, Special Issue, 64, p. 308–313.

Rotnicki, K., 1995. An outline of geomorphology and main problems of the Upper Quaternary of the Gardno-Łeba Coastal Plain. In: Polish Coast: Past, Present and Future (Rotnicki, K., ed.) Journal of Coastal Research, 22, p. 213–219.

Rotnicki, K. and Borówka, R.K., 1995. The Last Cold Period in the Gardno-Łeba Coastal Plain. In: Polish Coast: Past, Present and Future (Rotnicki, K., ed.) Journal of Coastal Research, 22, p. 225–229.

Rotnicki, K., Alexandrowicz, A.W., Pazdur, A., Goslar, T. and Borówka, R.K., 2009. Stages of the formation of the Łeba barrier-lagoon system on the basis of the geological cross-section near Rąbka (southern baltic coast, Poland): Studia Quaternaria, 26, p. 3–24.

Rotnicki, K. and Rotnicka, J., 2010. Poland. In: Encyclopedia of the World´s Coastal Landforms (Bird, C.F., ed.) Springer.

Roy, P.S., Cowell, P.J., Ferland, M.A. and Thom, B.G., 1994. Wave-dominated coasts. In: Coastal Evolution - Late Quaternary shoreline morphodynamics, Coastal Evolution in the Quaternary IGCP Project 274 (Carter, R.W.G., and Woodroffe, C.D., eds.) Cambridge University Press.

Sandmeier, K.J., 2013. Reflex-W: Karlsruhe, Germany.

Schwartz, R.K., 1982. Bedform and stratification characteristics of some modern small-scale washover sand bodies: Sedimentology, 29, p. 835–849.

Schwarzer, K., Diesing, M., Larson, M., Niedermeyer, R.O., Schumacher, W. and Furmańczyk, K., 2003. Coastline evolution at different time scales - examples from the Pomeranian Bight, southern Baltic Sea: Marine Geology, 194, p. 79–101.

Sedgwick, P.E. and Davis Jr., R.A., 2003. Stratigraphy of washover deposits in Florida: implications for recognition in the stratigraphic record: Marine Geology, 200, p. 31–48.

Shankar, R., Thompson, R. and Prakash, T.N., 1996. Estimation of heavy and opaque mineral contents of beach and offshore placers using rock magnetic techniques: Geo-Marine Letters, 16, p. 313–318.

Shaw, J. and Forbes, D.L., 1992. Barriers, barrier platforms, and spillover deposits in St. George's Bay, Newfoundland: paraglacial sedimentation on the flanks of a deep coastal basin: Marine Geology, 105, p. 119–140.

Short, A.D., 1999. Handbook of Beach and Shoreface Morphodynamics: Wiley, Chichester.

Smith, D.G., Simpson, C.J., Jol, H.M., Meyers, R.A. and Currey, D.R., 2003. GPR stratigraphy used to infer transgressive deposition of spits and a barrier, Lake Bonneville, Stockton, Utah, USA. In: Ground Penetrating Radar in Sediments (Bristow, C.S. and Jol, H.M., eds.) Special Publications, Geological Society, London, 211, p. 79–86.

Speer, J.H., 2010. Fundamentals of tree-ring research: University of Arizona Press, Tucson.

Storms, J.E., Weltje, G.J., Van Dijke, J.J., Geel, C.R. and Kroonenberg, S.B., 2002. Process-response modeling of wave-dominated coastal systems: simulating evolution and stratigraphy on geological timescales: Journal of Sedimentary Research, 72, p. 226–239.

Stuiver, M. and Reimer, J., 1993. Extended 14C data base and revised CALIB 3.0 14C age calibration program: Radiocarbon, 35, p. 215–230.

Switzer, A.D., Bristow, C.S. and Jones, B.G., 2006. Investigation of large-scale washover of a small barrier system on the southeast Australian coast using ground penetrating radar: Sedimentary Geology, 183, p. 145–156.

Switzer, A.D. and Jones, B.G., 2008. Large-scale washover sedimentation in a freshwater lagoon from the southeast Australian coast: sea-level change, tsunami or exceptionally large storm? The Holocene, 18, p. 787–803.

Sztobryn, M., Stigge, H.-J., Wielbińska, D., Weidig, B., Stanisławczyk, I., Kańska, A., Krzysztofik, K., Kowalska, B., Letkiewicz, B. and Mykita, M., 2005. Sturmfluten in der südlichen Ostsee (westlicher und mittlerer Teil): Berichte des Bundesamtes für Seeschifffahrt und Hydrographie, 39, p. 74.

Tamura, T., Murakami, F., Nanayama, F., Watanabe, K. and Saito, Y., 2008. Ground-penetrating radar profiles of Holocene raised-beach deposits in the Kujukuri strand plain, Pacific coast of eastern Japan: Marine Geology, 248, p. 11–27.

Tamura, T., 2012. Beach ridges and prograded beach deposits as palaeoenvironment records: Earth-Science Reviews, 114, p. 279–297.

Thom, B.G., 1984. Transgressive and regressive stratigraphies of coastal sand barriers in southeast Australia: Marine Geology, 56, p. 137–158.

Timmons, E.A., Rodriguez, A.B., Mattheus, C.R. and DeWitt, R., 2010. Transition of a regressive to a transgressive barrier island due to back-barrier erosion, increased storminess, and low sediment supply: Bogue Banks, North Carolina, USA: Marine Geology, 278, p. 100–114.

Tomczak, A., 1995a. Geological Structure and Holocene Evolution of the Polish Coastal Zone. In: Polish Coast: Past, Present and Future (Rotnicki, K., ed.) Journal of Coastal Research, 22, p. 15–31.

Tomczak, A., 1995b. Relief, geology and evolution of the Hel Spit. In: Polish Coast: Past, Present and Future (Rotnicki, K., ed.) Journal of Coastal Research, 22, p. 181–185.

Tsoar, H. and Blumberg, D.G., 2002. Formation of parabolic dunes from barchan and transverse dunes along Israel's Mediterranean coast: Earth Surface Processes and Landforms, 27, p. 1147–1161.

Tsoar, H., Blumberg, D.G. and Stoler, Y., 2004. Elongation and migration of sand dunes: Geomorphology, 57, p. 293–302.

Twinning, A.C., 1833. On the growth of timber: American Journal of Science and Arts, 24, p. 391–393.

Uścinowicz, S., 2006. A relative sea-level curve for the Polish Southern Baltic Sea: Quaternary International, 145, p. 86–105.

Uścinowicz, S., 2014. The Baltic Sea continental shelf. In: Continental shelfs of the world: Their evolution during the last glacio-eustatic cycle (Chiocci, F.L. and Chivas, A.R., eds.) Geological Society, London, Memoirs, 41, p. 69–89.

Van Dam, R.L. and Schlager, W., 2000. Identifying causes of ground-penetrating radar reflections using time-domain reflectometry and sedimentological analyses: Sedimentology, 47, p. 435–449.

Van Dam, R.L., Schlager, W., Dekkers, M.J. and Huisman, J.A., 2002. Iron oxides as a cause of GPR reflections: Geophysics, 67, p. 536–545.

Van Dam, R.L., 2012. Landform characterization using geophysics—Recent advances, applications, and emerging tool: Geomorphology, 137, p. 57–73.

Van Dam, R.L., Hendrickx, J.M.H., Cassidy, N.J., North, R.E., Dogan, M. and Borchers, B., 2013. Effects of magnetite on high-frequency ground-penetrating radar: Geophysics, 78, p. H1–H11.

van Heteren, S. and van de Plassche, O., 1997. Influence of relative sea-level change and tidal-inlet development on barrier-spit stratigraphy, Sandy Neck, Massachusetts: Journal of Sedimentary Research, 67, p. 350–363.

van Heteren, S., Fitzgerald, D.M., McKinlay, P.A. and Buynevich, I.V., 1998. Radar facies of paraglacial barrier systems: coastal New England, USA: Sedimentology, 45, p. 181–200.

van Heteren, S., Huntley, D.J., van de Plassche, O. and Lubberts, R.K., 2000. Optical dating of dune sand for the study of sea-level change: Geology, 28, p. 411–414.

Wang, P. and Horwitz, M.H., 2007. Erosional and depositional characteristics of regional overwash deposits caused by multiple hurricanes: Sedimentology, 54, p. 545–564.

Westervelt, P.J., 1963. Parametric acoustic array: The Journal of the Acoustical society of America, 35, p. 535–537.

Wilson, P., Orford, J.D., Knight, J., Braley, S.M. and Wintle, A.G., 2001. Late-Holocene (post-4000 years BP) coastal dune development in Northumberland, northeast England: Holocene, 11, p. 215–229.

Witkowski, A., Latałowa, M., Borówka, R.K., Gregorowicz, P., Bąk, M., Osadczuk, A., Święta, J., Lutyńska, M., Wawrzyniak-Wydrowska, B. and Woziński, R., 2004. Palaeoenvironmental changes in the area of the Szczecin lagoon (the south western baltic sea) as recorded from diatoms: Studia Quaternaria, 21, p. 153–165.

Wojciechowski, A., 1995. Holocene deposits and molluscan assemblages in Lake Łebsko, Gardno-Łeba Coastal Plain. In: Polish Coast: Past, Present and Future (Rotnicki, K., ed.) Journal of Coastal Research, 22, p. 237–243.

Wojciechowski, A., 2011. Stages of the evolution of the South Baltic coast as recorded in the molluscan fauna: Journal of Coastal Research, Special Issue, 64, p. 711–715.

Yao, Z.Y., Wang, T., Han, Z.W., Zhang, W.M. and Zhao, A.G., 2007. Migration of sand dunes on the northern Alxa Plateau, Inner Mongolia, China: Journal of Arid Environments, 70, p. 80–93.

Zhang, W., Deng, J., Harff, J., Schneider, R. and Dudzinska-Nowak, J., 2013. A coupled modeling scheme for longshore sediment transport of wave-dominated coasts—A case study from the southern Baltic Sea: Coastal Engineering, 72, p. 39–55.

Ziegelmeier, E., 1966. Die Schnecken(Gastropoda Prosobranchia) der deutschen Meeresgebiete und brackigen Küstengewässer: Helgoländer wissenschaftliche Meeresuntersuchungen, 13, p. 1–61.

Ziekur, R., Hoffmann, G. and Grelle, T., 2009. Facies architecture of the subsurface of the Holocene coastal lowlands on the SW Baltic Sea (Germany) - insights from ground penetrating radar surveys: Zeitschrift Der Deutschen Gesellschaft für Geowissenschaften, 160, p. 79–91.

Acknowledgments

First of all, my special thanks go to Christian Betzler and Sebastian Lindhorst who initiated this project and entrusted me with the responsibility to research this topic. For your guidance throughout my time at the institute, revising and discussing figures and texts as well as decisive suggestions and ideas I would like to express my sincere gratitude. Furthermore, I would like to thank you for the opportunity to participate in ship cruises that gave me valuable insights into different scientific questions and methods.

I am particularly grateful to Prof. Borówka, Dr. Krystyna Osadczuk, Andrzej Osadczuk and Agnieszka Strzelecka for sharing their profound knowledge of the Łeba barrier and dunes as well as the Świna area, their support during the first fieldwork, and their tireless help with any administrative procedure in Szczecin as well as in Łeba. For the initiation of the Polish-German cooperation Prof. Dr. Jan Harff is greatly acknowledged.

The administration of both, the Słowinski National Park and the Wolin National Park, are greatly acknowledged for allowing me to conduct fieldwork in the natural protection areas. Malgorzata Knitter and her team are greatly thanked for inestimable on-site help in solving technical and logistical challenges and for providing biological and historical facts of the Łeba area.

I wish to express my gratitude to the Helmholtz-Zentrum Geesthacht (especially Volker Dzaak) for providing a time slot to use the RV Ludwig Prandtl in order to obtain hydroacoustic and seismic data in the Pomeranian Bight. The ship crew of the RV Ludwig Prandtl is greatly acknowledged for any support and Heiko Gembert is thanked for doing everything possible to get the ship as close to the shore as possible.

The Helmholtz Climate Initiative REKLIM (Regional climate change) is greatly acknowledged for funding (CLISCODE). Their financial support facilitated several fieldworks, the participation in meetings and a full-time focus on the aims of the project.

Svenja Bierstedt is gratefully thanked for her patient explanations and for providing re-analyzed wind data. In this regard, thanks are also due to Birgit Hünicke and Eduardo Zorita.

Jutta Richarz and Eva Vinx are thanked for their contributions in the laboratory, including grain size measurements and the preparation of sediment samples. Furthermore, I owe them gratitude for introducing the Bachelorstudents to their duties.

Nora Goretzki, Anna Rowold, Lion Schumann, Tobias Geiling, and Wolfgang Erbe are thanked for their helpful contributions to fieldwork and for supporting this project with results of their Bachelor and Master theses.

I address special thanks to all my helping hands during fieldwork: Dirk Eggers, Nestor Karafotis, Ilona Schutter, Marco Wunsch, Iria Costas, Leonie Ulferts, Svenja Bierstedt, Martin Hincke, the Bsc.

and Msc. students, and the team of the Szczecin University. Thank you so much for supporting me – also and especially in bad “stay at home” weather conditions – and for sharing a great time and work experience! Especially the time in Łeba during the harsh but deserted winter months and the “special eating places” will be an unforgettable and unique experience. For a smooth workflow and a great time during the ship cruise in the Pomeranian Bight I would like to express my sincere gratitude to Sebastian Lindhorst, Nestor Karafotis, Wolfgang Erbe, Marco Wunsch, Dirk Eggers, Michał Bugajny, and Andrzej Osadczuk. Sönke Reiche, special thanks for your incredible patience explaining the seismic procedure, from the preparation to the post-processing, and your assistance during the first half of the cruise!

Thank you so much, Marco and Martin, for proofreading the final version of my thesis and for any helpful revisions.

I thank you, Huaqing Bai, for being a great office companion during the last four years (time is flying), for very interesting discussions about your home country and your patience with me during the more stressful days. For an entertaining time in the office I thank you, Nestor and Ron.

I am endlessly and deeply grateful to Ilona, Bene, Marco, and Martin who have been such lovely and important company during my ups and downs at the Geomatikum. I already miss our regular coffee breaks, the much-needed work-distracting and amusing chats and the fantastic nights out in Hamburg. I wish only the best for all of you!